

Final Engineering Project Proposal

submitted to

The ME 450 Design & Manufacturing III Class Instructors

University of Michigan

A Novel Device for Tension-Torsion Testing of Micro-Wires

May 29, 2009

Team 24

Thomas Fick
Paula Harrison
Kristin King
Gretchen Miller

Sponsor

Samantha H. Daly
Assistant Professor of Mechanical Engineering
University of Michigan

Section Instructor

John Hart
Assistant Professor of Mechanical Engineering
University of Michigan

EXECUTIVE SUMMARY

In the current era of micro and nanotechnology, the inability of the traditional laws governing permanent deformations to predict plastic behavior in small-scale devices is a critical issue. A driving force behind miniaturization is the idea that “smaller is stronger”. Some experiments have been completed to study the material properties of small-scale wires, but more experiments need to be done to verify the theory. Our team will design and build a miniature tension-torsion tester to be used for experimentation and validation. The system will be interfaced with a computer controller, which allows the user to define specific loading paths and to view the results graphically and numerically in real-time or instantaneously when the test is complete.

The three most critical customer requirements, and the corresponding engineering specifications and target values are given below in Table 1. Our full quality function deployment (QFD) can be found in Appendix A.

Table 1. Top Six Critical Customer Requirements and Engineering Specifications

Mandatory Customer Requirements	Critical Engineering Specifications	Specification Target Value
Grips micro-wires without slipping	Alignment tolerance	0.5 °
Maintains wire and grip alignment	Tension Resolution	4.98(10 ⁻⁴) N
High testing resolution	Torsion Resolution (at 5 mm)	2.49(10 ⁻⁹) N

A micro-wire can be put under tension and torsion by pulling and twisting the wire. After completing a functional decomposition, and looking at the customer requirements and engineering specifications, we identified three modules to focus on: gripping of the micro-wires, alignment of the wire and grips, and data sensitivity and resolution. Our most critical module was the sensors, including the rotational and linear encoders; load cell; and, most importantly, the flexure, amplification bar, and capacitance probe design. We will use the displacement of the bar measured by the capacitance probes to calculate the torsion load. The design of the tension-torsion tester for micro-wires is complete, and all parts have been received. Most of the assembly is complete and a few tests have been run. Initial testing confirmed that the machine is capable of performing and measuring the tension loads on a wire. Our grips do not allow for wire slip and do not break the wire provided the clamp is not screwed on too tightly. For the torsion test, it is known that the wire can be twisted and that the capacitance probes can measure the extremely small loads that we require. These results are from initial testing with the machine in Professor Awtar’s lab. However, the drift of the sensors has caused problems because of the resolution required, 1-2 nm. The sensors currently drift and we have found it hard to stabilize them. We hypothesize that the drift is due to thermal fluctuation in the room causing thermal expansion of the amplification bar and wing. Other possibilities include electromagnetic fields around the probes (having the bar not ground well enough, air currents, vibrations, and sensor drifts).

We recommend further testing with the capacitance probes, such as in the Michigan Nanofabrication Lab, so that different variables can be isolated. After this, a new flexure can be designed and a torsion test will be possible. A few things still need to be made or fixed on our prototype such as the grip alignment plate, the groove lathed in dowels, and the current grip alignment. In addition, the LabView program is still in the development stage.

TABLE OF CONTENTS

1. INTRODUCTION.....	5
2. BACKGROUND.....	5
3. RESEARCH & INFORMATION SOURCES	5
3.1 Gripping and aligning the micro-wires	6
3.2 Data sensitivity/resolution.....	7
4. CUSTOMER REQUIREMENTS & ENGINEERING SPECIFICATIONS.....	7
5. PROBLEM DECOMPOSITION.....	8
6. BRAINSTORMING & CONCEPT GENERATION PROCESS	9
7. CONCEPTS.....	10
7.1 Gripping	10
7.2 Alignment.....	13
7.3 Sensing.....	15
7.3.1 Displacement Sensors	15
7.3.2 Torsion Load and Force Sensors.....	15
8. CONCEPT SELECTION PROCESS.....	16
8.1 Gripping	17
8.2 Alignment.....	18
8.3 Sensors	19
8.4 Final Concept Selection	20
9. PRELIMINARY ANALYSIS	20
9.1 Gripping	21
9.2 Alignment.....	22
9.3 Sensors	22
9.4 Drive Train.....	22
10. FINAL DESIGN & ANALYSIS.....	22
10.1 Description of Final Design	22
10.2 Bill of Materials	26
10.3 Engineering Design Parameter Analysis.....	28
10.3.1 Sensors	28
10.3.2 Drivetrain	29

10.3.3	Flexure	29
10.3.4	Material Selection	31
10.4	Safety Analysis.....	33
10.5	Environmental Analysis	33
11.	PROTOTYPE MANUFACTURING & ASSEMBLY PLAN	36
12.	USABILITY ANALYSIS	37
13.	VALIDATION PLAN.....	38
13.1	Flexure Functionality	38
13.2	Gauge length	38
13.3	Travel	38
13.4	Backlash	38
13.5	General Dimensions and Quantities.....	39
13.6	Test Height	39
13.7	Motor Loads and Speeds	39
13.8	Gripping Force and Coefficient.....	39
13.9	Alignment Tolerance.....	39
14.	CHALLENGES, RISKS, & COUNTERMEASURES	39
14.1	Design Changes.....	39
14.2	Flexure Design and Modification.....	40
14.3	Capacitance Probes and Calibration Issues	41
14.4	Next Steps	42
14.4.1	Manufacturing.....	43
14.4.2	Integration of the LabVIEW Program	43
14.4.3	Calibration of the Torsion Flexure.....	43
15.	TESTING PROCEDURES AND LABVIEW USER MANUAL.....	44
16.	CONCLUSION	45
17.	REFERENCES	46
	APPENDIX A.....	48
	APPENDIX B	52
	APPENDIX C	55
	APPENDIX D.....	58
	APPENDIX E	60

APPENDIX F.....	63
APPENDIX G.....	64
APPENDIX H.....	66
APPENDIX I	67
APPENDIX J	68
APPENDIX K.....	73
APPENDIX L	74
APPENDIX M	78
APPENDIX N.....	81
APPENDIX O.....	95

1. INTRODUCTION

In the current era of micro and nanotechnology, the inability of the traditional laws governing permanent deformations to predict plastic behavior in small-scale materials is a critical issue. A driving force behind miniaturization is the idea that “smaller is stronger”. However, the conventional equations governing plasticity neglect the strain gradient, and therefore cannot predict size effects at these small scales. Some work has been done with strain gradients as a result of small-scale bending and indentation, but more experiments are needed to generalize the effect of these gradients. Our team worked with Professor Daly, our sponsor, to design and build a miniature tension-torsion tester in order to experimentally examine the effect of strain gradients on metallic and carbon micro-wires with diameters ranging from 10-200 microns. The system will be interfaced with a computer controller that will allow the user to define specific loading histories to look at the interaction between statistically stored versus geometrically necessary dislocations.

2. BACKGROUND

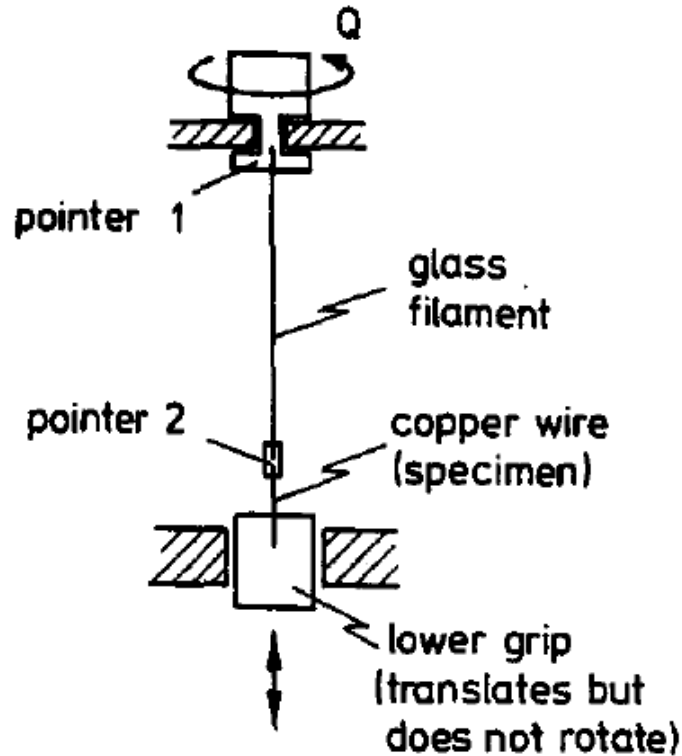
In materials science, the conventional laws governing plasticity do not incorporate a length scale; therefore, the effect of size on a material’s strength is not well known. The conventional laws cannot be used to predict plastic behavior in small-scale devices. According to Fleck and Hutchinson [1], both strain and strain gradients determine yield stress, but “strain gradient strengthening plays an increasingly dominant role with decreasing wire diameter.” This is because the effects of geometrically necessary dislocations become more pronounced as the material size decreases, and strain gradient is proportional to the density of dislocations. Geometrically necessary dislocations appear due to the geometry of loading or because of a plastically inhomogeneous material. Material hardening is controlled by the density of dislocations, and therefore related to the gradient of strain. As a result, it is postulated that the smaller the diameter of a wire, the stronger it is. The purpose of this project is to build a miniature tension-torsion device for testing micro-wire so that this theory can be explored and expanded. The device must examine the response of micro-wires under no strain gradient (i.e. under tension, where no size effect should be seen), strain gradients (i.e. under torsion, where size effects are predicted), and a combination of tension and torsion loading paths. It must test wire of materials ranging from carbon fiber to steel with diameters between 10-200 microns.

If our team is able to build a successful tension-torsion device, the impact it can have on research and theory is far-reaching. The current state-of-the-art, shown in Figure 1 on the next page, came from Fleck and Hutchinson, and their tests have not been repeated since 1993. The material properties of micro-wires are simply unknown. If the theory can be verified and further refined through better experimentation, the field of material science could potentially use this theory to develop new and unique materials, and be able to correctly predict the material’s behavior.

3. RESEARCH & INFORMATION SOURCES

After reviewing the project specifications with our sponsor and examining our QFD, we came up with a set of specifications that will be the most difficult to achieve, and focused our research and benchmarking efforts on these topics.

Figure 1. Schematic of Torsion Test Rig from Fleck and Hutchinson



3.1 Gripping and aligning the micro-wires

One of the most difficult specifications to meet is that of gripping the micro-wires without slippage and ensuring perfect alignment of the wire during the entire duration of the test. In the search for a possible method for gripping the micro-wires, our group conducted research on gripping and alignment methods for optical fibers, as well as examined products out on the market that are used for tensioning yarn or fine wires.

One method that we found for gripping these wires which was common in both patents and journal articles was to use a V-groove etched in a substrate, and then some sort of clip (e.g. cantilever clips [2]) or clamp (e.g. leaf spring clamp [3]) to hold the wire in the V-groove. In already existent tension devices, the main methods used to grip wires or cables involves wrapping the wire around some sort of post. In one method the wire was wrapped around a curved capstand [4], while another method used a bollard style grip, basically wrapping the wire around a cylindrical post [5].

When looking at existing alignment methods, the main sources found were journal articles. Many articles accomplished the alignment using a V-groove as was mentioned in the previous paragraph [6]. Other methods involved constraining all but one degree of freedom, which was left unconstrained for self alignment. An example of this is a device used to align an optical fiber using a ball that is clamped but still allowed to rotate [7].

3.2 Data sensitivity/resolution

Another difficulty that our group faced was to allow a large range of materials to be tested while also maintaining a reasonable amount of resolution for our data.

When looking for methods of measuring small forces with high resolutions, we first looked at different off-the-shelf options. During this research, we followed calculation that were recommended by Interface Force [8], a load cell company, and determined that an off-the-shelf sensor would meet our needs for the tension load. We also had conversations with different sales engineers and technical support assistants from various torsion load transducer companies and from these conversations, determined that our torsion resolution could not be obtained using an off-the-shelf option [9]. Therefore, our team had to create a new method for measuring these forces. One possible method for this measurement was to use a diaphragm in order to convert the force into a deflection (or strain) and then measure that deflection. The team researched many different methods for measuring that deflection including strain gages and capacitance probes [10]. In addition to researching methods for measuring these deflections, we also researched methods for manufacturing a diaphragm. These methods include using photo/chemical etching [11] or using wire EDM [12].

4. CUSTOMER REQUIREMENTS & ENGINEERING SPECIFICATIONS

There are a number of design requirements for the tensile-torsion testing device to function correctly and so that it yields viable results. Through talking with Professor Daly, we have identified the following as the most critical criteria for success:

- Micro-wire grips do not slip
- Wire and grip alignment maintained throughout test
- High testing resolution
- Fits under a SZX16 Olympus Stereo microscope
- Programmable load path
- Stable

Here “stable” is defined as the device rests securely on a tabletop without being prone to tipping or shaking. The above criteria are mandatory and must be incorporated into our design.

To determine the engineering specifications, we examined the customer requirements and generated a list of what specifications those would depend on. Over a couple meetings with Professor Daly, we were able to create a “wish list” of target values. We also had to derive some target values through calculations and research. Maximum tensile and torsion loads needed to test micro-wires of diameters 10 to 200 μm were calculated for a number of materials that Professor Daly expressed interest in testing. Equations used in calculating the loads, tabulated loads for seven materials, and a plot of load versus micro-wire diameter can be found in Appendix B. The top six engineering specifications and their target or limit value are shown in Table 2 on the next page.

Table 2. Top Six Critical Engineering Specifications and their Target or Limit Value

Critical Engineering Specifications	Target/Limit Value [13]
Gauge length	1–75 mm
Gripping force	175 N
Gripping friction coefficient	0.25
Alignment tolerance	0.5 °
Tension Resolution (50 pts)	4.98(10 ⁻⁴) N
Torsion Resolution (50 pts at 5 mm)	2.49(10 ⁻⁹) N*m

Here “gripping force” refers to the axial force applied to the wire by the grips so that slippage does not occur, i.e. the clamping force. This works in conjunction with the “gripping friction coefficient”. A more detailed summary of the relations between the design requirements and engineering specifications can be found in the QFD chart located in Appendix A. As can be seen by the specifications, the most critical requirements and specifications pertain to the micro-wire grips and sensors. The security of the grips, their alignment relative to each other, and sensing will determine the accuracy of the test data. A justification for each target or limit value is given in Appendix C.

5. PROBLEM DECOMPOSITION

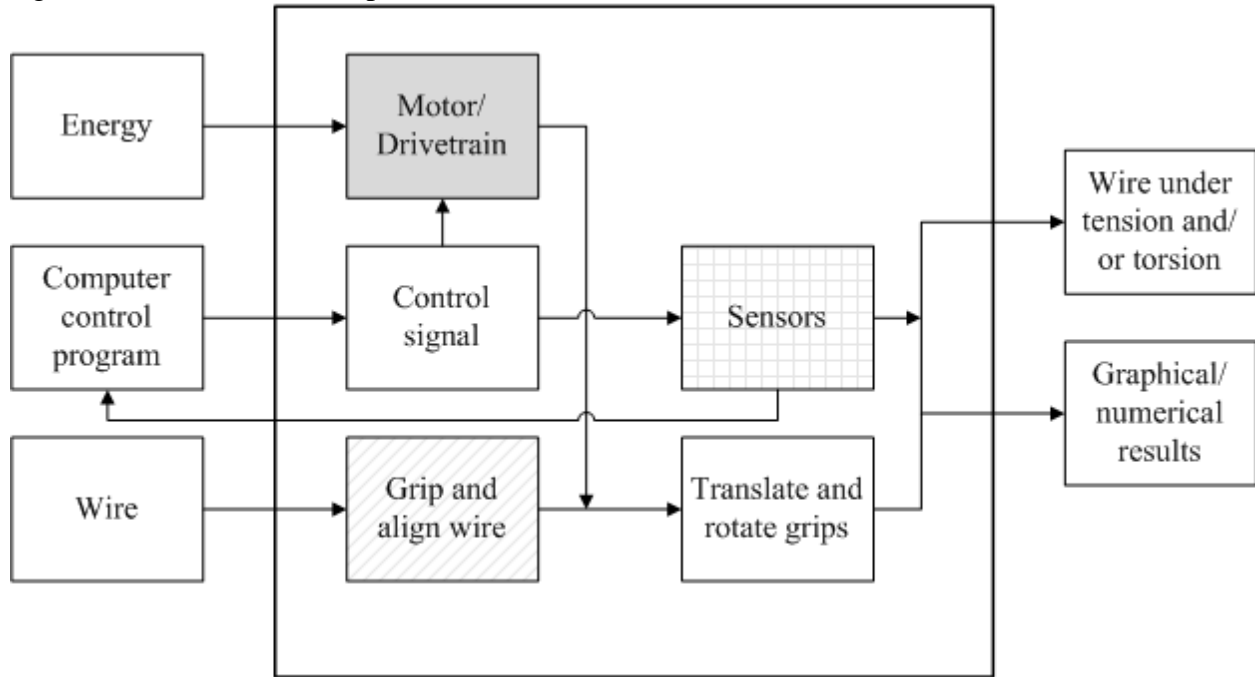
After meeting several times with our sponsor, generating a QFD, and brainstorming, the main design problems became clear. We first identified our strategies for putting the wire under tension and torsion. For our application, the only strategy for accomplishing this is by pulling and twisting the wire, exactly like tension-torsion tests on bars. We then generated a simple functional diagram, see Figure 2 on the next page, to show how our team decomposed the problem and focused our efforts on three modules: gripping, alignment (both through the grips and drivetrain), and sensing.

For our device, a human will load the wire into the grips and then go to a computer to begin the test using a program such as LabView. Once the human starts the test, energy travels to the motor and drivetrain. Together, the control signal, grips, and motor/drivetrain translate and rotate the grips. Therefore, the wire is under tension and/or torsion. The sensors also begin taking data when the test starts. The sensors send the recorded data back to the computer control program and the user sees graphical and numerical results on the screen.

One of the most challenging problems was that of gripping and aligning the wires, as shown in the *striped box* in Figure 2. The main reasons why gripping is such a problem are: the small surface area with which to grip the wire, many different wire material properties, and feasibility/manufacturability of the gripping mechanism. Our team had many brainstorming sessions only related to gripping and many of our concepts incorporated some sort of grip design. The main reason why aligning the wire is problematic is that if the wire were to be misaligned by only a few degrees, the results could be severely skewed. Alignment is closely related to gripping because, first, the grips themselves must be aligned, and, second, the way the grips hold onto the wire must maintain wire alignment. We must keep our inclusion angle to below 0.5°.

See Appendix A for our QFD with values of grip force, coefficient of friction, and tolerance angle.

Figure 2. Functional Decomposition of a Miniaturized Tension-Torsion Device



Another difficult aspect of our tension-torsion device is the sensors, shown in the *checkered box*, which will measure force, torsion load, linear displacement, and angular displacement. These must not only have a wide range, but also a high resolution. Our team has used off-the-shelf devices as much as possible, but through calculations (see Table 2 for the sensing resolution), we knew that some unique methods for sensing must be developed. Specifically, the torsion load measurement is one of our major challenges. The smallest torsion load we need to measure is $1.24(10^{-7})$ N*m, but to obtain the 50 points of resolution requested, the device will need to measure torsion loads as small as $2.49(10^{-9})$ N*m. Therefore, the torsion loads must be amplified in some way; this topic is discussed more in Section 10.3.3. In general, sensors that will measure variables on such a small scale are nearly impossible to find. With the help of our professors, we have devised a new way to measure these small-scale variables while maintaining accuracy and precision.

The motor and drivetrain, shown in the *gray box*, also require consideration because they are important to alignment. Since, the drivetrain will be translating and rotating the grips, it is essential that the methods through which we translate and rotate maintain wire alignment. If misalignment occurs, the results could be useless. Our initial concepts for all three modules are presented in Section 7 with our final concept shown in Section 10.

6. BRAINSTORMING & CONCEPT GENERATION PROCESS

Our initial brainstorming began during our preparation for the first design review. However, our brainstorming was not structured, just more of jotting down ideas as they came to mind. From those base ideas, we obtained the rough concepts for our first design review. After that, our

group took the Friday (9/26) and Saturday (9/27) following the review to come up with individual concepts on any of the main areas of focus. These areas include grips, alignment, sensors, and overall design. We wanted to give ourselves at least a few days for broad concept generation in order to generate as creative concepts as possible. Then our group met on that Sunday (9/28) in order to present our individual ideas, and to try to fully understand the ideas of others. We tried to keep criticism to a minimum and instead of immediately tagging an idea as impossible, we thought about how we could alter the idea or how we could use a similar mechanism in a way that was more plausible. We also spent about half an hour at our meeting going through a group brainstorming session and then reviewing those ideas. We found that once one person came up with an idea, it was easy to improve upon that idea until we came up with a much more developed and appropriate design.

We spent the next three days on focused brainstorming. Once again we worked separately on concept generation and then each evening we would meet for about an hour to review these concepts, improve upon them, and brainstorm as a group. We spent a day each on the areas of gripping, alignment, and sensors. In reality, our brainstorming and concept generation process was not confined to a certain time period. After doing some calculations and initial research into available torsion load sensors, our team soon realized that it would be extremely difficult to measure the torsion load variable and began to focus more of our efforts on this. The measurement for torsion load has required our team to revise our concepts or start over at the brainstorming phase. For example, at the end of our focused brainstorming session, we had the benefit of meeting with a professor at the university, Professor Awtar, who specializes in precision motion systems at small scale. When we met with him, we presented our basic problem specifications and our concept ideas up to this point, and then he recommended alterations to our gripping and alignments ideas. Over multiple meetings with Professors Awtar, Hart, and Daly, they were also able to help us generate some concepts for sensing the incredibly small torsion loads. The initial idea, which came from Professor Awtar, was to use very thin diaphragms with small strain gauges; however, after doing initial mathematical and FEA analysis for the diaphragm, we realized that there was not enough strain in the material to be measured by strain gauges. We then met with our professors to revise the concept and began looking into capacitance probes. The idea morphed into a thin flexure that will have an amplification bar attached to its center. The flexure will deflect when subjected to a force and capacitance probes will measure the displacement of the wings. More about the flexure is discussed in Section 10.3.3. Our initial concepts for each module (gripping, alignment, and sensing) are presented in the next section with our final design in Section 10.1.

7. CONCEPTS

After a lot of brainstorming, our team drew up some of our concepts for our three major modules: gripping, alignment, and sensing. Here we present three of our top concepts for gripping and alignment, and talk about the options for sensors, including our diaphragm.

7.1 Gripping

Figure 3 - Compressive Sleeve Design

This concept is centered around the ability to create a uniform pressure on the wire preventing the creation of stress concentrations. Two rubber or epoxy halves are put over the wire and then

placed inside the compression sleeve. This sleeve constricts as the screw is tightened around the inserts. The compression sleeve does not have a constant diameter; it is thicker at one end. This creates an increased force at the end of the wire when the screw is tightened.

Figure 3. Compression Sleeve Gripping Concept

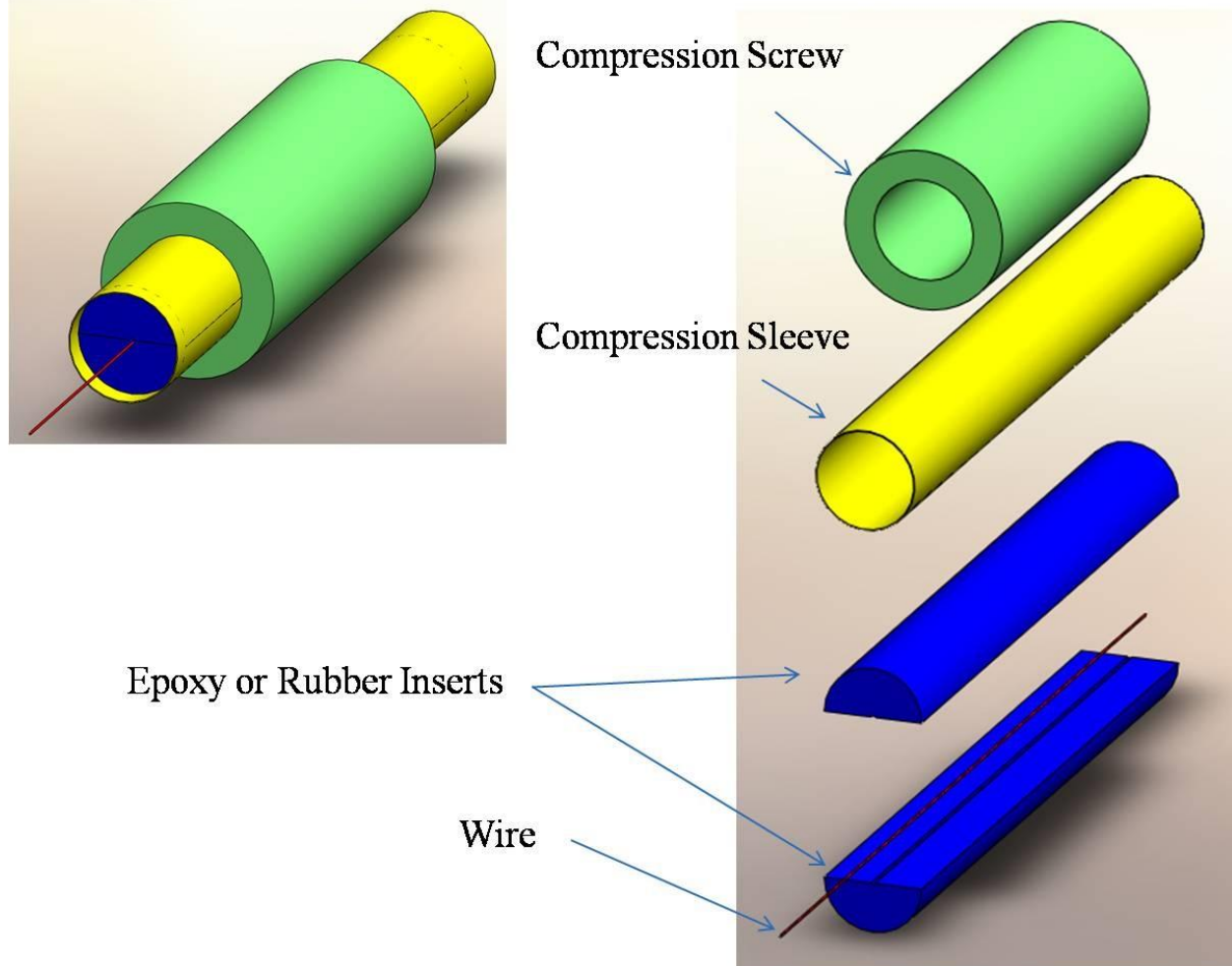


Figure 4 - Rubber or Soft Metal Clamp with Post

For the soft metal gripping concept, shown on the next page, alignment is achieved by wrapping the micro-wire around a post behind the clamping mechanism and gluing it in place. The wire is held in place during testing by two rubber or soft metal plates. The number of retention mechanisms in this design may be excessive. Both the post and soft grips were proven to independently hold the wire in baseline testing.

Figure 5 - V-Groove Clamp

For this concept, found on the next page, alignment is achieved by placing the micro-wire in an etched v-groove. The wire is held in place by a metal plate bolted down on top of it. The need to manufacture grips with different sized v-grooves is avoided by machining out the middle for a flat interface with the plate. While this gripping concept would be simple to use, it has two major drawbacks. First, the metal clamping plate design would introduce a stress concentration at the edges. Second, the geometry limits how short the testing length of the wire can be.

Additional designs for gripping, including the “Disposable V-Groove Tray with Epoxy” and “Epoxy Only” designs, are included in Appendix D.

Figure 4. Rubber or Soft Metal Clamp with Post Gripping Concept

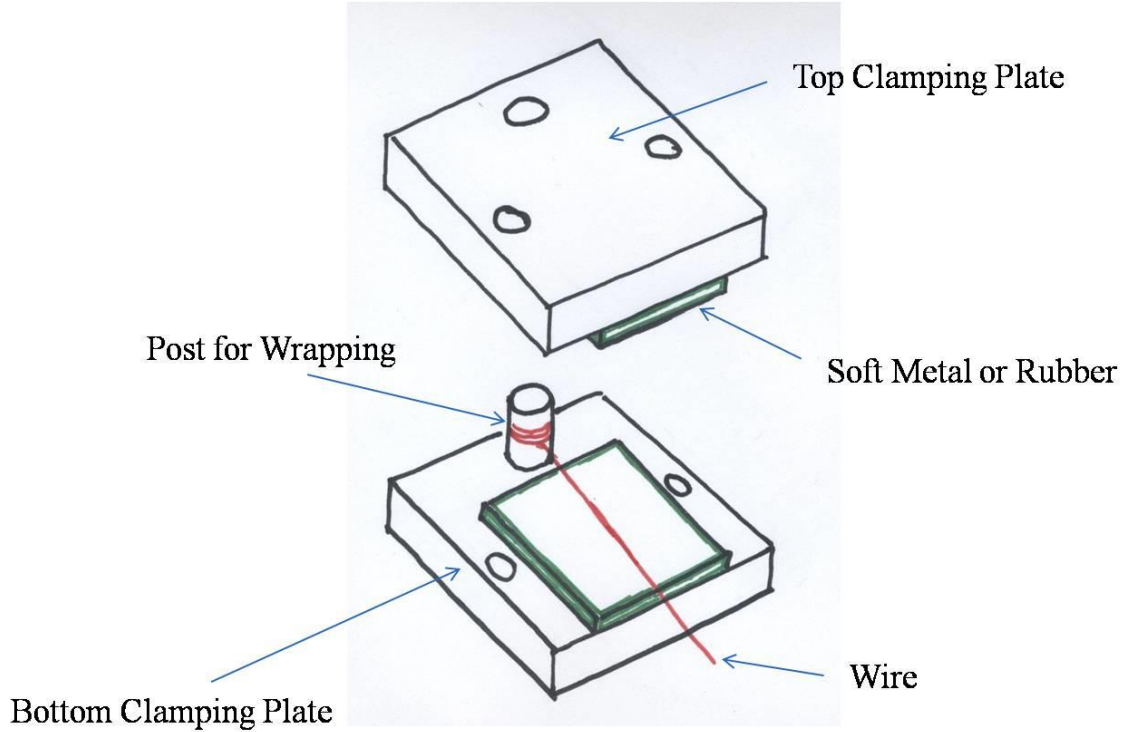
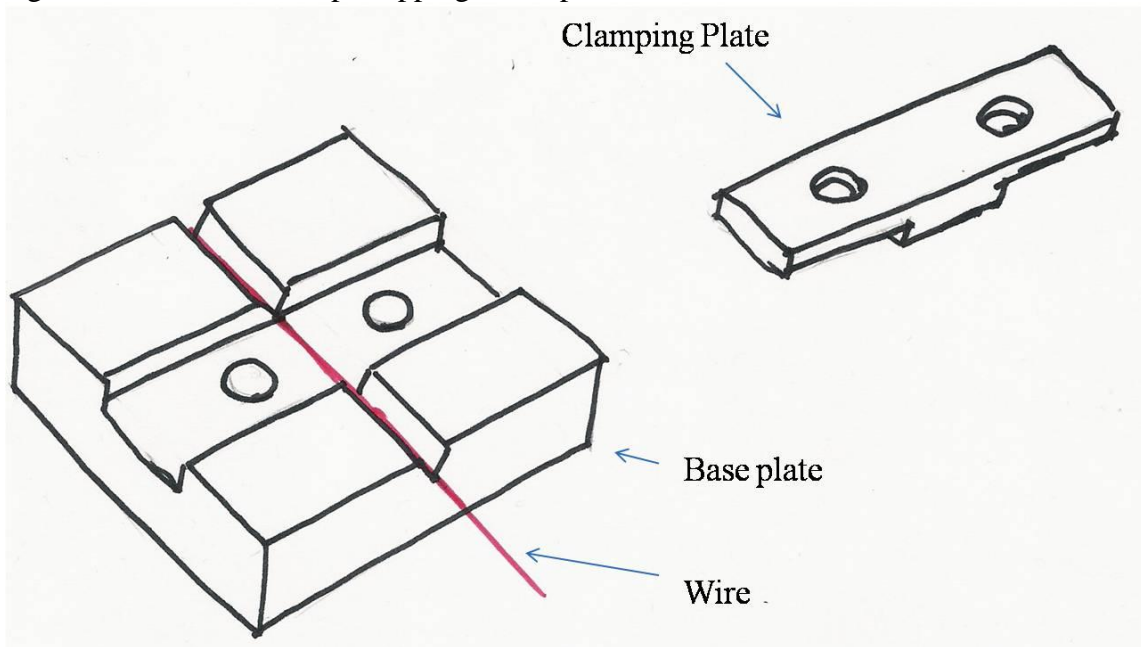


Figure 5. V-Groove Clamp Gripping Concept



7.2 Alignment

Micrometer

In order to initially align the wires in either the horizontal or vertical plane, one of our ideas was to use a micrometer. The micrometer would be a very precise way to move the grips into the correct position. We would have to use another mechanism along with the micrometer in order to determine the correct position for the grips to ensure wire alignment. Another possibility was to use a laser along with the micrometer and to manually move the grip using the micrometer until the laser indicates that the wire is aligned.

Figure 6 - Cylindrical Joint

For this concept, alignment is achieved by allowing the wire holder to pivot about one axis. Figure 6 shows the micro-wire glued into a v-groove on the holder. Alternatively, the holder could have a spindle or small clamping mechanism. The cylindrical holder fits down into the fixture and rotates freely. The grip at the other end of the wire could be rotated ninety degrees to further improve alignment. However, considering the small loads being tested, there is no guarantee that the force from misalignment would be enough to rotate the holder.

Figure 6. Cylindrical Joint Alignment Concept

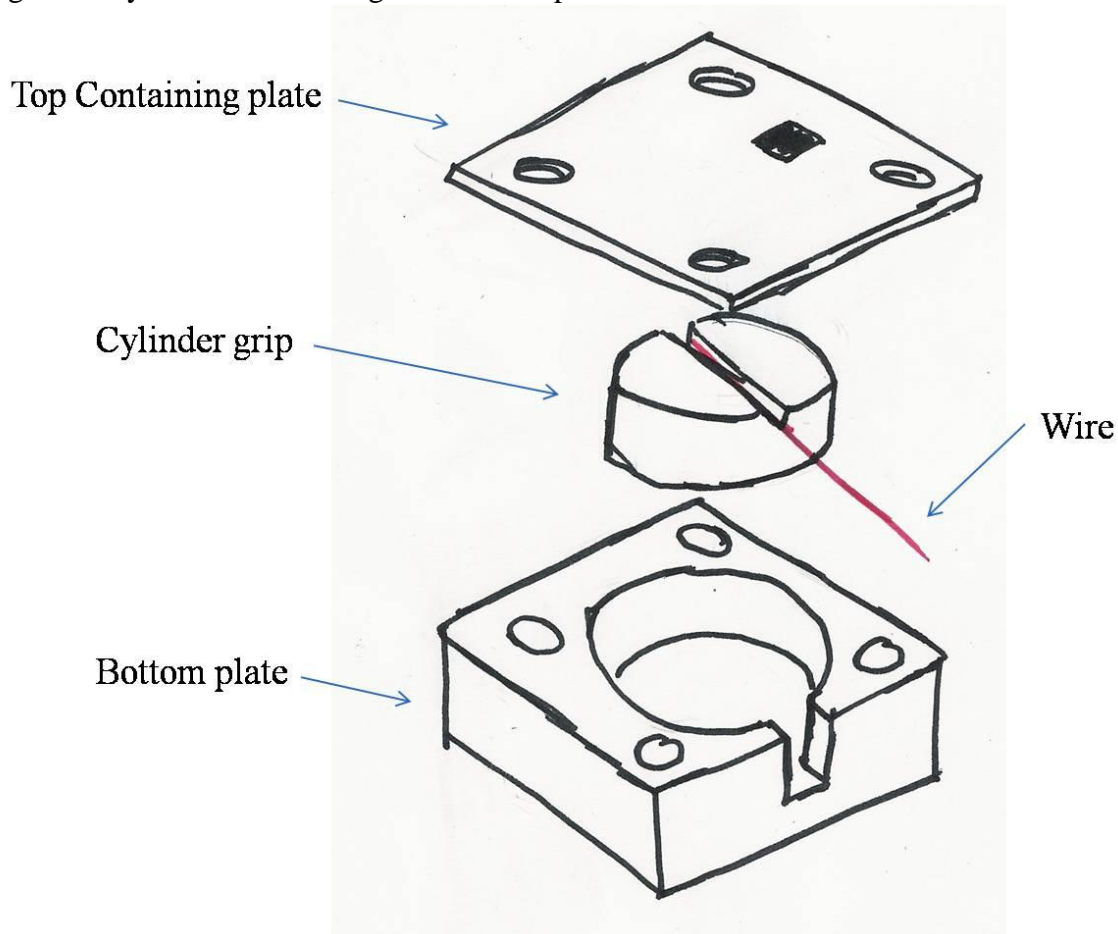


Figure 7 - Thrust Bearing Clamp

Alignment is achieved in this concept shown below by clamping the micro-wire between two thrust bearings and allowing the wire to align itself about one axis. The gripping mechanism employed would introduce a stress concentration on the wire. Our team considers this our “wacky” concept because while it may work for alignment, there are a few disadvantages once thought through in depth, such as the stress concentration and the possibility that the wire force would not be strong enough to actually turn the bearings.

Figure 7. Thrust Bearing Clamp Alignment Concept

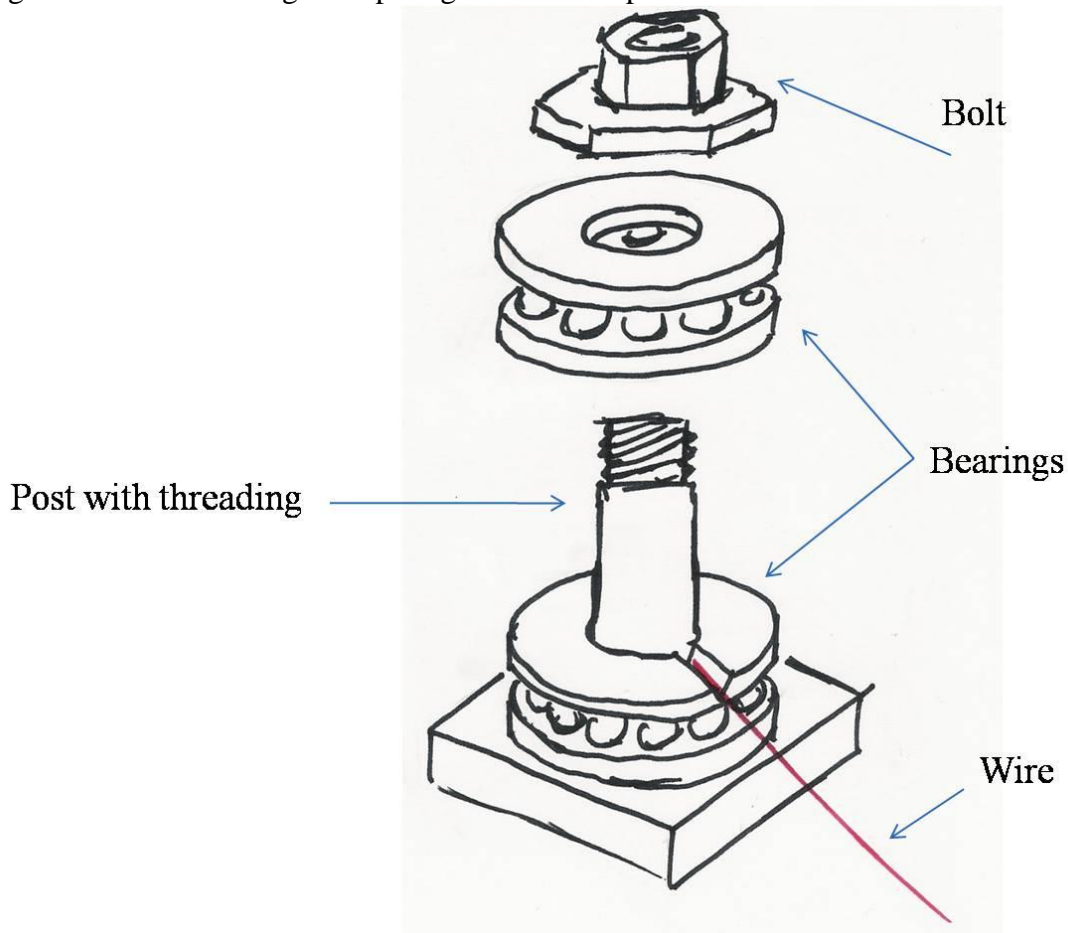
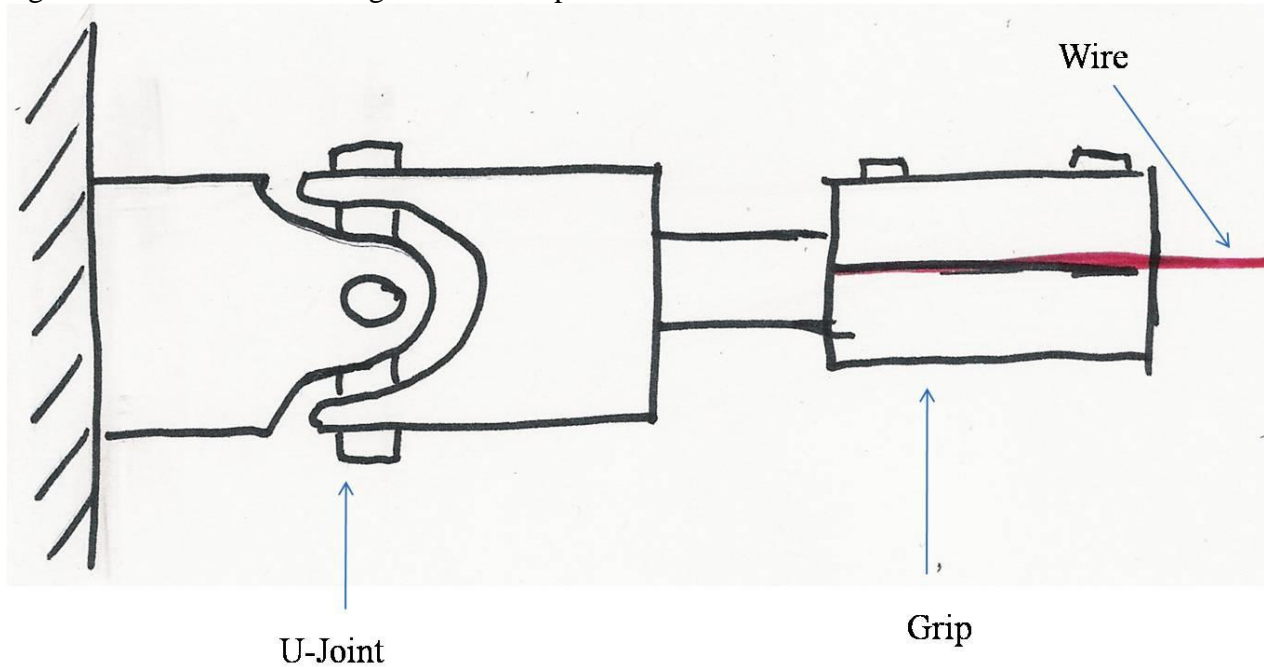


Figure 8 - Universal Joint

With the Universal Joint, found on the next page, alignment is achieved by attaching the grips to a universal joint. Universal joints are commonly used in applications involving misaligned rotating parts. The greatest flaw in this concept is the weight of the joint. The micro-wires are not strong enough to support the weight of the joints and grips in tension.

An additional design, a “Spool”, for alignment is included in Appendix D.

Figure 8. Universal Joint Alignment Concept



7.3 Sensing

When we began this project, our group assumed that the gripping and alignment would be the most difficult to achieve. After working on concept generation and some initial analysis, we have determined that instead, the most difficult and most necessary to our design is the sensor module.

7.3.1 Displacement Sensors

The displacement sensors are not a big concern for this project; see Section 10.3.1. For displacement we are considering different off-the-shelf options such as Linear Variable Differential Transducers (LVDT) and optical (both rotary and linear) encoders.

7.3.2 Torsion Load and Force Sensors

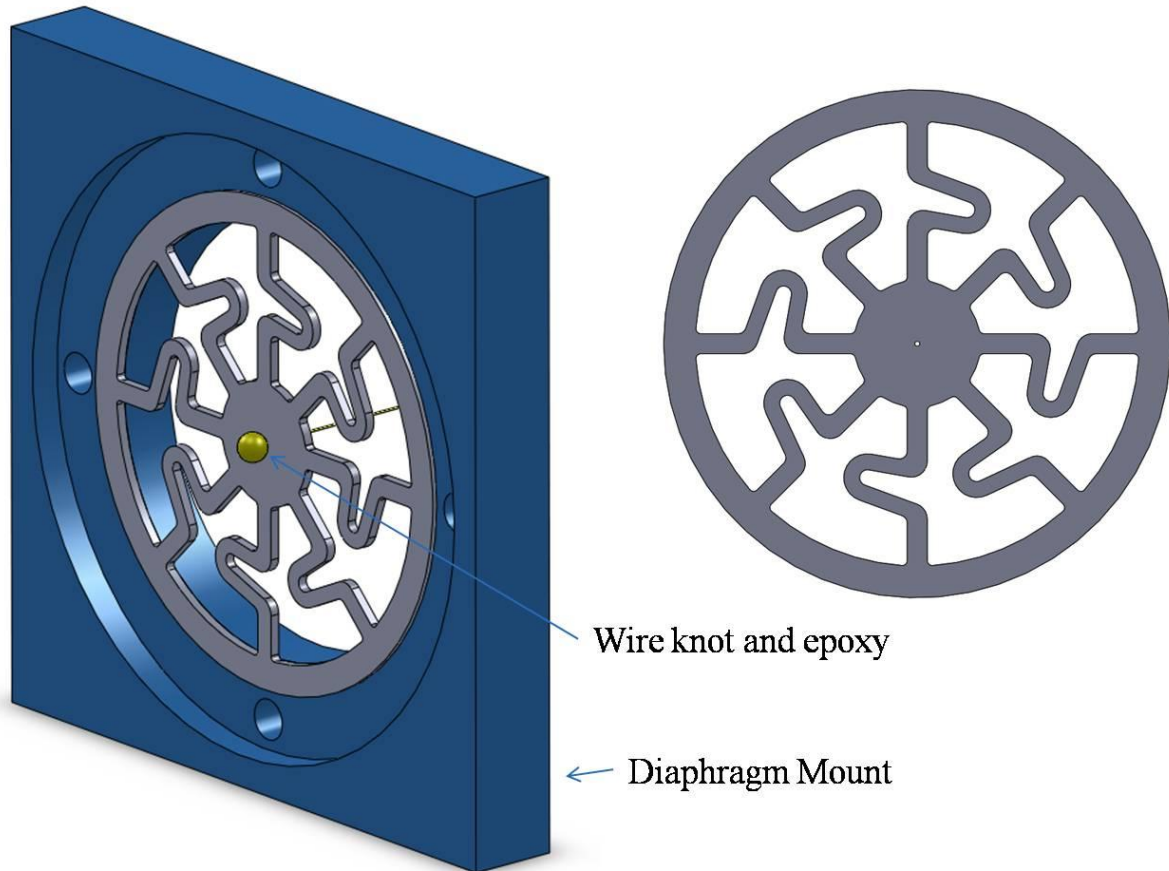
The big challenge is the ability to measure the wide range of loads required for our project with a high resolution. Also, some of our loads are quite small; our smallest torsion loads are on the order of 10^{-9} N*m and our tension loads are on the order of 10^{-4} N. Torsional and tensile loads this small are difficult to measure while still maintaining a reasonable resolution. After doing calculations and research, we found that the force sensor to measure the tensile load can be purchased off-the-shelf. The data acquisition system in the lab has enough resolution (24 bit) to measure the loads read by the load cell with a very high precision. However, the torsion load cannot be measured with any sensor already in existence. We have to find a new way to measure this. The most promising idea, explained below, was a diaphragm with strain gauges attached. Professor Awtar met with us and helped us generate this concept.

Figure 9 - Diaphragm with Strain Gauges

The diaphragm uses strain gages placed radially in order to measure the tension load and tangentially in order to measure the torsion load. It would be necessary to etch out a design on the torsion diaphragm in order to measure the smaller loads. The benefit of this concept is that, with sensitive enough strain gauges, it would most likely allow us to measure our small torsion

and tension loads with high resolution. We came up with an initial concept for attaching the wire to the diaphragm. The user would thread the wire through the small hole in the center of the diaphragm and then tie a knot in the wire. Then glue would be spread around the knot to make a ball, and this ball would also be glued to the back of the diaphragm in order to prevent the end of the wire from spinning during torsion.

Figure 9. Diaphragm Force Sensing Concept



8. CONCEPT SELECTION PROCESS

When going through the process of choosing the top designs from our concepts, our group created concept selection matrices. We approached this process by looking at the concepts from each of the modules (gripping, alignment, and sensors) individually. We felt that it would be a good start to first look at the best from each area and then try to combine these into one workable design. When creating these matrices, we used a generic datum, where '+' indicated that the concept met the specifications well, a '0' indicated that the concept somewhat met the specifications, and a '-' indicated that the concept did not meet the specifications. We also compared the devices used by Fleck and Hutchinson [1] using this datum in our matrices. When choosing the selection criteria for these matrices, our group looked at the different customer specifications, and used the ones that were most relevant for the specific module. We felt that only choosing the most relevant specifications would give us a better idea of the quality of our idea, rather than trying to figure out how our concept might distantly relate. Our top concepts for

gripping are the compression sleeve and rubber or soft metal clamp with post; the micrometer and cylindrical joint for alignment, and the diaphragm for sensing.

8.1 Gripping

When considering the gripping mechanism, the most important characteristic was making sure the device would actually function and hold the wire without slipping. Due to this basic necessity, some of our designs were flawed based on the preliminary analysis we performed and described in Section 9. Many of our concepts were either altered or eliminated after the conclusion that the epoxy would not have a high enough shear strength to hold the wire. Also, some of our concepts were ruled out because of excessive cost. In one of our ideas we considered using disposable trays with a v-groove etched onto them; however, we found that laser or chemical etching was not affordable when done in bulk. Table 3 below shows the selection matrix for our top four gripping concepts as of Design Review 2, which leaves out some of these flawed concepts, while the entire matrix can be found in Appendix E.

Table 3. Concept Selection Matrix with Top Ranked Designs for Gripping

Selection Criteria	Concepts				
	Fleck and Hutchinson	Compressive Sleeve	Rubber Clamp w/Post	Glued Knot	V-Groove Clamp
Grips wires without slipping	0	+	+	0	0
Consistent alignment	-	0	-	0	+
Cost	0	0	0	+	0
Tests wide range of materials	0	+	+	0	-
Ease of use	0	-	-	0	+
Stress Concentrations	0	+	+	-	-
Sum +'s	0	3	3	1	2
Sum 0's	5	2	1	4	2
Sum -'s	1	1	2	1	2
Net Score	-1	2	1	0	0
Rank	N/A	1	2	3 (tie)	3 (tie)
Continue?	N/A	Yes	Yes	Yes	No

Looking at the concept matrices, our top two concepts were our compressive sleeve and our rubber or soft metal clamp with post for wrapping. Both of these designs had the benefit of being able to test a wide range of materials by using the softer material to encase the wire, instead of a machined material, where you would have to etch different V-grooves for different diameter wires. Also, both of these designs eliminated the use of epoxy. When considering designs with epoxy, we realized that the part on which epoxy was applied would have to be disposable. Therefore, when we eliminated the use of epoxy, we reduced the number of disposable parts needed and reduced the cost. A final advantage that these two concepts have in common is that they use a softer material and offer lower stress concentrations than just using a hard metal clamp.

The major downfall to the compressive sleeve and our rubber or soft metal clamp ideas is that they are not as easy to use as some of our other designs. For the compressive sleeve design, the user would have to somehow feed two half cylinders into the sleeve while maintaining wire alignment between two smooth surfaces. For the rubber clamp with post, the user would have to manually wrap the wire around the post. An additional downfall to the rubber clamp with post idea is that wrapping the wire would cause some material waste, and the wire at such small diameters is quite expensive. To reduce excessive costs in this design, the user would have to limit the number of wrappings used.

One of our other considered concepts was glue around a knot in the wire, which we came up with to use with the initial diaphragm idea for sensing the loads, explained in Section 7.3.2 This is because the design of the diaphragms did not allow for the use of a bulky grip like those that we had previously come up with. This idea would have been inexpensive; however, it would have been difficult to keep the wire aligned perfectly and find enough surface area to transfer the torque load with a reasonable shear at the wire-diaphragm interface. Additionally, there was the possibility of high stress concentrations with the use of the knot.

The final concept found in the matrix above is a simple V-groove clamp. This concept has the benefit of being easy to use and would also allow the user to consistently align the wire in the grip. The downfalls to this idea are that it would require different sized V-grooves for different diameter wires, and depending on the range of diameters a V-groove could cover, this could lead to higher costs. Our group is also worried about having high stress concentrations at the edge of this grip on the wire.

8.2 Alignment

We had three top ranked alignment concepts: the micrometer, the cylindrical joint, and the spool. This is shown in the top ranked concept selection matrix on Table 4 on the next page, while the entire matrix can be found in Appendix E. These ideas are different in the way they are used for alignment. The micrometer would be a way to mechanically align the system before the test, while the cylindrical joint (also called “cylinder in casing”) would be used to maintain alignment during the test in two planes. The spool design would have the wire wound around two posts. The benefits to the micrometer are that it is easy to use and also would allow precise alignment. The drawbacks are that it is a manual operation and it would only initially align the wire. The main benefit to the cylinder in casing is that it would maintain alignment during the test. A drawback to this concept, however, is that it might be difficult to ensure that the cylinder can spin freely in the casing, which could cause issues with its ability to maintain proper alignment. To reduce the possibility of this issue, we could use grease on the bottom of the cylinder. Finally, the spool design would constantly align the wire in one plane with the wire constrained vertically by a groove cut into the post.

Other designs that we considered were a universal joint, a laser, and a thrust bearing design. We decided to rule out the universal joint idea (Section 7.2) when we realized that the weight of the joint would pull down on the wire, causing our device to not function correctly. Another idea was to use a laser to determine whether or not the system was actually aligned, however this idea is not being strongly considered because of the difficulty of aligning the laser directly on the axis

of the wire. An additional idea using two thrust bearings (Section 7.2) was ruled out because we were concerned it would stress the wire.

Table 4. Concept Selection Matrix with Top Ranked Designs for Alignment

Selection Criteria	Concepts			
	Fleck and Hutchinson	Micrometer	Cylindrical Joint	Spool
Resists buckling	0	0	0	0
Maintains alignment	0	0	+	0
Cost	0	0	0	+
Ease of use	0	+	0	0
Sum +'s	0	1	1	1
Sum 0's	4	3	3	3
Sum -'s	0	0	0	0
Net Score	0	1	1	1
Rank	N/A	1 (tie)	1 (tie)	1 (tie)
Continue?	N/A	Yes	Yes	Yes

8.3 Sensors

When looking over the different sensor options for our project, we also completed concept selection matrices. For the sensors, some of the designs were our original concepts, but some were already existent methods for measuring force or displacement. The selection process for our sensors was more straightforward than for the gripping and alignment. Therefore, the process will be described here in the text and the selection matrices can be found in Appendix E.

For the displacement sensors, our top design choice is an optical encoder. We are considering using an encoder because it is a high resolution device and could allow us to measure the entire range of materials requested by Professor Daly. The major drawback to using an optical encoder is that they can have a high cost, depending on the resolution desired. We also looked at Linear Variable Differential Transducers (LVDT), but we could not find one with the entire range that our project requires and, therefore, did not focus much further on these devices. We were able to find some with a lower range, for example from 0.5 – 2.5 millimeters (mm), and also some with a higher range, about 4–38 mm, but we were unable to find one with a wide enough range to accommodate our needs, which is from about 0.2 – 20 mm. We also compared our ideas to the method used by Fleck and Hutchinson for measuring displacement. Fleck and Hutchinson did not describe how they measured the linear displacement in their tests, but they did describe their method for measuring angular displacement, which was quite tedious. They used needle pointers and a protractor in order to measure these angles. The major drawbacks to this method are that it was not very easy to use and cannot obtain a high testing resolution.

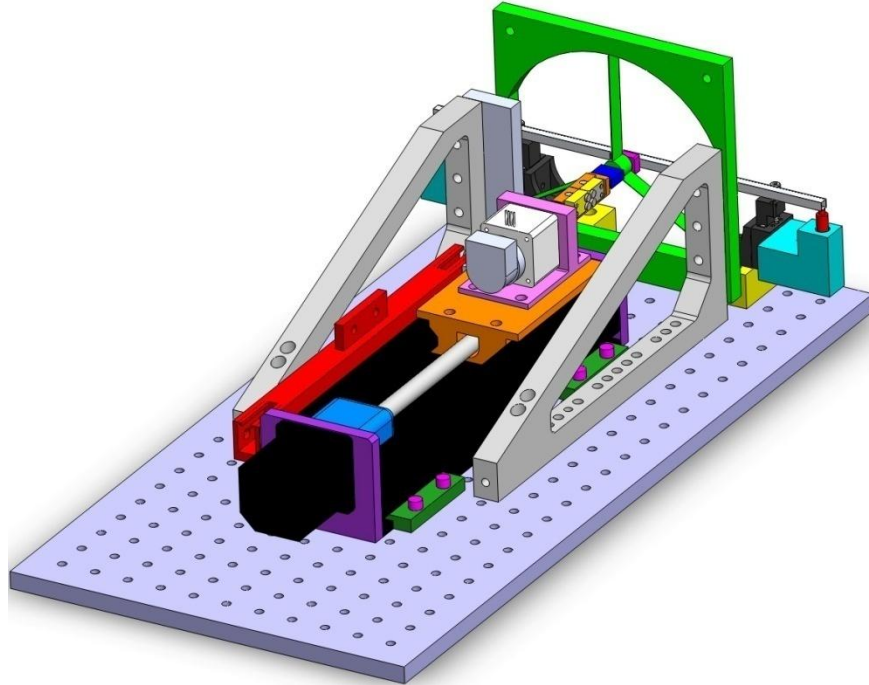
For the force sensors, we will be using a combination of off-the-shelf load cells for the tensile loads and a custom three beam flexure for the torsion load. Early in the project we considered a cantilever beam with strain gages for the tensile measurement. However, such a set up would require extensive calibration and with the data acquisition unit in the lab, the load cells that we

found will work well for the tensile loads in our project. We could not find load cells sensitive enough to handle our torsion loads. Because of this, we have moved towards a custom-made sensor. During our meeting with Professor Awtar, he helped us come up with an idea to use a metal diaphragm with strain gages to measure both the tension and torsion loads. After some analysis we concluded that in order to achieve a diaphragm strain sufficient to measure with a strain gauge, the diaphragm would have to be too thin to mount the gauges on and would deflect to an unacceptable amount under tensile loads. However, this concept led to our current flexure design. Our major concern with this idea remains the resolution at the lowest torsion loads.

8.4 Final Concept Selection

Our final design selection was highly dependent on the ability to measure the torsion loads on the wire. The lack of commercial torsion sensors capable of measuring such small loads dictated that we design our own. Analysis of the original diaphragm concept showed that it would be too flexible in tension and not sensitive enough in torsion. The design then progressed into a three beam flexure that would measure only torsion with a commercial load cell recording the tension load. The sensitivity of the flexure limited the weight that we could attach to it for gripping and alignment. Therefore, using a micrometer to adjust the alignment was ruled out. The cylindrical joint was abandoned because, without testing, we could not confirm how well it would function. Due to the complexity of the flexure design and analysis we opted for simplicity by ordering pre-made parts where we could. The translating grip will be guided by a BiSlide from Velmex which is available with an optical encoder attached. The grip design of a post and clamp was chosen based on our preliminary analysis. The assembled final concept is pictured below in Figure 10.

Figure 10. Final Design Concept



9. PRELIMINARY ANALYSIS

In order to direct our concept selection process toward a workable solution, it was necessary to do some basic analysis of our proposed systems. Our primary areas of concern were the micro-

wire grips, the alignment of the system, sensors, and motion control. The results of our experiments demonstrated that we should use a rubber gripping material or a wrapping technique with super glue. For a 5 mm wire the grips must be aligned within 0.044 mm, the motor needs to control the ball screw in 1.44° increments, and must have a step size of 0.096° for torsion. Optical encoders can be used to measure the angular and linear displacement; however, the torsion and tensile loads are more difficult.

9.1 Gripping

The ability to grip the micro-wire securely is a critical functional capability of the testing device. To ensure that our gripping solution would hold the micro-wire without slipping or damaging the wire, our group conducted some initial analysis and then testing in order to determine the quality of our gripping concepts.

By comparing the maximum loads the various micro-wires can sustain to their surface areas, we found that the shear strength needed at the wire/grip interface ranges from about 630 to 1380 MPa for metals (Appendix B) for a grip length of 25.4 mm. Unfortunately, product research indicates that epoxies offer a shear strength ranging from only about 13.8–34.5 MPa. Due to the high cost of the micro-wire, increasing the grip length to meet the low shear strength of the epoxy is cost prohibitive.

Our calculations led us to the conclusion that relying solely on epoxy to hold the micro-wires is impractical. An adhesive to hold the wire in place during fixturing is useful, but a second retaining method is necessary. The permanent nature of two-part epoxies prompted our group to move to super glue as our new adhesive. While super glue does not offer an advantage in shear strength, it can be removed with acetone and is inexpensive enough to couple with a second gripping method. The results from our bench level tests using super glue and different wrapping and clamping techniques can be found in Table 5 below.

Table 5. Results of Bench Level Experiments

Fixture	Failure Method			Grip Held
	Broke in Grip	Slipped From Grip	Broke at Wire Bend	
Vise	X			
Metal Plates	X			
Post Single Knot		X		
Post Double Knot			X	
Post with Epoxy				X
Flate Plate with Epoxy		X		
Rubber Grips				X

As shown in the table, when the wire was held using stiff objects, such as the vise or two metal plates, the wire broke in the grips. However, when we used a more forgiving material, such as rubber erasers, the grip held. When we wrapped the wire and used a knot to secure it around the post, the wire broke at the knot. However, when we used glue to secure the wrappings, the grip held. From these initial experiments, we have decided to move more towards a rubber material for clamping, super glue for adhesive, a wrapping technique, or any combination of these. For pictures of the bench-level experiments we performed for gripping, see Appendix F.

9.2 Alignment

The required alignment tolerance needed to meet our alignment goal of 0.5° is a trigonometric function of the wire length. For a 5 mm wire the grips must be aligned within 0.044 mm.

$$d = (5\text{mm}) \tan(0.5^\circ)$$

9.3 Sensors

In order to record the experimental data, the test mechanism needs very sensitive sensors with high resolution. Measuring the linear and angular displacements of the grips is relatively straight forward. The angular displacements for the shortest wires are too small to measure with an encoder directly from the grips with any significant resolution. The displacement can therefore be read from the optical encoder on the torsion drive motor. The linear travel can be measured with an encoder with a resolution equal to the drive step or better.

Measuring the tension and torsion loads on the micro-wires is difficult due to the low expected loads. For our smallest wires we hope to achieve a tensile resolution of 25–50 μN . After contacting SMD Sensors [9], we know that this is certainly possible with a load cell, although the load cell would have to be changed for larger wires. The resolution required for torsion loads is $2.4(10^{-9})$ Nm or smaller. There are no existing sensors capable of measuring such small loads directly. We are developing a flexure to measure displacements from the torsion load, which is described more in Section 10.

9.4 Drive Train

Precision in the powered elements of the test mechanism directly affects the quality of any experiments. Since we will be working with extremely small wires, small displacements are significant.

Assuming a 20 percent strain in a 1 mm long wire, the tension motor must be able to pull the grips apart in 4 μm increments to achieve sufficient resolution to plot a stress-strain curve. With our current actuation mechanism choice to use a ball screw with a 1 mm pitch, we will have to control the screw in 1.44° increments or 250 steps per revolution.

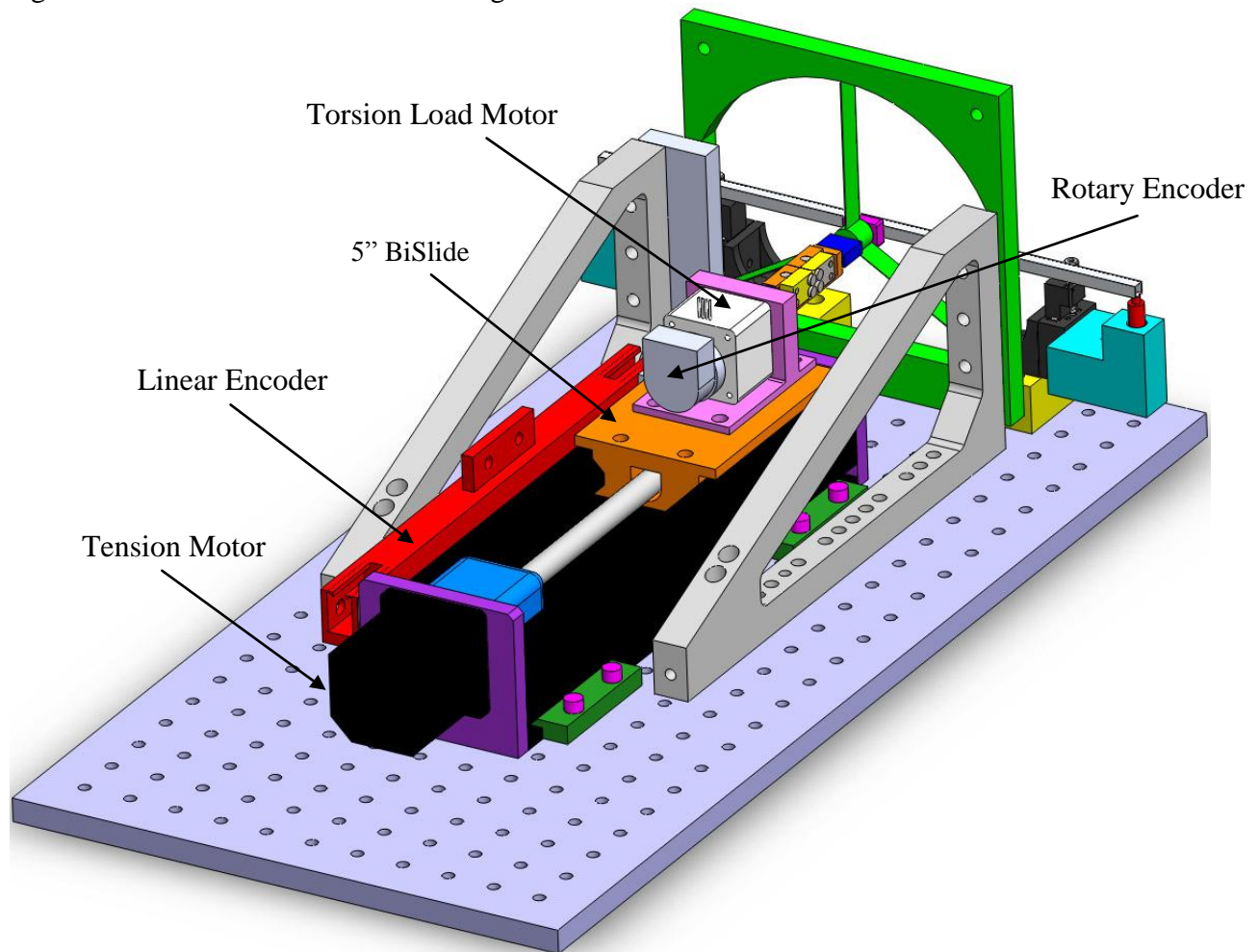
Similarly, our minimum expected angle of failure in torsion for a 1 mm wire is 4.78° . The motor driving the torsion component of the test mechanism will therefore have to be geared down significantly to achieve control in 0.096° steps.

10.FINAL DESIGN & ANALYSIS

10.1 Description of Final Design

The final design for our tension-torsion device is best explained by looking at the individual functions that it must perform. These functions are as follows: translating the tension grip and measuring that translation, rotating the torsion grip and measuring that rotation, measuring both the tension and the torsion forces, and holding the wire sample. Figure 11 on the next page shows the first view of our final design.

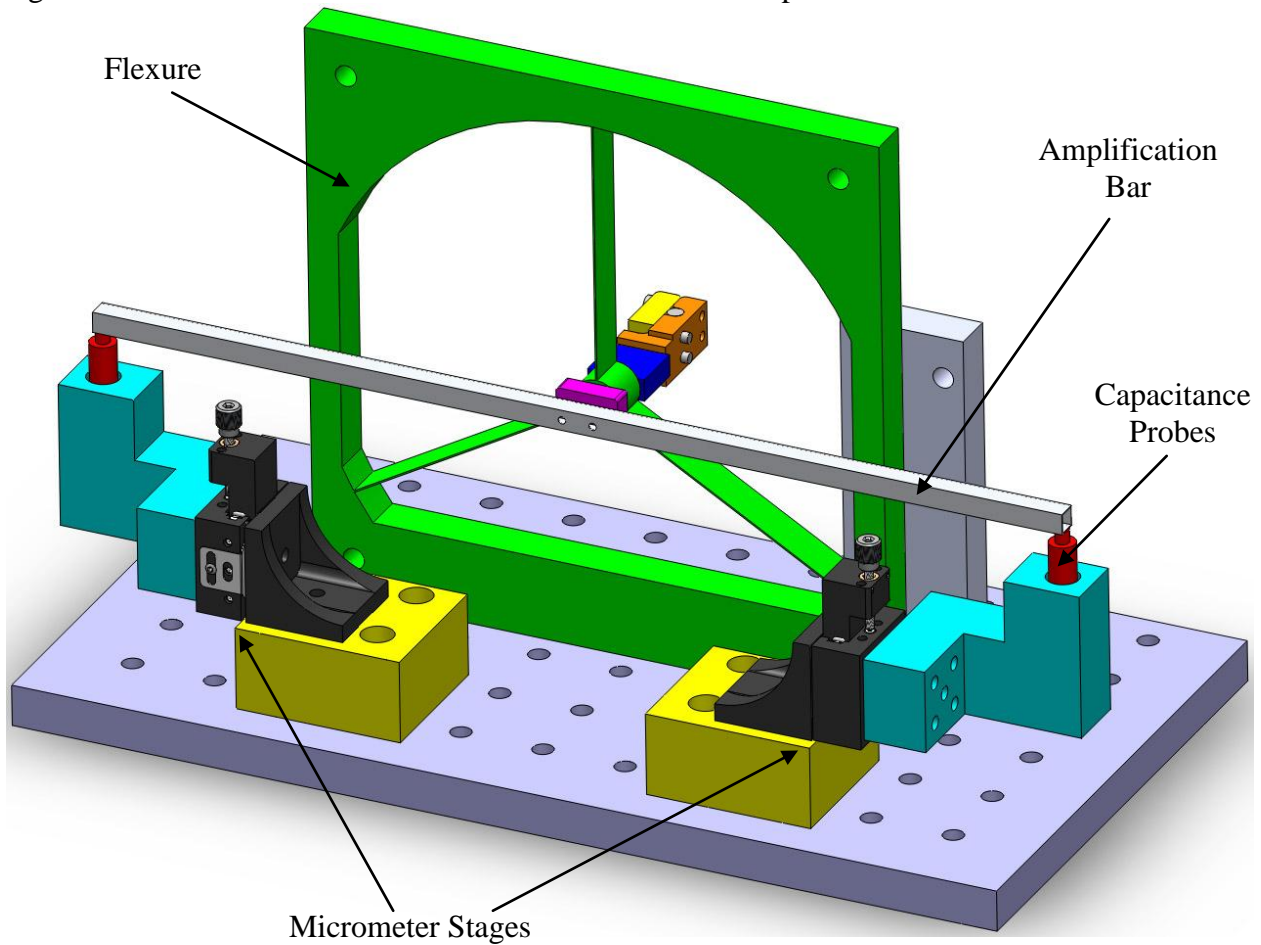
Figure 11. CAD Model of Overall Design



As shown in Figure 11 above, the method used to translate the tension grip is a Velmex BiSlide, which is a combination of a ball screw and a linear guide. The ball screw on the BiSlide is driven using a step motor, which is controlled by a controller with micro-stepping capabilities in order to keep the ball screw from pulling the wire too far with each step and jerking the wire during the test. Attached to the BiSlide is a linear encoder, which is used to measure the translation of the slide. A torsion step motor, which sits on top of the slide, is used to rotate the torsion grip. This motor has an attached damper, which helps reduce the vibrations caused by the motor, and also a rotational encoder, which measures the angular displacement of the torsion grip. In order to interface the two encoders directly to the computer, a PCI quadrature encoder is used. This encoder comes with a LabView driver which will allow us to incorporate the encoder measurements into our LabView program. The base of the system will be an optical breadboard. The reasoning for this is that Professor Daly would like to perform her testing underneath a stereo microscope, as well as on top of an optical table. Using an optical breadboard will allow the user to screw in posts with feet in order to raise the system above the base of the stereo microscope, and also to remove the posts and screw the system directly onto an optical table.

Figure 12 on the next page shows the second view of our overall design, which narrows in on the method used for measuring the torsion force.

Figure 12. CAD Model of Torsion Flexure and Attached Amplification Bar

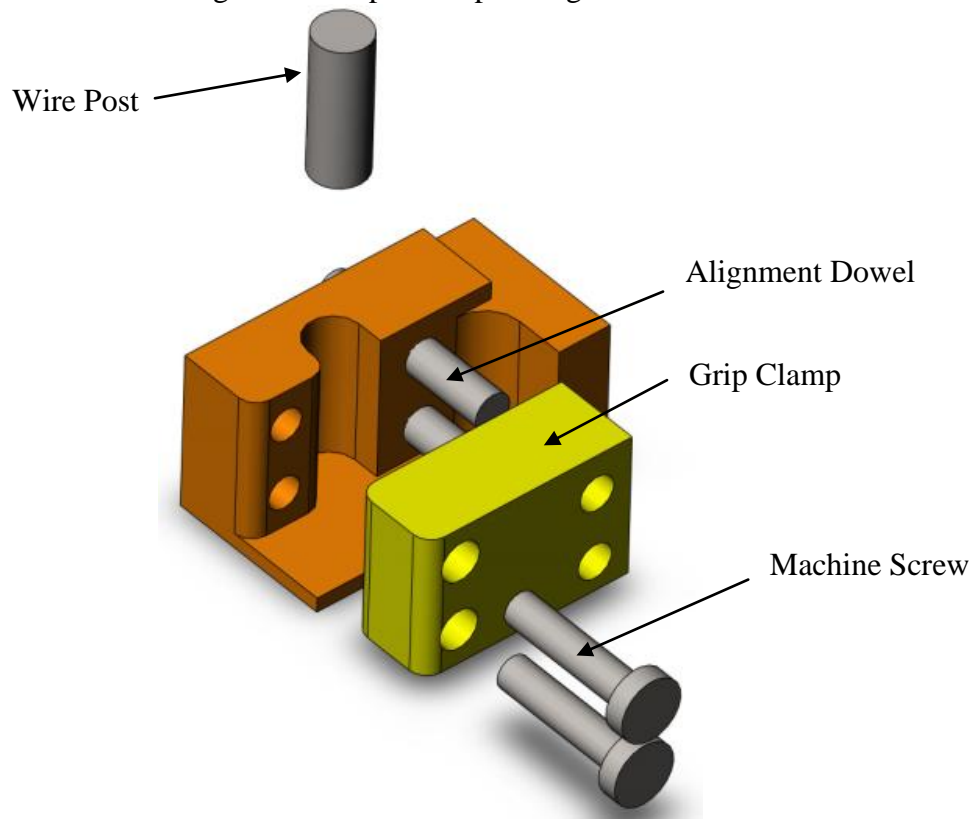


In order to measure the very small torsion loads, our group has decided to use a flexure. This flexure consists of a center which is held up by three cantilever beams. The flexure is made of 6061 Aluminum which allows the beams to bend slightly when the torsion load from the wire is transferred to the center of the flexure. The center of the flexure rotates slightly, and this rotation is then translated into a deflection using the amplification bar as shown in the figure. The deflection of the amplification bar is measured using two capacitance probes. These probes are able to measure small deflections with 1-2 nm or smaller resolution if needed. After the flexure is calibrated, we will be able to convert this deflection into a torsion load. The micrometer stages are attached to the breadboard via machined blocks and brackets. The capacitance probe holders are then attached to the micrometer stages, allowing the probes to translate vertically and to be positioned at a very accurate distance from the amplification bar. A set screw is used to hold the capacitance probes in the holder; however, the probes are first placed in a bronze bushing for protection. A band saw is used to cut the bushing along the long edge to ensure a tight fit.

The micro-wire samples will be held by a custom machined grip which can be aligned for each test. The wire will be wrapped around a dowel pin with a groove cut in it to determine the vertical placement of the wire. The pin will then be placed in the grip, and the grip and clamp will be bolted together. The alignment of the faces of the grips can then be checked and adjusted

by placing a precision drilled alignment plate over the dowels that protrude from the back of the grip. There are two different options for the dowel and alignment plate assembly: 1) a diamond dowel with a round hole machined into the plate or 2) a round dowel with a slot machined in the plate in which the dowel can slide back and forth. The diamond dowels are tough to find and are almost a custom part. Therefore, the round dowels are both more cost effective and easier to obtain, and are included in our current design. If the grip is misaligned, the motor mount plate holding the motor and grip to the rest of the assembly can be loosened and readjusted while the alignment plate is in place. The alignment plate must be removed before the test can be run. Both grips will be press-fit onto pins for mounting to the motor coupling and flexure. The pin on the flexure side will be threaded to connect to the load cell. An exploded view of one grip is shown below in Figure 13.

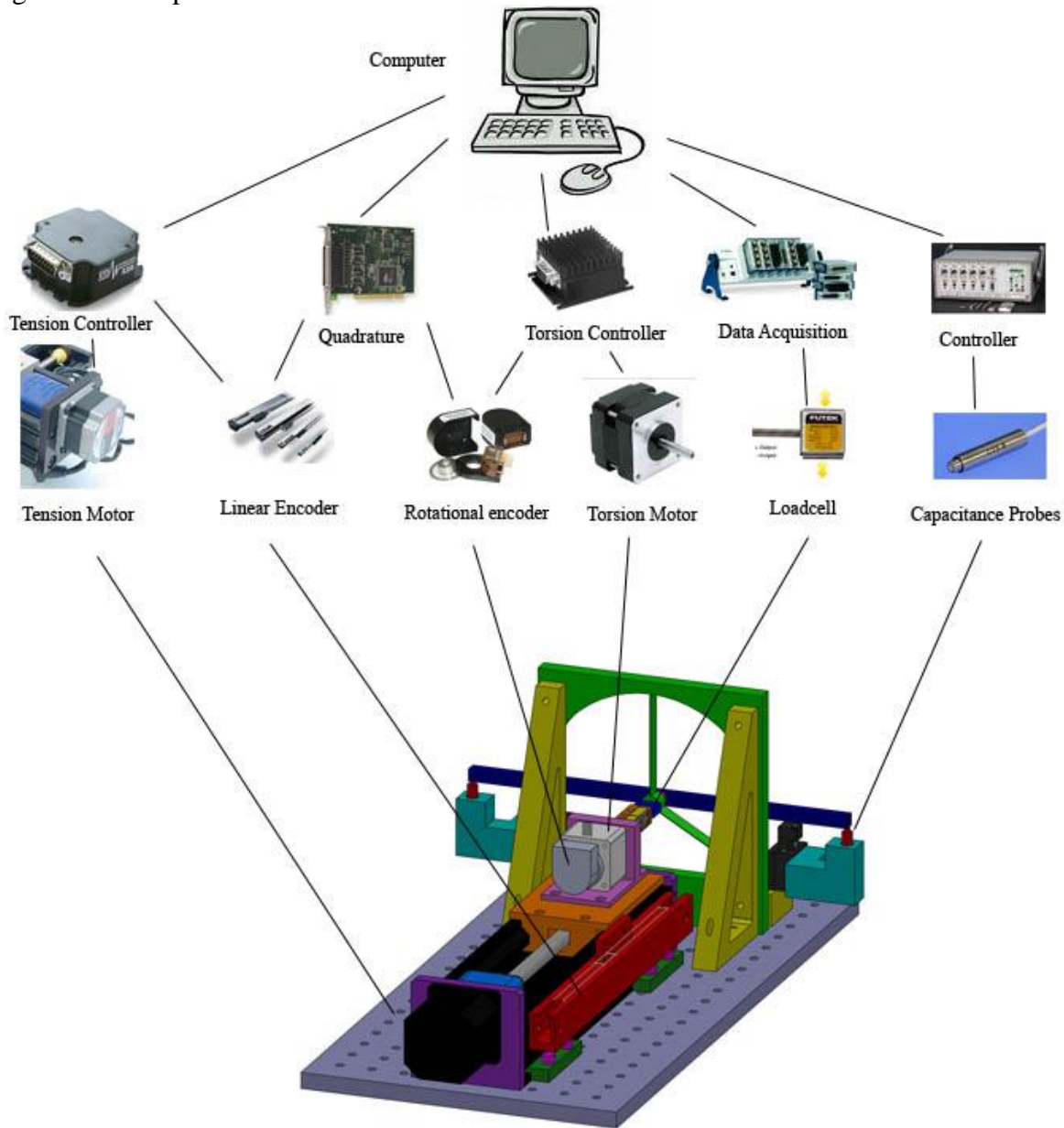
Figure 13. Grip Concept Design



A complete view of the component interaction is outlined on the next page in Figure 14. The computer will first send a signal to the controllers attached to the motors. The controllers control the step size the motors take. Depending on the parameters the user inputs, both or just one motor will activate when the program is told to run. With this, LabView will begin gathering data from the data acquisition systems of the different sensors: the load cell, linear encoder, rotary encoder, and capacitance probes. The program will plot the results in real time and run for a specified time. The data can be saved to a text file for further analysis.

Appendix N gives the engineering drawings for all of our custom parts.

Figure 14. Component Interaction



10.2 Bill of Materials

The bill of materials (BOM) for our project can be found in Appendix G. The BOM can be broken down into the basic functions required for our device. First, a BiSlide, stepper motor, and linear encoder were ordered from Velmex, which will be used to translate the tension grip and then to measure that translation. In order to rotate the torsion motor and measure that rotation, a stepper motor, controller, power supply, damper, and rotational encoder were purchased from Lin Engineering. We also ordered an additional controller in order to more precisely control the tension motor. Since we wanted to read the results from the encoders directly into our LabView program, a PCI quadrature encoder was ordered, which includes LabView drivers to integrate the information from the encoders into our LabView program. We also considered purchasing a less

expensive USB quadrature encoder; however, we felt that it would allow us more time for the calibration of the flexures to purchase the encoder with the LabView driver. Since our tension forces were not as small as our torsion forces, we were able to purchase an off-the-shelf load cell to measure these forces. As an addition to the load cell, we also ordered a Transducer Electronic Data Sheet (TEDS) chip, which contains electronic identification of the load cell. This means that the user does not have to physically enter in the calibration data for the load cell and makes it easier to swap load cells, if Professor Daly ever has a need to do so. The data acquisition system for the load cell was available to us in the lab since it had already been set up for a similar device.

The measurement of the torsion force has become one of the most challenging aspects of our project. In order to accomplish this goal, our team has decided to use capacitance probes. In addition to these probes, it is also necessary to purchase electronics that are specific to the probes. The combined cost of this capacitive sensor system is nearly \$9000. Due to this large cost, our group has decided to delay the purchase of these items until some initial testing has been performed. This initial testing will not only give us the confidence to purchase this system, but will also allow us to have a better idea of the resolution that is required from these sensors. We have gathered various lead times for the capacitance probes. The vendor informed us that the typical lead time for this system is 4-6 weeks; however, when we explained the situation, he seemed confident that he could reduce that time to 3 weeks. Professor Awtar has stated that they could take up to 3 months to arrive so we are unsure what the actual lead time will be. For our BOM, we used the quoted lead time of 3-6 weeks.

Some additional items we purchased were miscellaneous items from Thor Labs. These items include vertical brackets made for breadboards, which we will use as a holder for our flexure, an optical breadboard to be used as the base of our system, and a micrometer stage, which will allow us to vertically translate the capacitance probes in a precise manner. Other items, such as dowels, bolts, materials, and

The final design included a few components that could not be purchased off of the shelf as they are custom designed. There is a cost associated with the material to be used for manufacturing the flexure, motor mount, capacitance probe stand, and other miscellaneous components. Both the flexure and motor mount machining were donated to us, which saved about \$850 in machining costs. The flexure and motor mount were machined by Henze Industries and Arnold Tool & Die Co., respectively. In addition to these, we had our grips sent out to a professional machinist in order to ensure tight tolerances, which adds to the cost of the material and the machining to our budget.

Fortunately, our sponsor allowed us to expand the budget whenever performance was going to be compromised. This device will be the state-of-the-art when completely finished so high performance was absolutely necessary for the project to be successful. Our group did not therefore encounter any major tradeoffs between cost and performance. The most cost prohibitive parts of our device are the sensors and drivetrain, together totaling 75-80% of our projected budget total of \$14,000. The raw material costs are small compared to this being under \$200.

10.3 Engineering Design Parameter Analysis

There were three main areas in which analysis was performed in order to design our system: the selection of the sensors (excluding the torsion sensor), the selection of the motors, and finally the design of the flexure (the torsion sensor). When looking at the sensor portion of the analysis, the main tools used were knowing the resolution required by our system and then using a bit of electrical engineering knowledge to see if that level of resolution could be obtained using our data acquisition system. The motors were fairly simple to choose as we had specific requirements for the system to work properly. The torsion loads were very low so we could use a standard motor with micro-stepping capabilities. The most extensive analysis performed was in the design of the flexure. This consisted of creating a mathematical model to approximate the system using beam theory, doing an extensive finite element analysis of the system, and then comparing the two. This analysis drew on many of the different classes that we have taken, but the two most relevant were solid mechanics (ME 211 and ME 311) and finite element analysis (ME 305). In order to complete this analysis as thoroughly as possible, our team met with different solid mechanics professors to confirm the validity of our mathematical model and also met with our finite element GSI in order to improve our finite element model. Many of the practical tools gained through previous design and manufacturing classes (ME 250 and ME 350) and involvement in student teams were also very useful, such as the theory behind screws, bearings, and motors.

10.3.1 Sensors

When selecting the encoders (linear and rotational) for the system, the analysis was minimal. We needed to determine the resolution required and then choose a sensor that could achieve this resolution. For the linear travel, a resolution of $4\ \mu\text{m}$ was required when using the smallest gauge length (1 mm) and striving for at least 50 data points of resolution. Therefore, a linear encoder with a $1\ \mu\text{m}$ resolution was chosen. For the rotary encoder, we first narrowed our search down to those offered by Lin Engineering so that the company can assemble the motor, damper, and encoder before shipping. Adding the damper and encoder require an additional shaft to be added. To choose between the two offered for the motor size we selected (NEMA 17), we mainly looked at the cycles per revolution (CPR). We chose the one with the higher number of CPR since that one will give us more data points. Our encoder has a maximum of 1,250 CPR, which means it will take a reading every 0.288° . If we use a 1.8° step motor with 32x micro-stepping, we should be able to take a reading every 5.12 steps the motor takes. We would like the encoder to read about every 1 step; however, 1,250 cycles was the maximum offered and we will also be able to gather step data from the controller. The encoder can therefore act as a feedback system for the controller.

When choosing the tension load cell, we required a resolution of $4.98(10^{-4})\ \text{N}$ (Appendix B). This value was obtained by considering the smallest tension load at failure (0.025 N) and striving for at least 50 data points of resolution. From talking to other students in Professor Daly's lab, we found that our lab already has a Data Acquisition System (DAQ) with 24 bit resolution. In order to save Professor Daly the expense of purchasing a new system, we decided to design our system around the existing DAQ. Our maximum tension load is approximately 22 N and therefore we knew we would need at least one load cell with this capacity. We found through our calculations (Appendix H) that using the existing DAQ and a 22 N load cell, we are able to achieve a $1.65(10^{-5})\ \text{N}$ resolution, which is even smaller than the resolution that we were hoping

to achieve. One benefit to the use of the load cell chosen is that the company offers different capacities of this load cell of the same shape and size. This would allow Professor Daly to purchase an additional load cell of larger capacity if she decides later to use larger diameter wires, or it allows us to purchase a lower capacity load cell if for some reason we are not obtaining the expected resolution with the 22 N load cell.

10.3.2 Drivetrain

The first part of the drivetrain needed was the ball screw that would translate the grips to put the wire under tension. We knew that Professor Daly wanted to test wires as short as 1mm so we looked for ball screws with a 1 mm pitch. We also knew that we needed to have a linear guide so that the grips and wires could maintain alignment throughout the test. Velmex was one of the only companies that met these needs. The “BiSlide” (model M01) from Velmex was a combination linear guide and ball screw, and has a pitch of 1 mm. From there we picked the motor to translate the BiSlide.

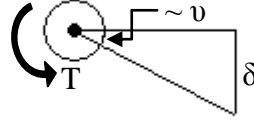
The translational motor was fairly easy to choose. From our analysis, we knew we needed to translate no more than 4 μm each step of the motor. The motors offered by Velmex have a step size of 1.8° but have half-stepping (0.9°) capabilities. That is 400 steps per revolution; therefore, each time you half-step the motor, the BiSlide moves 2.5 μm . To do this calculation, take the pitch length divided by the number of steps per revolution. From here, we used torque vs. load curves provided by the company to find the torque required. We knew our normal or translational and thrust loads would be less than 5 lbs. According to the graphs, shown in Appendix I, we needed a peak torsion load of about 90 oz-in and a holding torque of about 45 oz-in. The speed of the motor was not critical so using the above parameters, a tension motor was selected.

For the torsional motor, we had a maximum holding torsion load of $2.16(10^{-3})$ and a peak torque of about twice this. Since this torque is so small, most motors can handle this. Speed was also not important because the speeds at which we will spin the wire do not diminish the torque to below our requirements. There was no torque vs. speed curve provided by the chosen vendor, Lin Engineering, however, technical support at the company ensured us that the motor can handle our range of loads. The bigger consideration was step size. To achieve 50 points of resolution, we need the step size to be 0.096° . Lin Engineering supplies controllers that can do micro-stepping, which allowed us to choose a standard motor with a step size of 1.8° . There is a wide range of micro-steps, but we will most likely use the 32x micro-step option. The more standard motor also keeps the costs down, and allows us to attach a damper and encoder to the torsional motor.

10.3.3 Flexure

The driving design parameter for the torsion flexure was flexibility in torsion and rigidity in tension. The deflection of the flexure due to torsion will be measured at the ends of the amplification bar. Achieving a deflection of 10 nm or more at our resolution torsion load will allow the use of less expensive measurement equipment. However, we want to minimize the deflection of the flexure in tension as this displacement will introduce an error in the strain measurement of the wire. Using the assumption that any deflections due to torsion would be very small, our initial design was based on standard beam theory as taught in ME 211 and ME 311.

We used the equations listed below, and derived in Appendix M, which were double-checked and re-derived by both Professor Lu and Professor Wineman. The diagram shows the relationship between the flexure deflection, v , and the deflection of the amplification bar, δ .



$$v = \frac{TL^3}{3rbh^3E}$$

$$\delta = \frac{TL^3L_w}{3r^2bh^3E}$$

T = torsion load

L = beam length

E = Young's Modulus

v = flexure deflection

L_w = length of amplification bar

r = inner radius

b = beam depth (axial direction)

h = beam thickness (bending direction)

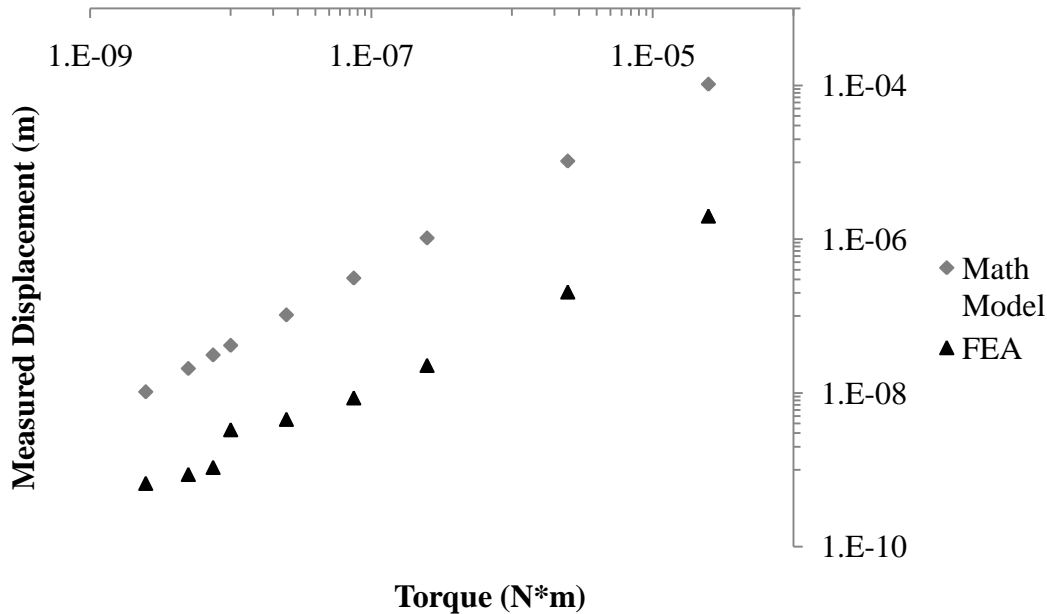
δ = amplification bar deflection

Once we had a suitable geometry according to the beam theory calculations, we ran the geometry through three finite element programs. SolidWorks CosmosWorks, two and three dimensional models in Altair Hypermesh with Nastran, and Abaqus all calculated smaller deflections for our over-constrained geometry in torsion than predicted from our mathematical model despite the small deflections involved. See Appendix L for example FEA simulations. The beam equations, however, were fairly accurate in predicting the deflections of the flexure in tension. Figure 15 on the next page summarizes the predictions of the displacement due to torsion as predicted by the two analysis methods.

As can be seen in the graph, under the effect of gravity, the measured displacement of the amplification bar in FEA is not linear with the torsion load for very small loads. We believe that this is due to the three legs of the diaphragm being under different loading conditions with the vertical beam in tension and the lower beams in compression. As the torsion load increases all beams are brought back into tension and the flexure begins to exhibit the expected linear spring behavior.

By varying the geometry of the flexure in CAD we were able to determine that the finite element software computed an unusual dependence on the inner radius. With our current knowledge we are unable to derive an equation that accounts for the discrepancy between the models. As they are inexpensive, we have decided to have a flexure made based on the beam theory math model and conduct real-world tests. The planned test is described in Section 13.

Figure 15. Predicted Displacement as Calculated by the Math Model and SolidWorks CosmosWorks for an 6061 Aluminum Flexure with $L = 80\text{mm}$, $r = 0.75\text{mm}$, $b = 12.7\text{mm}$, and $h = 0.05\text{mm}$

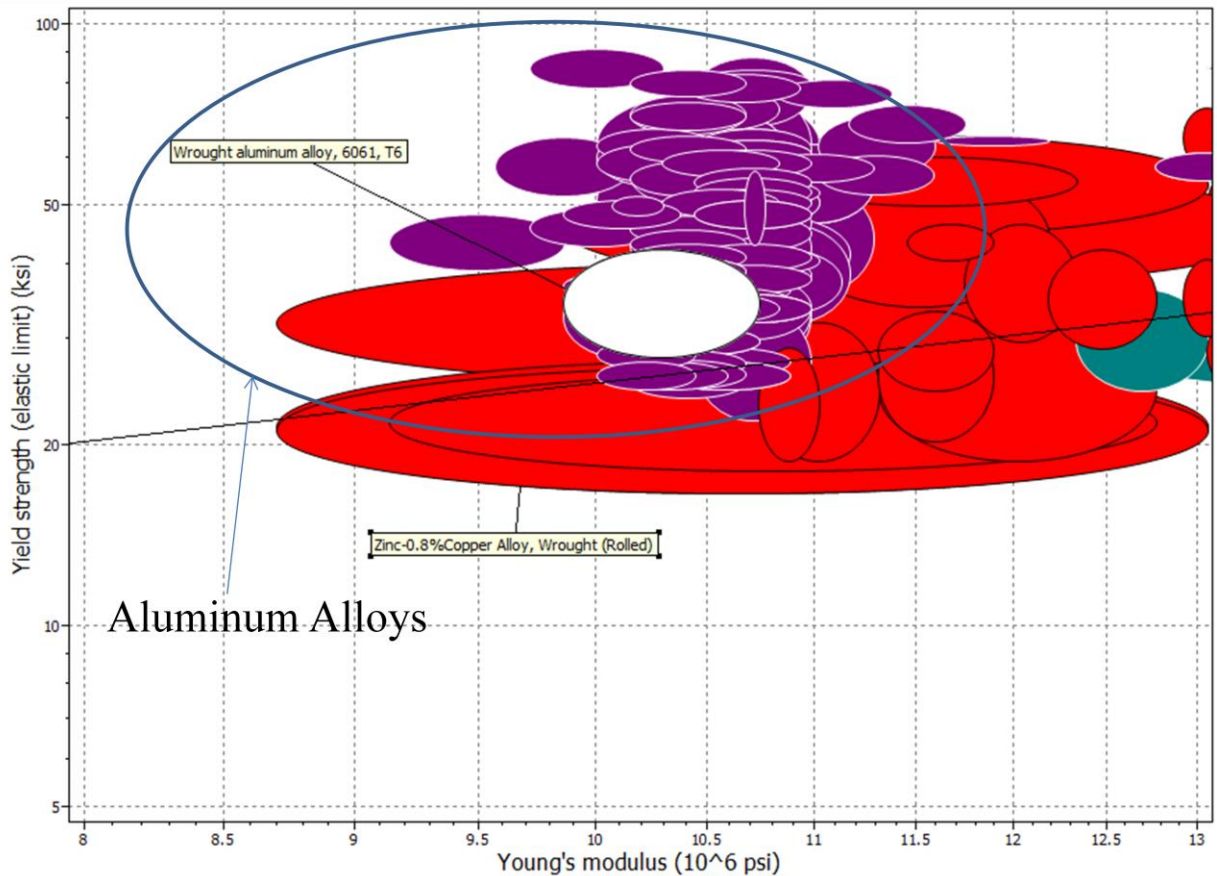


10.3.4 Material Selection

Proper material selection is imperative to the success of our design. When considering the materials to be used, there were three main components of our design, which required proper material selection: the flexure, amplification bar, and grips.

The most important material decision made by our team was the material of the flexure. For the flexure, the most important characteristic was the Young's modulus. We wanted to choose a middle of the range Young's modulus because if the flexure were too stiff, the beams would not be able to bend and we would not be able to obtain a deflection. We also did not want a low Young's modulus because the flexure has to be stiff enough for the beams to support the center of the flexure, and also to remain rigid when the tension force is applied. Another characteristic which we considered was the yield strength of the material. We wanted to choose a material with high yield strength in order to avoid yielding of the flexure due to the stresses caused by the different applied forces. It is imperative to keep the flexure material in the elastic range during testing. We performed an analysis in CES looking for high yield strength and a moderate Young's modulus and the results of this analysis are in Figure 16. The line on the figure represents a performance index of 1 because we weighted the importance of high yield strength and a moderate Young's modulus equally. Although the loads that will be applied to the diaphragm are low in comparison to the yield strength of most materials, we still looked for high yield strength in order to achieve a high safety factor. We found that the materials that best fit these characteristics were aluminum alloys and this is the material we have chosen for our flexure. The specific alloy that we have been using for our initial flexure and for our modeling is 6061 because it has high yield strength and is commonly available.

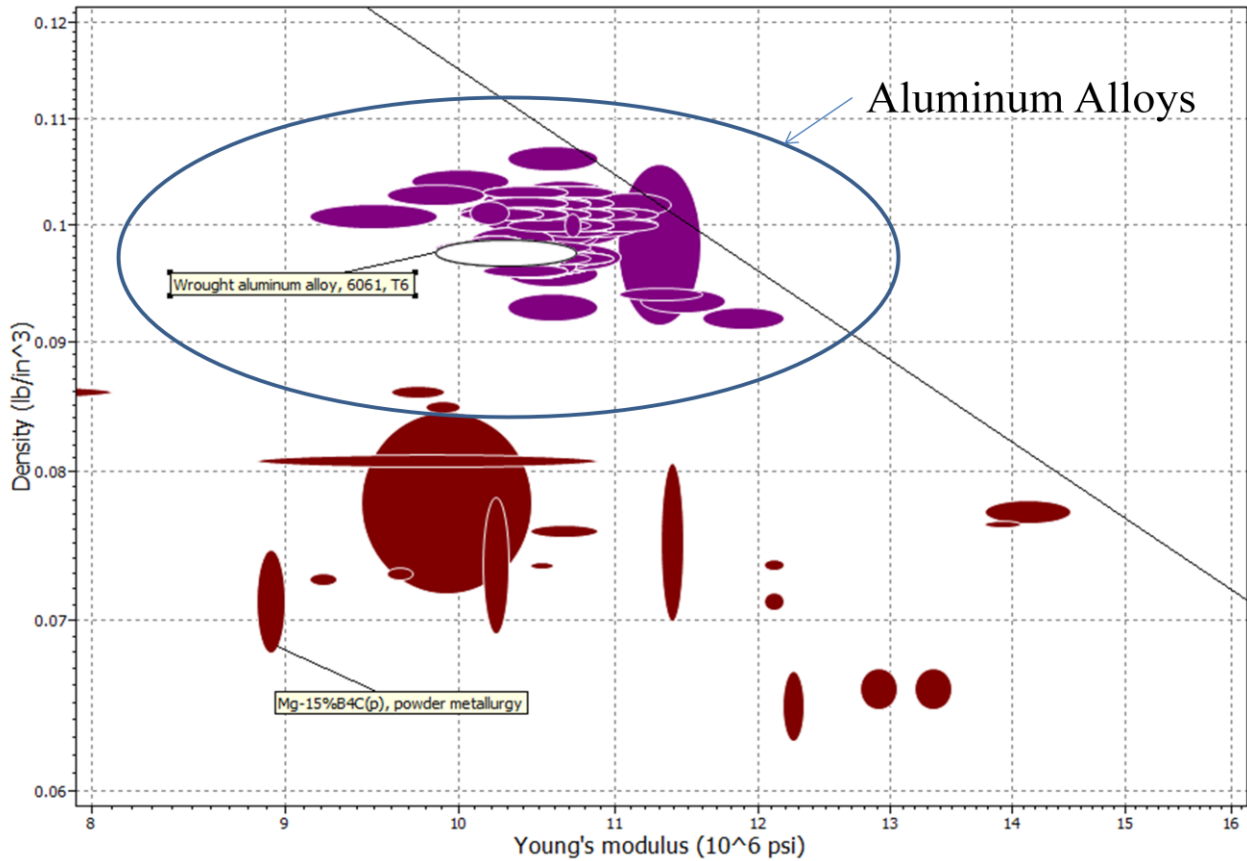
Figure 16. CES Analysis for Flexure Material Selection



The next two material choices were directly related to the flexure. Since both the grips and the amplification bar are attached directly to the flexure, it was important to use a light material for both of these components. For the material selection of the amplification bar, in addition to the light weight requirement, it was also important for the amplification bar to be stiff because the capacitance probes work properly only when measuring materials with a flat surface. Finally, the material had to be a good conductor in order to be used with the capacitance probes. It would not be reasonable to use a different material for the bar and then just add a conductive material to the end, because the bar must be grounded to complete the circuit with the capacitance probes. Therefore, when beginning a CES analysis to choose a proper material, we looked specifically at metals because the majority of conductors are metallic. The other two important characteristics: light weight and stiff, were translated into CES as density and Young's modulus. We determined that it was more important for the amplification bar to be light weight than stiff, and so we focused our analysis more on low density than on high Young's modulus, therefore we limited Young's modulus on the graph. Also, we decided that we could use a different shape for our cross section, such as an I-beam or a box beam, instead of a simple beam in order to make the amplification bar stiffer. The line on the figure corresponds to a performance index of 1, because after limiting the Young's Modulus, we decided that low density and high Young's modulus were of equal importance. The results from our CES analysis can be found in Figure 17. The lowest density metals with a stiff enough Young's modulus were a group of aluminum alloys, and also some magnesium alloys that are used mainly for casting. From these results, our group

has decided to use an aluminum alloy for the material of the amplification bar. From this analysis, we also decided that an aluminum alloy would be the best material for the grips as well, mostly because of its low density and therefore low weight on the flexure.

Figure 17. CES Analysis for Wing Material Selection



10.4 Safety Analysis

Since our design has only a few moving parts and is relatively small, the safety risks are relatively small. The risks come from the electronics and motors, and the translation of the BiSlide along its track. There is the potential for the user to get their hand in the way of the slide as it is moving. We did not find that this was a big risk, but a guard or shield can be placed around the device to eliminate this possibility. The electronics present the risk of shock. To help prevent this, we will make sure that everything is grounded properly and by providing a setup procedure for the electronics. There is no way for us to address the weight of the device short of keeping it as light as possible. There will always be a risk during transport; however, this is a minimal risk. The failure modes are summarized in Table 6 on the next page.

10.5 Environmental Analysis

The environmental impact of our device is minimal due to the fact that it does not take a vast amount of resources to make nor does it take many resources to run. We used SimaPro to estimate the environmental impact of making our device as well as the environmental impact of a single use of our device.

Using SimaPro, we estimated the environmental impact of making our device by the amount of aluminum we used in our design, which was estimated conservatively to be 15 kg. As shown in Figure 18 on the next page, the total amount of environmental emissions for generating this much aluminum is about 350 kg with about 125 kg of that being emitted to the air. We would have to focus more on how to reduce these emissions if this device was going to be mass produced; however, because only one is being made, this is reasonable. Additional information can be found in Appendix J.

Table 6. Failure Mode and Effect Analysis for the Device; O (Occurrence Rating), S (Severity Rating), D (Detection Rating), RPN (risk priority number)

Function	Failure Mode	Effects	S	Cause	O	Current Controls	D	CRIT	RPN
Flexure	Fracture	Loss of torsion load measurement reliability	8	Excessive flexing	2	Design of flexures so flex is within the elastic region	8	Yes	128
Wiring	Improper wiring	Loss of measurement reliability	10	Setup done wrong	4	Procedure will be put in place to avoid this	7	Yes	280
Electrical	Lack of grounding	Shock of user	6	Setup done wrong	3	Procedure will be put in place to avoid this	4	No	72
Vibration	Vibration	Loss of measurement resolution	10	Building noise	8	Use of optical table and if necessary experiments can be done later in day.	2	Yes	160
Vibration	Vibration	Loss of measurement resolution	10	Torsion motor vibrations	8	Use of torsion motor dampener	2	Yes	160
Vibration	Vibration	Loss of measurement resolution	10	BiSlide/Tension motor vibrations	8	Will determine if additional action is needed at later date	2	Yes	160

Each run of our device only requires a few inches of micro-wire and some glue, both of which have minimal impact on the environment because their quantities are so small. We used SimaPro to estimate the environmental impact of each use of our device based on epoxy, copper, and acetone used during a typical run of the equipment. The emissions, seen in Figures 19 thru 22, are minimal. The maximum amount of emissions is less than a gram. Even if this device was used once a day, every day for a year, the emissions would still only be a few grams per year. Additional information can be found in Appendix J.

The total energy consumption is around 208 Watts, which results in a cost of \$0.0174 per hour. The biggest consumers are the computer (~65 W), monitor (~35 W), the motors (~50 W) and the capacitance probes (~50 W).

Figure 18. Environmental emissions: water, raw, and air due to manufacture of device

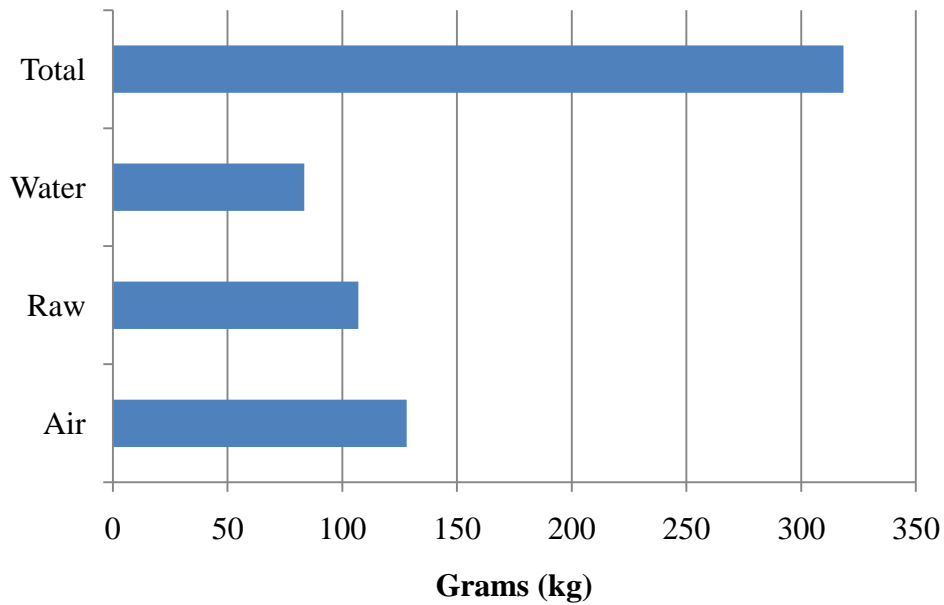


Figure 19. Water environmental emission per use of device

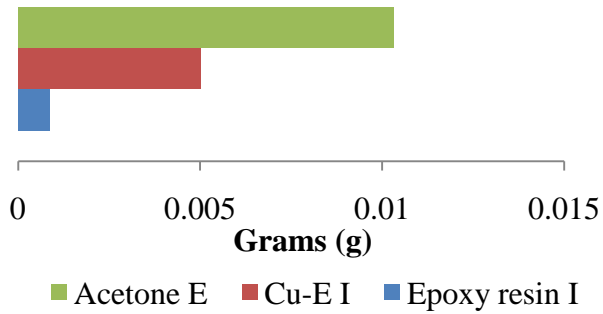


Figure 20. Air environmental emission per use of device

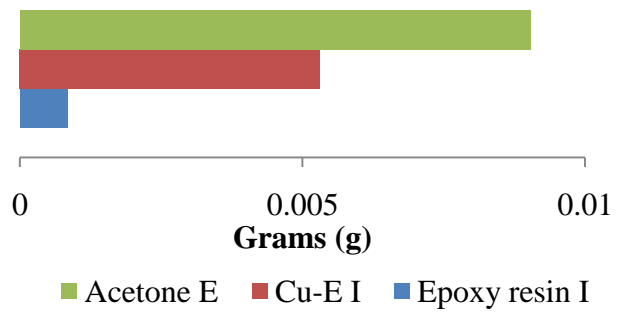


Figure 21. Raw environmental emission per use of device

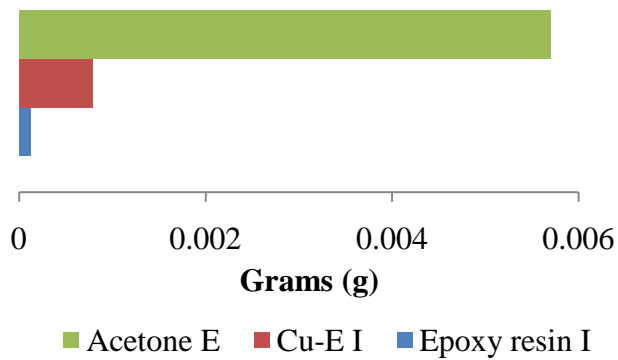
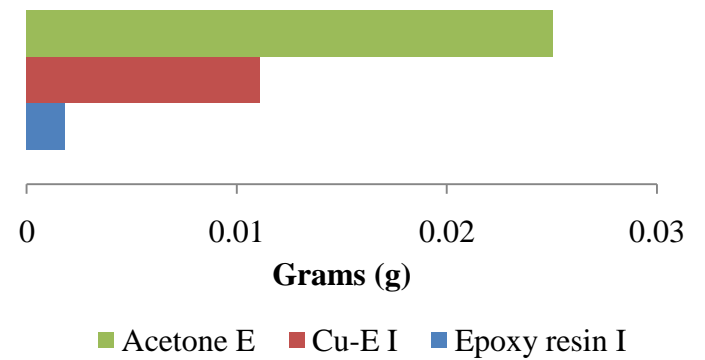


Figure 22. Total environmental emission per use of device



11.PROTOTYPE MANUFACTURING & ASSEMBLY PLAN

The large majority of our parts will be purchased, including all the electronics and sensors as well as the BiSlide and motors. Despite this there are still some parts that have to be manufactured either by custom order or in-house. We have decided that the parts that are done in-house will be done on a manual mill to reduce the time spent manufacturing the pieces. The parts that have to have high tolerances need to be done on a CNC mill or with another precise machining technique, which we will send out to be done custom for us. Table 7 shows which parts are being manufactured and where.

Table 7. Manufacturing Plan for Parts That Cannot Be Purchased

Part	Process	Where
Capacitance probe stand	Manual mill, drill press	In-house
Torsional motor mount	CNC mill, drill press	Arnold Tool & Die Co.
Micrometer stage blocks	Manual mill, drill press	In-house
Flexure	Wire EDM	Henze Industries
Grips	CNC Mill	Custom (Malaysia)
Grip plate for alignment	Manual mill	In-house

The assembly has been set up in such a way to maximize alignment and to eliminate stress points in the structure. We purchased an optical breadboard to help us maintain alignment throughout assembly. Breadboards have precision drilled and aligned bolt holes. The first step in assembly is the drivetrain, which provides a starting point for assembling the grips and flexure. The BiSlide, including the linear encoder and motor, is first attached to the breadboard by cleats. The torsion motor is then mounted to the BiSlide, which completes the main parts to the drivetrain. A coupling is mounted to the torsion motor shaft and a shaft that has been press fit into the grip.

Following linearly along the device, brackets made specifically for breadboards are screwed to the board; the width of the BiSlide and the hole spacing dictate the overall width of the flexure. Height is also a concern. The flexure and amplification bar (attached by two small screws) will be screwed to the brackets so we must ensure that the height of the middle hole on the flexure is aligned with the middle of the torsion motor shaft. After attaching the flexure to the brackets, the load cell can be press-fit into the flexure using a shoulder screw. The grip is also then screwed to the load cell, and this completes the assembly of the main components of our prototype.

The grip alignment and height of the flexure will be verified using a plate that bolts into the grips and kept aligned through cylindrical dowel rods. At least one of the rods can travel along a slot cut into the plate. If the grips are misaligned in the horizontal plane, the motor mount can be unscrewed and adjusted slightly. If the heights of the grips are different, shim stock can be added underneath the motor mount. It might also be possible to move the flexure higher or lower on the bracket. One should be careful of introducing unknown stresses when adjusting the motor mount, grips, or flexure. It is recommended that if adjustment is needed, everything assembled after the point of adjustment should be re-assembled.

12.USABILITY ANALYSIS

There are four main use cases for our tension-torsion device: performing an actual test, cleaning the posts after the tests, changing the flexure in between tests, and finally moving the system from an optical table to a microscope.

The main use for this device is performing a tension-torsion test. The most difficult step for the user in this process is loading the wire into the grips. First the wire will have to be wrapped around the posts and glued. We are currently working on a plan to make this process easiest for the user, but the basic process follows. The two posts will be placed in a tray (which has not been designed yet), which will allow the user to place them a specific distance apart, in order to obtain a predetermined gauge length. Then the user will lay the wire in the groove of each post and place a ball of glue on a marked location on the post. Next the user will wait approximately 5-10 minutes for the glue to harden, and then wrap the wire twice around each post. The user will apply additional glue around the wrappings to ensure a solid hold, and then will allow the glue to set overnight in order for it to properly harden. Therefore, many wire posts are needed to perform multiple tests per day. The wire posts are inexpensive, and we do not feel that this is a problem. After the glue has hardened, the user will pick up both posts and place them in the slots on the grips. In order to align the grips before the test, an alignment plate will be placed onto the dowels on the back of the grips; then the gripping plate is placed on the dowels on the front of the grips. Next the user will tighten the bolts on the gripping clamp and remove the alignment plate before beginning the actual test. The rest of the process will consist of the user entering information about the test to be performed into the LabView interface.

In order to reuse the posts for the tests, it is necessary to remove the super glue. The process for this is quite simple. After the test is performed the posts will be placed in a small beaker filled with acetone for 1-2 hours. Then the posts can be wiped off with a paper towel and reused for further testing. Also, we will have a few different sets of posts so that the user doesn't have to wait until the post is clean to perform another test.

When performing tension-torsion tests with our device, there will sometimes be the need to change the flexure to one with different properties, depending on the diameter and type of wire used. This step will not necessarily be performed in between every test, especially if the individual is running multiple tests on wire with the same material and similar diameter. In order to replace the flexure, the individual will need to simply remove the four bolts which hold the flexure onto the brackets, remove the flexure, and finally bolt the new flexure onto the brackets. The brackets remain attached to the base of the system permanently.

Another possibility is the need to move the entire system to a different location. The two main places where this device will be used is on an optical table and then on a normal table underneath a stereo microscope. In order to make this transition as simple as possible, the base of our system will be an optical breadboard. When using an optical breadboard, there are simple posts that are made to be screwed directly into the breadboard. These posts can be used to hold the system above the bottom of the microscope and can be removed in order to screw the base directly onto the optical table.

13.VALIDATION PLAN

Many of the engineering specifications for the tension-torsion device are a function of the final hardware designs and can be verified by measurement or part dimension. Additionally, many of the operational parameters will be simple to test as they are controlled by both an input signal and a feedback encoder. The most difficult specification to verify will be the torsion sensing, which will require extensive calibration with capacitance probes and known torsion loads.

The first validation to be done is on the torsion flexure. We have received a first iteration part for testing, assembled our prototype, and have begun testing on the flexure. Professor Awtar has generously allowed us to use his capacitance probes for these tests. Please refer to Section 14 for more of a discussion on the flexure testing as it stands thus far.

Once all the parts have been manufactured or procured, many of the engineering specifications can be validated by simple measurement. However, the operational engineering specifications will require full assembly of the device and program debugging before they can be verified.

13.1 Flexure Functionality

The prototype flexure will be bolted to an optical table with a capacitance probe under one end of the amplification bar. The first readings we will take will be at steady state to determine the effect of room air currents and ambient vibrations on the bar position. If air currents are a significant problem, all following tests will occur with the assembly covered. We will then calibrate the flexure by placing pieces of wire at different locations on the bar to simulate a torsion load. The wire we will use as weights is the inexpensive 196 μ m copper wire used for grip concept testing. Since its density and diameter are known, we will be able to accurately calculate torsion load applied to the flexure.

13.2 Gauge length

Minimum gauge length is a function of the radius of the grip fillets and the jig used for assembling the wires on the posts. With the fillets necessary to avoid stress concentrations the minimum gauge length is 3.175 mm. This can be measured with a pair of calipers.

13.3 Travel

The BiSlide acquired for the tension portion of the device has a specified travel of 12.7 cm. This can be verified quickly by measuring the distance between the ball screw carriage and the end of the slide with a pair of calipers, running the carriage through its full travel, and re-measuring.

13.4 Backlash

The backlash of the BiSlide will be determined by reversing the direction of the BiSlide motor and comparing the travel calculated from the motor controller to the travel measured by the optical linear encoder. This can be done quickly when the LabView programming is being tested. However, we do not anticipate running a test both forwards and backwards so backlash should not be a large problem.

13.5 General Dimensions and Quantities

The weight, overall height, depth, and footprint of the tension-torsion device are not design critical and are intended to facilitate ease of use and portability. Once the device is assembled these parameters can be measured by a scale and a measuring tape.

13.6 Test Height

The test height of the device is important when using the microscope to view tests being run. The test height has been designed into the device. Any variation in that actual assembly can be dealt with by adjusting the microscope focus.

13.7 Motor Loads and Speeds

The chosen motors have been oversized to ensure no operational problems. Attempting to prove or disprove the manufacturer data sheets could result in damage to the motors.

13.8 Gripping Force and Coefficient

The gripping force and coefficient can be verified by loading a wire in the grips, marking the wire, and running the tension portion of the device while viewing the grip under the microscope. If the wire is seen to slip in the grips, the grip screws can be tightened further. The orientation of the screws will then be marked on the grips for future reference.

13.9 Alignment Tolerance

During use, the alignment of the grips will be achieved by placing a precisely drilled plate on the grips as the wire is loaded. For the initial assembly, the alignment will be verified using the microscope to check the inclusion angle of the wire.

Engineering specifications that will not be tested include tension force, sensor resolution, deflection of the mechanism due to vibration, and the Young's Modulus of the materials used to construct it. Tension force will not be tested extensively because all components were selected or designed to carry the maximum expected wire loads. We can still run a test to maximum force in order to test for operability ranges. The sensors we will be using come pre-calibrated or with appropriate circuitry to automatically zero. Both the deflection of the device due to vibration and the Young's Modulus of the materials would be extremely difficult to measure. In order to record good measurements, tests will have to be run with the device isolated from external vibration on an optical table. The Young's Modulus was specified before the final design was known with the intention of building a very rigid device. As the base will be made out of half inch aluminum optical breadboard, disruption of the device will be minimal if it is moved.

14. CHALLENGES, MODIFICATIONS, & FUTURE WORK

14.1 Design Changes

There have been a few slight design changes since Design Review 3. In the interest of time, we decided to purchase the angle brackets to mount the flexure. The angle brackets from Thor Labs do not meet up with all of the bolt holes on the flexure, but the flexure is still sufficiently constrained. An added benefit is that the whole assembly fits under the stereo microscope better than with our original design. The other cosmetic change resulted from unexpected spacers that were between the Bi-Slide and the linear encoder when they arrived. A plate to move one of the

angle brackets outward had to be added to provide room. Other changes included enlarging the holes in the capacitance probe mounts to fit a larger bushing to make the system compatible with Professor Awtar's equipment and reducing the size of the amplification bar due to material availability. One change that remains to be made is the replacement of the torsion motor coupling. We were given the suggestion to use a helical coupling to help maintain the alignment of the grips. In practice, suspending the grip from the flexible coupling induces excessive vibration. Additionally, one of the wire grips must be re-made due to an important hole being drilled at an angle.

There have been some successes with the first iteration parts. Basic testing has shown that the grips can exert enough force to hold a large copper wire in both tension and torsion. Although programming is not complete, both motors are functional. From initial testing we have learned that the torsion tests will need to be run with a feed-back control from the load cell as the wire buckles when only the torsion motor runs.

14.2 Flexure Design and Modification

The current flexure was designed based on the mathematic model derived from classic beam theory (Appendix M) as the finite element model is highly sensitive to element size. The easiest way to increase the deflection while maintaining a small flexure was to make the beams as thin as possible in the torsion direction. We therefore set this value on the edge of manufacturability at 0.5 mm. After receiving the flexure from the manufacturer, we measured the beams and found that their thickness varies suggesting that an even thinner beam would not be feasible. The inner radius was set at 7.5 mm in order to allow sufficient space to mount both the load cell and the amplification bar. The remaining parameters were chosen to yield a predicted deflection of 10 nm for the resolution torque of a 10 μm nickel wire while facilitating manufacturing. A beam length of 80 mm combined with stock half-inch aluminum plate resulted in almost exactly the desired predicted deflection.

Based on the limited existing test data, the current flexure should be able to handle most materials that may be tested. We believe that it should be capable of measuring loads for wires with predicted torsion failure of $5.22(10^{-6}) \text{ N}\cdot\text{m}$ or greater. This would include 30 μm diameter copper, nickel and aluminum samples, 25 μm diameter 303 stainless steel samples, and 15 μm carbon samples. The limiting factors on the upper load end are the axial displacement under tension that can be tolerated, the five pound load capacity of the load cell, and the six pound axial load capacity of the torsion motor. Tensile deflection can easily be reduced by making a new flexure out of thicker material but torsion deflection will be reduced as well.

Altering the flexure design to expand the testing range will be an educated guess. The limited calibration testing results we were able to obtain suggest that the flexure follows neither model exactly but is closer to the finite element model. When altering the computer geometry, we were able to determine that the finite element and the mathematic models behave similarly with changes to the dimensions of the flexure beams. However, we were unable to explain the odd relationship between the finite element predictions and the central radius.

We have several recommendations for future flexure redesigns. Due to unpredictable effects of a different inner radius, any future flexure design should keep the 7.5 mm central radius and alter

only the beam dimensions. Following from the math model, increasing the beam length should have a cubic effect on the deflection and increasing the depth should have a linear effect. With the current set-up, the beam length could be expanded to about 130 mm without modifications to other parts. However, the upper corners would have to be cut inward to allow the machine to continue to fit under the microscope. The flexure could be made larger still if an appropriately sized spacer was to be placed under the torsion motor mount and larger blocks made to lift the capacitance probe mount higher. If the depth of the flexure is changed, the bar spacer will need to be changed accordingly to maintain the alignment of the capacitance probes. We do not recommend reducing the thickness of the beam as going smaller than the current dimension of 0.5 mm would likely not be manufacturable.

14.3 Capacitance Probes and Calibration Issues

In all four testing sessions the capacitance probes showed a significant amount of drift. By speaking with the probe manufacturer, we found out that the drift should not be an electrical problem with the controller or probes themselves. We then considered that the controller was not grounded well to the amplification bar. Using a multi-meter we were able to determine that if the ground was connected to part of the anodized frame, the circuit was disrupted. Therefore, the ground should be attached to the flexure itself.

The idea that thermal expansion of the set-up was a significant source of the sensor drift was first suggested by Gaurav Parmar, a graduate student working for Professor Awtar. The extent of the possible variability of the bar height can be calculated as shown in the equation below. In order to prevent the thermal effects from masking the torsion displacement, the thermal expansion would preferably be less than 5 nm over the course of the test. For our 6.35 mm bar, this translates to holding the temperature of the bar constant to within 0.06 K. Additionally, the thermal effects would apply to the flexure. Using the equation below again, in an unloaded state, each beam of the flexure would grow 1.89 $\mu\text{m}/\text{K}$. Since the ends of the flexure beams are constrained and a load and moment are applied to the center, the thermal load manifests as unknown stresses and deformations in each beam.

$$\Delta L = \alpha L(T_F - T_I)$$

ΔL = change in Length

T_F = final temperature in K

L = initial length

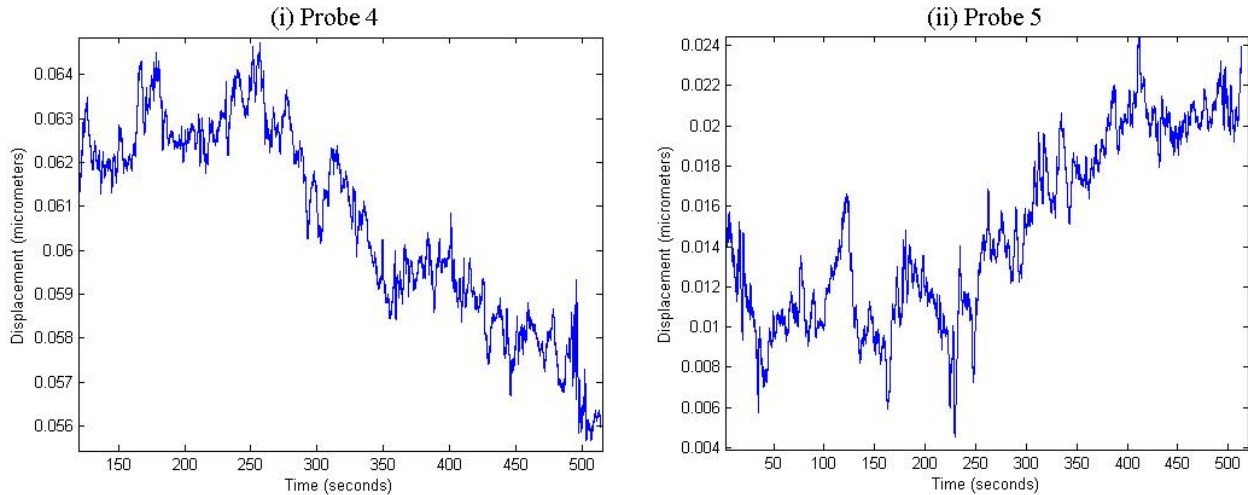
T_I = initial temperature in K

α = coefficient of thermal expansion = 23.6 $\mu\text{m}/\text{m}\cdot\text{K}$ for 6061-T6 Aluminum

Despite the large thermal effects, we believe the issue can be resolved. Our final steady-state test was run with no one standing in the near vicinity and with fairly stable room temperature. As seen in Figure 23, the measured drift was small and slow enough to run a test without severely distorting the results. Due to our limited access to using the capacitance probes, we only had sufficient time to achieve one steady run. This steady behavior could be more consistently achieved by using an insulated cover for the machine and running tests only when room temperature is steady and traffic is minimal. The expansion of the bar can be reduced by manufacturing a replacement out of graphite or other conductive material with a low coefficient of thermal expansion.

In addition to the thermal effects and grounding problems, we have looked into vibrations inherent to the surroundings, air currents, and sensor drift. After talking with GSIs, professors, and the manufacturers, these do not seem to be the cause of our problems; however, we hope to be able to isolate all of these variables to determine where exactly the problems lie.

Figure 23. Plots of sensor drift from most steady run where (i) Probe 4 drifted 9 nm in six minutes (ii) Probe 5 drifted 20 nm in eight minutes



Due to the large discrepancy between the math model and the finite element analysis, one of our major goals was to roughly characterize the real-world flexure. We cut small pieces of our inexpensive copper wire and weighed them using an analytical balance. We then placed the wire pieces on the amplification bar at measured distances to apply known torques. In order to reduce the effect of the sensor drift, we took multiple measurements of three different torques. The averaged results are plotted in Figure 24 on page 43 with the predicted results from the finite element and math models. As can be seen in the figure, the measured displacements fall between the finite element and the mathematical predictions. Notable sources of error include the sensor drift, the need to touch the amplification bar in order to place and remove the wire, and an incomplete set-up with the capacitance probes placed too close to the center of rotation. Full calibration needs to be done with a more accurate set-up. Even then, matching the data to the prediction models may prove difficult as the thickness of the flexure beams is inconsistent due to machining limits. However, from the data we have, we can conclude that the finite element model can be used as a lower bound for future flexure design with a significant safety factor to resolve small torques.

14.4 Next Steps

The team created a prototype device to be used for the tension-torsion of micro-wires; however, this prototype still needs additional work before it can operate as a successful research instrument. There are three main areas that still require further attention: manufacturing, integration of the LabVIEW program, and calibration of the torsion flexure.

14.4.1 Manufacturing

One of the most prominent manufacturing issues experienced by the team was a misaligned hole on the grips, which we had sent out to be manufactured. The main hole, which is to be used to connect the grips to the load cell, is visibly misaligned, which makes it impossible to properly align the grips. A new grip must be manufactured. Additional items which were intended to be manufactured, but were not completed due to time constraints are as follows: the alignment plate, lathing a groove into the dowels, using a ban saw to cut a slit into the bronze bushings for the capacitance probe holders, and the loading tray. The team has conducted multiple tests using the grips without wrapping the wire around the post, and as long as the clamping plate wasn't bolted on to the grips too tightly, the wire held in the grips and broke halfway in between the two grips during the test.

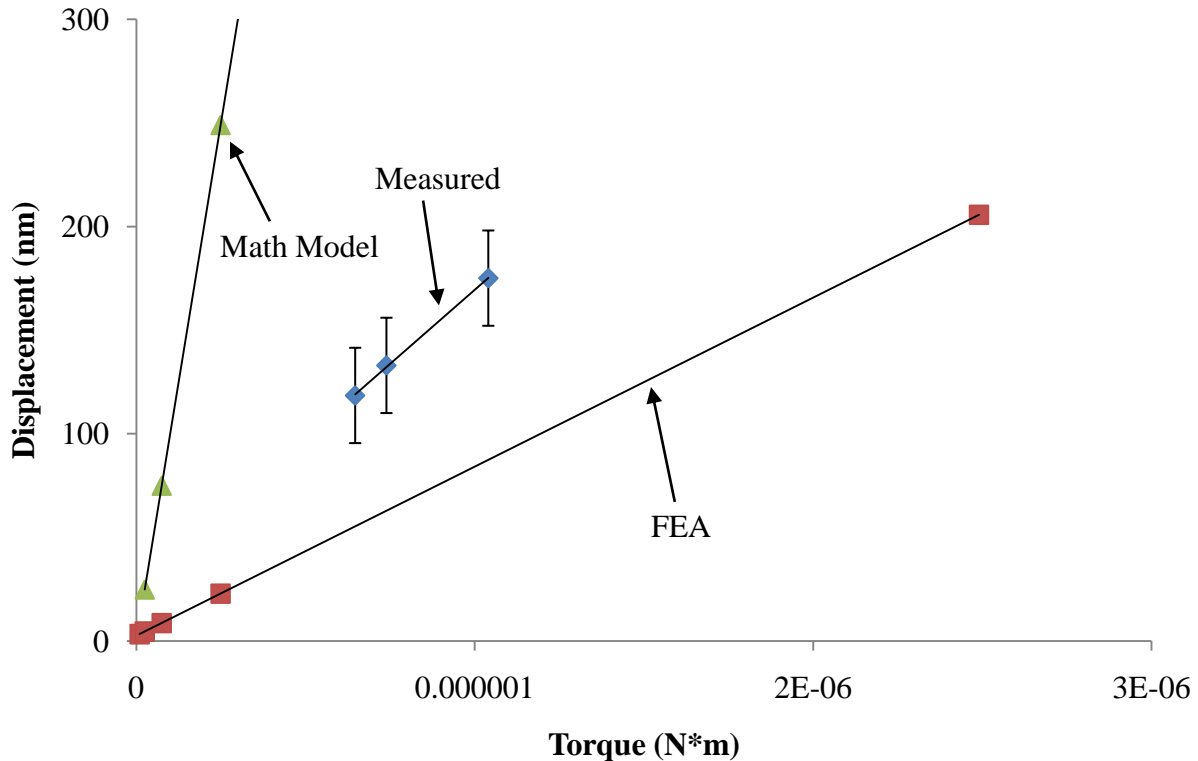
14.4.2 Integration of the LabVIEW Program

As was previously stated in the procedure, due to time constraints and a limited knowledge of LabVIEW, the team was unable to complete the LabVIEW program as intended. The current working program demonstrates how to acquire data from the two encoders and also how to acquire data from the load cell. One issue with the current program is the inability to acquire distance values at the same time step as the load values are acquired. The team also has a separate LabVIEW with which to control the motors. The capacitance probe tests are currently being run using a separate program; however, there are LabVIEW drivers available for the capacitance probes after purchase and it is recommended that these are used to integrate the capacitance probes into the overall LabVIEW program.

14.4.3 Calibration of the Torsion Flexure

After experiencing significant sensor drift during the initial capacitance probe tests run, our team spent considerable time trying to determine the source of this drift and solve this issue. Because of this, the team has not yet purchased the capacitance probes to be used for the torsion sensor. The capacitance probes and associated controller are quite expensive, and the team did not feel comfortable making this investment without gaining more substantial data from the capacitance probe tests. Our team recommends running additional tests using these probes under controlled conditions to try to isolate the variables and determine the main source of the sensor drift. If the issue is due to thermal drift as hypothesized, we recommend running the tests with the system thermally insulated (use of a foam box) or to change the wing or diaphragm material to one with a lower coefficient of thermal expansion.

Figure 24. Measured displacement of the amplification bar compared to model-predicted values



15. TESTING PROCEDURES AND LABVIEW USER MANUAL

1.) In order to run a tension-torsion test with this device, the first step is to load the micro-wire into the grip and align the two grips.

- a.) First place the two posts into the designated holes on the loading tray (Appendix N), which still remains to be manufactured.
- b.) Then place the wire into the groove and glue the wire onto the post. Wait 5-10 minutes for the glue to harden.
- c.) Next wrap the wire once around each post and apply additional glue to hold the wrappings in place. Wait 30-60 minutes for the glue to harden.
- d.) While waiting for the glue to dry, use the motor controller LabVIEW program (serial.vi) to drive the grips close enough together to attach the alignment plate (still remains to be manufactured) using the dowels.
- e.) Minor adjustments might need to be made to the setup at this point in order to allow for the attachment of the alignment plate. The motor mount allows for some movement in either horizontal direction. Also, if there is an issue with misalignment in the vertical direction, shims can be placed underneath the motor mount.
- f.) After the glue is dry and the grips are aligned, place the posts into the slots in the grips and bolt the clamping plate onto the grips to hold the posts in place.

2.) The next step is to use zero both the load cell and the capacitance probes.

- a.) In order to zero the load cell, first run the load cell and encoder LabVIEW program (Load cell and encoder.vi).
 - b.) Then, use dial on the front panel of the program which allows the user to zero the load cell.
 - c.) In order to zero the capacitance probes, first the user must alter the vertical position of each capacitance probe using the micrometer stages until the controller indicates that the probe is approximately in the middle of the desired measuring range.
 - d.) In order to zero the capacitance probes, a computer program must be used to convert the voltage readings into a filtered deflection. The program currently being used for this purpose is not a LabVIEW program; however, it is advised in the future to somehow integrate this into the main LabVIEW program. Using one such program, rotate the dials (first the coarse, then the fine) on the controllers to zero the probes, until both probes reach zero deflection.
- 3.) The final step is to run the actual test.
- a.) The load cell and encoder program should already be running. Then use the motor controller program to control either the tension or torsion motor, depending on the test being run. A full list of commands for controlling the motors can be found in the controller's manual [15].
 - b.) The current LabVIEW program will save a file into a specified folder giving values for load versus time and also linear displacement versus time.
 - c.) After the test is completed, use Acetone to remove the glue from the posts for further use.

Note: It was the goal of the team to have a fully working LabVIEW program with all of the modules integrated into one program. However, due to time constraints and a limited knowledge of LabVIEW, the program has not been fully completed. The current working program demonstrates how to acquire data from the two encoders and also how to acquire data from the load cell. One issue with the current program is the inability to acquire distance values at the same time step as the load values are acquired. The team also has a separate LabVIEW with which to control the motors.

16.CONCLUSION

The effect of strain gradient on strength in small-scale devices has not been thoroughly researched. The conventional laws governing plastic behavior in materials cannot be used for micro-wires because they do not incorporate a length scale. To examine the size dependence of a material's strength, our team will build a machine capable of performing tension and torsion tests on wires sized from 10-200 microns. After talking with Professor Daly and creating a QFD, we determined that the most important customer requirements include: the micro-wire can be gripped without slipping, wire and grip alignment is maintained throughout the test, the sensors have a high resolution, the device fits under a microscope, the mechanism has a programmable load path, and the machine is stable. When considering how to approach our concept generation process, our group broke up our problem into three main modules: gripping, alignment, and sensors. After generating concepts for these individual modules, our group formed a proposed final concept. Preliminary analysis has been done on the final concept, all CAD models are complete, parts have been ordered and received, and the prototype is near completion. Optical

encoders will be used for the displacement sensors, and the loads will be measured by a load cell for tension. A novel idea utilizing a flexure, amplification bar, and capacitance probes for torsion has been devised. A prototype of the flexure has been received and some validation testing is done. The wire will be gripped by a clamp using a grooved post for initial alignment while a BiSlide will guide the grip as it travels during the test. These gripping and alignment mechanisms were not the top ranked concepts from our selection matrices. They were chosen in order to work around the design of the flexure because the sensing mechanism has become the most critical module in our project to achieve.

We are currently experiencing some issues with the validation testing of the flexure. The drift makes the error of our readings larger than the readings themselves. We were able to achieve stability in only one of our tests with the capacitance probes but hope to be able to repeat this with further testing. Due to our limited access to the capacitance probes, it has been difficult to determine the main cause of the drift. However, a new flexure cannot be designed with much certainty until testing is complete. We recommend further testing with the capacitance probes, specifically to test our hypothesis of thermal drift and to isolate other variables. In addition, there are a few things left to finish on the prototype, such as lathing the dowels, machining the alignment plate, and fixing the alignment of the grips. Lastly, the LabView program is still in the development stage and cannot be completed for the end of this semester.

Appendix O includes a matrix showing our design goals versus current operating capabilities.

17. REFERENCES

- [1] Fleck et al. (1994). "Strain Gradient Plasticity: Theory and Experiment." *Acta Metallurgica et Materialia*, 42, 475-487.
- [2] Liu et al. (2001). "Optimal design of optical fibre-holding microclips with metamorphic development." *Journal of Micromechanics and Microengineering*, 11, 195-201.
- [3] Grois et al. (1998). U.S. Patent No. 5,761,360. Washington, DC: U.S. Patent and Trademark Office.
- [4] Instron. (2004). 2714 Series Pneumatic Cord and Yarn Grips. Retrieved September 20, 2008, from <http://www.instron.us/wa/library/default.aspx>
- [5] Tinius Olsen. (2004). Bollard Style Tensile Grips. Retrieved September 20, 2008, from <http://www.tiniusolsen.com/index.html>
- [6] Kanda et al. (2006). *U.S. Patent 7,151,877*. Washington, DC: U.S. Patent and Trademark
- [7] Wu et al. (2006). *U.S. Patent 7,073,952*. Washington, DC: U.S. Patent and Trademark
- [8] Interface Advanced Force Management. (2008). Load Cell Resolution. Retrieved October 14, 2008 from <http://www.loadcelltheory.com/loadCellResolution.html>

- [9] SMD Sensors “Sensors” Retrieved on September 20, 2008.
<http://www.smdsensors.com>\
- [10] Lion Precision. (2008). *Capacitive Sensor Operation and Optimization*. Retrieved October 14, 2008 from <http://www.lionprecision.com/tech-library/technotes/cap-0020-sensor-theory.html>
- [11] Precision Micro. “Photo Etching”. Retrieved on September 24, 2008.
<http://www.precisionmicro.com/updocs/photoetching.pdf>
- [12] Precision Micro. “Wire EDM”. Retrieved on September 24, 2008.
<http://www.precisionmicro.com/updocs/wireedm.pdf>
- [13] Automation Creations, Inc. (1996-2008). Matweb. Retrieved on September 13, 2008.
<http://www.matweb.com>
- [14] ThomasNet Industrial Newsroom. (2008) Retrieved on October 6, 2008.
<http://news.thomasnet.com/fullstory/527517>
- [15] Lin Engineering. (2008). Retrieved on December 9, 2008.
<http://www.linengineering.com/LinE/contents/stepmotors/R356.aspx>

APPENDIX A

QFD

Row Number	Demanded Quality (a.k.a. "Customer Requirements" or "Whats")	Weight / Importance	Relative Weight	Competitive Analysis (0=Worst, 5=Best)					
				Fleck and Hutchinson	Istron Microtorsion Series				
1	Fits under microscope	11	9.17	5	0				
2	Grips micro-wires without slipping	11	9.17	5	0				
3	Suitable gauge length	7	5.83	2	3				
4	Robust	4	3.33	3	5				
5	High testing resolution	11	9.17	2	2				
6	Mobile	6	5.00	3	2				
7	Wide range of strain rates	4	3.33	2	3				
8	Resists buckling	8	6.67	3	3				
9	Maintains alignment	11	9.17	3	3				
10	Performs multiple revolutions	9	7.50	5	5				
11	Programmable load path	10	8.33	0	3				
12	Tests wide range of materials	4	3.33	0	5				
13	Tests to sample failure	4	3.33	3	5				
14	Stable	10	8.33	3	5				
15	Ease of use	6	5.00	2	4				
16	Cost	4	3.33						

Relationship Between Requirements:
 9 - Strong 3 - Moderate 1 - Weak

Row Number	Max Relationship Value in Row	Relative Weight	Quality Characteristics (a.k.a. "Functional Requirements" or "How's")	Demanded Quality (a.k.a. "Customer Requirements" or "Whats")	Column Number																							
					1	2	3	4	5	6	7	8	9	10	11	12	13	14	15	16	17	18	19	20	21	22	23	24
Max Relationship Value in Column					9	9	9	9	9	9	9	9	9	9	9	9	9	9	9	9	9	9	9	9	9	9	9	
Requirement Weight					211.67	211.67	152.5	103.33	87.5	280	65	102.5	132.5	140	195	150	12.5	162.5	82.5	55	160.83	152.5	110.83	30	170	170	122.5	132.5
Relative Weight					6.63	6.63	4.78	3.24	2.74	8.77	2.04	3.21	4.15	4.38	6.11	4.70	0.39	5.09	2.58	1.72	5.04	4.78	3.47	0.94	5.32	5.32	3.84	4.15
Difficulty (0=Easy to Accomplish, 10=Extremely Difficult)					8	6	4	2	1	2	2	2	1	0	10	4	0	2	4	3	5	4	6		7	10	4	4
Minimize (▼), Maximize (▲), or Target (x)					▲	▲	▼	x	▼	x	x	x	x	x	x	x	x	▼	▼	▼	▼	x	▼	x	▲	▲	▼	▼
Target or Limit Value					175 N	0.25	40 lbs.	> 31 mm	300 mm	1-75 mm	0.2 Nm	10 ⁻⁶ - 10 ⁻³ m/s	15 mNm	60 gpm	0.5°	5 mN - 33 N	210 Gpa	0.18 m ²	15 mNm	250 mm	2 μm	125 mm	0.1 mm	\$5,000	5*10 ⁻⁴ N	9.5*10 ⁻⁹ N	4 μm	0.086°
1	9	9.17	Fits under microscope	Gripping force			3	9	9	3																		
2	9	9.17	Grips micro-wires without slipping	Gripping friction coefficient	9	9																		3	3			
3	9	5.83	Suitable gauge length	Weight			1		9																			
4	9	3.33	Robust	Treat height	9	9				3	3	3	3	9	1				1		1							
5	9	9.17	High testing resolution	Depth				9		3		3	9				9			9			9	9	9	9	9	
6	9	5.00	Mobile	Gauge length		9										9		3										
7	9	3.33	Wide range of strain rates	Tension motor load	9	9					9												3	3	9	9		
8	9	6.67	Resists buckling	Tension grip speed	3	3			9					3	9													
9	9	9.17	Maintains alignment	Torsion motor load	1	1			3					9	1				9	9								
10	9	7.50	Performs multiple revolutions	Torsion grip speed								9	9															
11	3	8.33	Programmable load path	Alignment tolerance						3	3	3	3															
12	9	3.33	Tests wide range of materials	Tension Force	9	9			9	9	3	9	3	9										3	3			
13	9	3.33	Tests to sample failure	Young's Modulus	3	3			9					9							9			3	3		3	
14	9	8.33	Stable	Footprint		9										9			3	9	3	3						
15	3	5.00	Ease of use	Stall Torque			1	3	1							3		3			3							
16	9	3.33	Cost	Overall Height								3										9	9	9	3	3		

Correlations: Positive (+) or Negative (-)

Row Number	Column Number	1	2	3	4	5	6	7	8	9	10	11	12	13	14	15	16	17	18	19	20	21	22	23	24
	Quality Characteristics (a.k.a. "Functional Requirements" or "Hows")	Gripping force	Gripping friction coefficient	Weight	Test height	Depth	Gauge length	Tension motor load	Tension grip speed	Torsion motor load	Torsion grip speed	Alignment tolerance	Tension Force	Young's Modulus	Footprint	Stall Torque	Overall Height	Deflection due to vibration	Travel	Backlash	Budget	Tension Resolution	Torsion Resolution (at 5 mm)	Travel Step Size	Twist Step Size
1	Gripping force																								
2	Gripping friction coefficient																								
3	Weight																								
4	Test height			+																					
5	Depth			+																					
6	Gauge length			+																					
7	Tension motor load	+	+																						
8	Tension grip speed	+	+				+	-																	
9	Torsion motor load	+	+																						
10	Torsion grip speed	+	+				+				-														
11	Alignment tolerance						-																		
12	Tension Force	+	+					+	-																
13	Young's Modulus							+		+				+											
14	Footprint			+		+	+																		
15	Stall Torque							+	+	+	+														
16	Overall Height			+											+										
17	Deflection due to vibration			-			+	+		+	-			-											
18	Travel	+	+	+			+	+				-	+		+				+						
19	Backlash								+		+								+						
20	Budget																				-				
21	Tension Resolution													+								+			
22	Torsion Resolution (at 5 mm)													-								+			
23	Travel Step Size																						-		
24	Twist Step Size																							-	

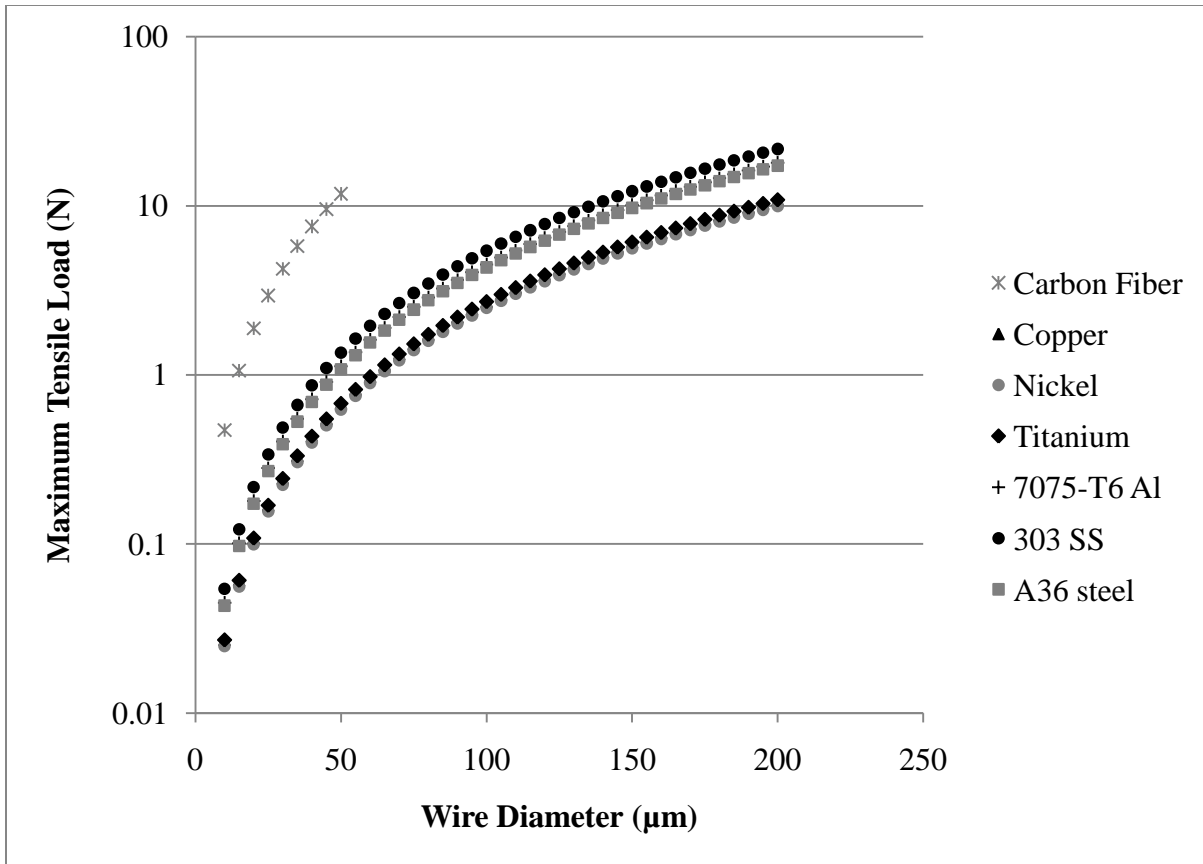
Row Number	Quality Characteristics (a.k.a. "Functional Requirements" or "Hows")	Minimize (▼), Maximize (▲), or Target (x)	Target or Limit Value	Max Relationship Value	Requirement Weight	Relative Weight (Relative Importance)
1	Gripping force	▲	175 N	9	211.67	6.63%
2	Gripping friction coefficient	▲	0.25	9	211.67	6.63%
3	Weight	▼	40 lbs.	9	152.50	4.78%
4	Test height	x	> 31 mm	9	103.33	3.24%
5	Depth	▼	300 mm	9	87.50	2.74%
6	Gauge length	x	1-75 mm	9	280.00	8.77%
7	Tension motor load	x	0.2 Nm	9	65.00	2.04%
8	Tension grip speed	x	10 ⁻⁶ - 10 ⁻³ m/s	9	102.50	3.21%
9	Torsion motor load	x	15 mNm	9	132.50	4.15%
10	Torsion grip speed	x	60 rpm	9	140.00	4.38%
11	Alignment tolerance	x	0.5 °	9	195.00	6.11%
12	Tension Force	x	5 mN - 33 N	9	150.00	4.70%
13	Young's Modulus	x	210 Gpa	1	12.50	0.39%
14	Footprint	▼	0.18 m ²	9	162.50	5.09%
15	Stall Torque	▼	15 mNm	9	82.50	2.58%
16	Overall Height	▼	250 mm	3	55.00	1.72%
17	Deflection due to vibration	▼	2 μm	9	160.83	5.04%
18	Travel	x	125 mm	9	152.50	4.78%
19	Backlash	▼	0.1 mm	9	110.83	3.47%
20	Budget	x	5000	9	30.00	0.94%
21	Tension Resolution	▲	5*10 ⁻⁴ N	9	170.00	5.32%
22	Torsion Resolution (at 5 mm)	▲	9.3*10 ⁻⁸ N	9	170.00	5.32%
23	Travel Step Size	▼	4 μm	9	122.50	3.84%
24	Twist Step Size	▼	0.096°	9	132.50	4.15%

APPENDIX B

Load by Material

Material	Ultimate Stress (MPa)	Shear Modulus (GPa)	Diameter (μm)	Maximum Tensile Load (N)	Maximum Torsion Load (N*m)	Grip Shear (MPa)
Carbon						
Fiber	6000		10	4.71E-01	2.36E-06	1.63E+03
	6000		50	1.18E+01	2.95E-04	1.63E+03
Copper	344	46	10	2.70E-02	1.35E-07	9.34E+01
	344	46	100	2.70E+00	1.35E-04	9.34E+01
	344	46	200	1.08E+01	1.08E-03	9.34E+01
Nickel	317	76	10	2.49E-02	1.24E-07	8.60E+01
	317	76	100	2.49E+00	1.24E-04	8.60E+01
	317	76	200	9.96E+00	9.96E-04	8.60E+01
Titanium (grade 9)	689	45	10	5.41E-02	1.35E-07	9.36E+01
	689	45	100	5.4113933	1.35E-04	9.36E+01
	689	45	200	21.645573	1.08E-03	9.36E+01
7075-T6						
Al	572	26.9	10	4.49E-02	2.25E-07	1.55E+02
	572	26.9	100	4.49E+00	2.25E-04	1.55E+02
	572	26.9	200	1.80E+01	1.80E-03	1.55E+02
303 SS	690	86	10	5.42E-02	2.71E-07	1.87E+02
	690	86	100	5.42E+00	2.71E-04	1.87E+02
	690	86	200	2.17E+01	2.17E-03	1.87E+02
A36 steel	550	79.3	10	4.32E-02	2.16E-07	1.49E+02
	550	79.3	100	4.32E+00	2.16E-04	1.49E+02
	550	79.3	200	1.73E+01	1.73E-03	1.49E+02

Material	Diameter (μm)	Twist Angle per Length	Angle at Failure Torsion Load at 1mm (rad)	Angle at Failure Torsion Load at 1mm (deg)	Resolution (50 points, deg)
Carbon Fiber	10				
	50				
Copper	10	2991.30	2.991E+00	1.714E+02	3.428E+00
	100	299.13	2.991E-01	1.714E+01	3.428E-01
	200	149.57	1.496E-01	8.569E+00	1.714E-01
Nickel	10	1668.42	1.668E+00	9.559E+01	1.912E+00
	100	166.84	1.668E-01	9.559E+00	1.912E-01
	200	83.42	8.342E-02	4.780E+00	9.559E-02
Titanium (grade 9)	10	3066.67	7.874E+00	4.512E+02	9.023E+00
	100	306.67	7.874E-01	4.512E+01	9.023E-01
	200	153.33	3.937E-01	2.256E+01	4.512E-01
7075-T6 Al	10	8505.58	8.506E+00	4.873E+02	9.747E+00
	100	850.56	8.506E-01	4.873E+01	9.747E-01
	200	425.28	4.253E-01	2.437E+01	4.873E-01
303 SS	10	3209.30	3.209E+00	1.839E+02	3.678E+00
	100	320.93	3.209E-01	1.839E+01	3.678E-01
	200	160.47	1.605E-01	9.194E+00	1.839E-01
A36 steel	10	2774.27	2.774E+00	1.590E+02	3.179E+00
	100	277.43	2.774E-01	1.590E+01	3.179E-01
	200	138.71	1.387E-01	7.948E+00	1.590E-01



List of Equations

$$\text{Maximum Torsion Load} = \frac{\text{Ult. Stress}}{R/2J}$$

$$\text{Angle at Failure Torque at 1 mm} = \frac{\text{Torque}_{max} * 1\text{mm}}{J * \text{Shear Modulus}}$$

$$\text{Maximum Tensile Load} = \text{Ult. Stress} * \text{Area}$$

$$v = \frac{TL^3}{3rbh^3E}$$

T = torque

L = beam length

E = Young's Modulus

r = inner radius

b = beam depth in the axial direction

h = beam thickness in the bending direction

APPENDIX C

Justification of QFD Values

Gripping Friction Coefficient and Gripping Force

The gripping friction coefficient was determined under the assumption that the test wire was not glued to the test grips. To ensure that the needed gripping force calculated would be sufficient for all wire materials, the value was chosen to be in the low range of metal-on-metal friction coefficients.

The gripping force was calculated based on the chosen friction coefficient and twice the maximum tensile load expected as calculated in Appendix B. As a check, the calculated force is also sufficient to resist the maximum expected torque with a safety factor of 1.2.

Mass

In the interest of mobility, the target value of 40 pounds was chosen as a mass that a single person would be able to move when setting up tests.

Test Height and Depth

The test height and base depth values are dependent on the base dimensions of the stereo microscope that will be used in testing. The apparatus must clear the 31 mm high base. The distance from the center of the microscope lens to the support column is 150 mm. Doubling this dimension yields the maximum mechanism depth of 300 mm.

Gauge Length

Professor Daly requested that the mechanism be able to test wire samples 1 - 75 mm in length. Due to stress concentrations at the edge of a blunt grip, the shortest wire we will be able to test will be no shorter than 3.175 mm.

Tension Motor Load

The tension motor load was calculated based on the maximum expected tensile load calculated in Appendix B. The maximum load was multiplied by the maximum torque necessary to raise one kN as listed on <http://www.nookindustries.com/ball/BallMetricAvailability.cfm>. The resulting torque on the ball screw was then multiplied by 10 to ensure that the motor will be able to overcome any friction in the grip guide system. While the torque factor was most likely higher than the ball screw we will use, it is better to oversize the motor than undersize it.

Tension Grip Speed

Professor Daly requested that the mechanism be able to test strain rates as high as 10^{-2} . For a 100 mm test wire, this translates to 1 mm/s.

Torsion Motor Load

The torsion motor load was determined from the maximum test torque as calculated in Appendix B with a safety factor of 3.5 to ensure that the motor can overcome system friction.

Torsion Grip Speed

The maximum torsion grip speed was chosen to be 60 rpm. The mechanism must be able to compensate for lengthening of the wire under torsion loads to prevent the wire from buckling. Verification that the wire is not buckling will be done by sight and the operator must have time to react. This value is likely faster than tests will be run anyway.

Alignment Tolerance

Professor Daly requested that the mechanism be able to hold the micro wires with an alignment error of 0.5° or smaller. This translates to an allowable grip alignment error of 0.087 mm for a 10 mm wire.

Tension Force

The tensile loads needed to break wires of several materials are listed in Appendix B. A safety factor of 1.5 was applied to the highest expected load for design criteria to ensure that the mechanism does not break.

Young's Modulus

We expect to make the mechanism frame out of 6061 Aluminum. The Young's Modulus will be used in the mechanical analysis.

Footprint

A larger footprint will ensure a more stable test platform. Initially we specified a maximum footprint of 0.18 m^2 allows for a frame that is 300 mm deep and 600 mm wide. The final mechanism requires a footprint that is 254 mm deep and 457.2 mm wide for an area of 0.12 m^2 .

Stall Torque

To avoid jerking the wire, we would like to minimize the stall torque of the torsion motor. In very small motors, the stall torque is high relative to the continuous torque of the motor. The stall torque was therefore listed as $15 \text{ mN}\cdot\text{m}$, the same as a maximum operating torque specified, with the intent to find a motor with as small of stall torque as is available for a reasonable price.

Overall Height

Keeping in mind the need to work with the mechanism around the microscope, we have set the maximum mechanism height to be 250 mm with the intent to make the final design much shorter.

Deflection due to Vibration

The mechanism will be driven by two motors and will therefore be subject to some small amount of vibration. To avoid influencing the data, we have set a target of a maximum deflection of $2 \mu\text{m}$ with hopes of an even stiffer design.

Travel

Professor Daly requested that the mechanism be able to test micro wires from 1-75 mm in length with strains exceeding 20%. To ensure the mechanism can break all samples, we are designing for 125 mm of travel.

Backlash

Typical backlash for a ball screw is about 0.1 mm. The acquisition of a more precise ball screw will be subject to budget constraints.

<http://www.nookindustries.com/ball/BallCarryInfo.cfm?id=21>

Sensor Resolution

Measurements of the very small loads on the thinner wires will be difficult to measure. We are hoping to find sensors to measure 0.001N in order to take readings before the smaller wires yield.

Budget

Professor Daly initially specified a budget of \$5000. Due to the instrumentation costs to measure such small loads, the budget has been increased. Current estimates of final cost are approximately \$9000 - \$10,000 including the capacitance probes.

Tension Resolution

As shown in Appendix B, the smallest tensile load we expect to see a wire break at is $2.49E-2$ N. In order to plot an accurate elasticity curve, a minimum of 50 data points is desirable. This translates to a tension load resolution of $5E-4$ N.

Tension Resolution

As shown in Appendix B, the smallest torsion load we expect to see a wire break at is $1.24E-7$ N*m. In order to plot an accurate elasticity curve, a minimum of 50 data points is desirable. This translates to a torsion load resolution of $2.49E-9$ N*m. This load is far below any off the shelf torsion sensor.

Travel Step Size

For most of the metals that will be tested on this machine we expect approximately a 20% elongation before breaking. For a 1 mm wire sample this would mean a $200\mu\text{m}$ travel throughout the test. In order to record 50 data points this translates to a linear travel step size of $4\mu\text{m}$. For a ball screw with a 1 mm lead this equates to a motor step of 1.44° .

Twist Step Size

As shown in Appendix B, the smallest twist we expect to see a 1 mm wire fail is 4.8° . Since the torsion motor is connected to the rotating grip without any gearing, in order to record 50 data points the motor step size must be 0.096° or less.

APPENDIX D

Additional Concept Drawings

Figure D1. Disposable V-groove Trays with Epoxy Grip Concept Drawing

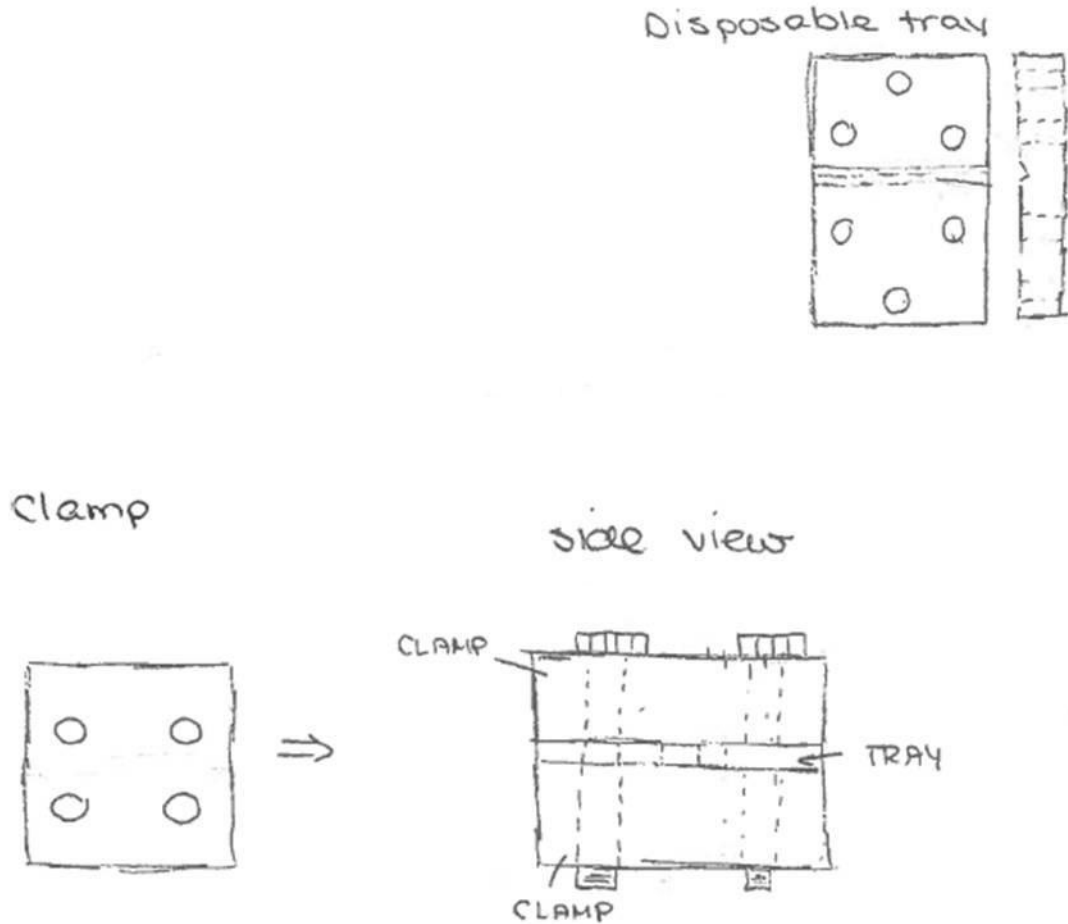
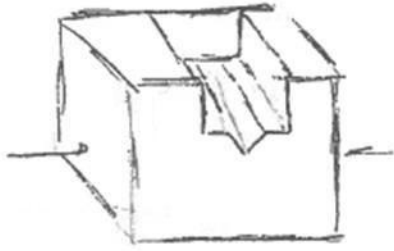


Figure D1 show the concept idea for disposable V-groove trays with epoxy. The disposable V-groove trays would be made out of some type of plastic or thin metal. The idea would be to lay the wire into the V-groove and then paint epoxy over this V-groove. The entire disposable tray would then be clamped into a grip.

Figure D2. Epoxy Only Grip



Epoxy into slot over
wire and grip
entire block

Figure D2 above shows the epoxy only grip concept. The epoxy only grip was a simple design using a block of wax or other material into which a cube is milled out. The wire is then laid into the etched out cube and then the cube is filled in with epoxy. The entire cube can be gripped using a clamping mechanism.

Figure D3. Spool Design Alignment Mechanism

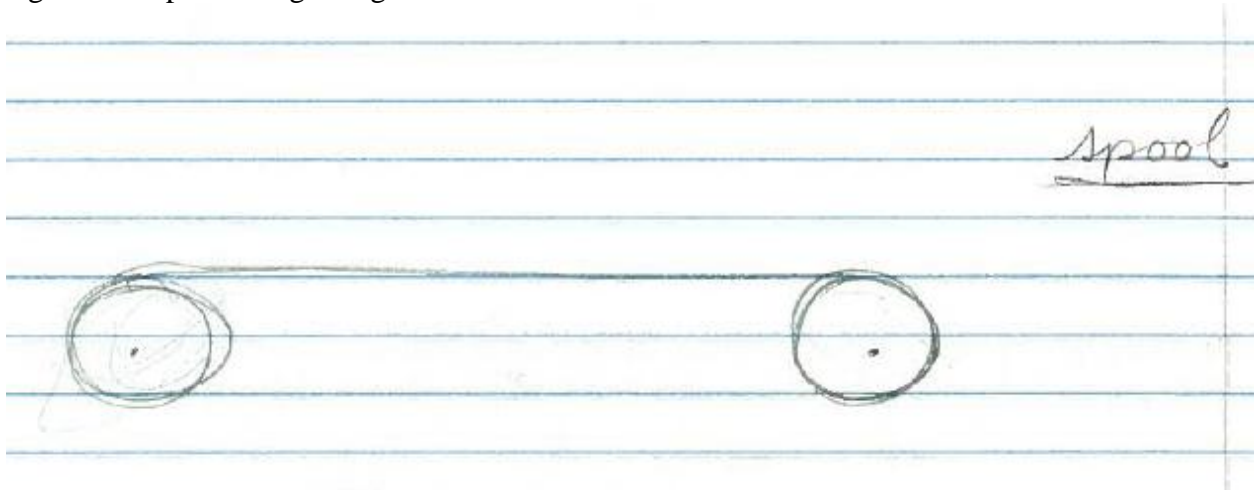


Figure D3 shows a general idea for aligning the wires. If the wires were wrapped around two spools or posts and the posts were aligned, then the wire would also be aligned because they would be tangent to the spools. This method would not maintain alignment in the vertical plane.

APPENDIX E

Concept Selection Matrices

Table E1. Complete Concept Selection Matrix for Gripping

Selection Criteria	Concepts							
	1	2	3	4	5	6	7	8
Grips wires without slipping	0	+	+	0	0	0	0	-
Consistent alignment	-	0	-	0	+	+	+	0
Cost	0	0	0	+	0	0	-	+
Tests wide range of materials	0	+	+	0	-	-	-	-
Ease of use	0	-	-	0	+	0	0	0
Stress Concentrations	0	+	+	-	-	-	0	0
Sum +'s	0	3	3	1	2	1	1	1
Sum 0's	5	2	1	4	2	3	3	3
Sum -'s	1	1	2	1	2	2	2	2
Net Score	-1	2	1	0	0	-1	1	-1
Rank	N/A	1	2	3 (tie)	3 (tie)	4 (tie)	4 (tie)	4 (tie)
Continue?	N/A	Yes	Yes	Yes	No	No	No	No

Table E2. Concept Numbers with Corresponding Descriptions

Concept	Description
1	Fleck and Hutchinson
2	Compressive Sleeve
3	Rubber Clamp w/Post
4	Glued Knot
5	V-Groove Clamp
6	Thrust Bearings
7	Disposable Trays
8	Epoxy Only

Table E3. Complete Concept Selection Matrix for Alignment

Selection Criteria	Concepts						
	Fleck and Hutchinson	Micrometer	Cylindrical Joint	Spool Design	Thrust Bearing	Laser	U-Joint
Resists buckling	0	0	0	-	0	0	0
Maintains alignment	0	0	+	0	+	0	-
Cost	0	0	0	+	0	0	0
Ease of use	0	+	0	0	-	-	0
Sum +'s	0	1	1	1	1	0	0
Sum 0's	4	3	3	2	2	3	3
Sum -'s	0	0	0	1	1	1	1
Net Score	0	1	1	0	0	-1	-1
Rank	N/A	1 (tie)	1(tie)	2 (tie)	2 (tie)	3 (tie)	3 (tie)
Continue?	N/A	Yes	Yes	Revise	No	Revise	No

Table E4. Concept Selection Matrix for Displacement Sensors

Selection Criteria	Concepts		
	Fleck and Hutchinson	Optical Encoder	Linear Variable Differential Transducer
Suitable gauge length	0	+	-
High testing resolution	-	+	0
Low Cost	0	-	0
Tests wide range of materials	0	+	-
Ease of use	-	+	0
Sum +'s	0	4	0
Sum 0's	3	0	3
Sum -'s	2	1	2
Net Score	-2	3	-2
Rank	N/A	1	2
Continue?	N/A	Yes	No

Table E5. Concept Selection Matrix for Force Sensors

Selection Criteria	Concepts		
	Diaphragm with Strain Gages	Load Cell	Cantilever with Strain Gages (Fleck and Hutchinson)
High testing resolution	+	-	+
Cost	-	0	0
Tests wide range of materials	0	-	-
Maintains alignment	0	0	-
Ease of use	0	+	-
Sum +'s	1	1	1
Sum 0's	3	2	1
Sum -'s	1	2	3
Net Score	0	-1	-2
Rank	1	2	3
Continue?	Yes	Revisit	Revisit

APPENDIX F

Bench Level Experiment Figures

Figure F1. Successful Post Wrapping Experiment



Figure F1 above shows a test being performed with 196 μm copper wire wrapped around a bolt which is being used as a post. During this test, the grip held and the wire broke halfway in between the bolt and the pliers.

Figure F2. Successful Rubber Clamp Experiment



Figure F2 above shows a test being performed using two rubber erasers as a rubber clamp. This grip held as well with the wire breaking halfway between the grip and the pliers. The right hand portion of the figure shows what the wire looked like in the grip after the experiment. This shows that the wire did not slip in the grip because it retained its original bent position.

APPENDIX G

Bill of Materials

Vendor	Part #	Item name	Qty	Unit	Unit price	TOTAL	Note
Velmex	MN10-0050-M01-21	BiSlide, travel=5 inch, 1mm/rev, limits, NEMA 23	1	ea	\$744.00	\$744.00	
Velmex	PK264-03A-P1	Vexta Type 23T1, Single shaft stepper motor	1	ea	\$120.00	\$120.00	
Velmex	MC-2	Cleat Standard BiSlide	4	ea	\$5.00	\$20.00	
Velmex	MB-1	BiSlide Bolt 1/4-20x3/4" (10 pack)	1	pack age	\$3.00	\$3.00	
Velmex	585271-06-bis	Acu-Rite Linear Encoder, 1 micrometer, SENC150	1	ea	\$659.00	\$659.00	
Lin Engineering	4018S-01D-XX	1.33" Standard Motor, 1.8 degree step with damper and encoder	1	ea	\$175.00	\$175.00	
Lin Engineering	N/A	R256 Controller, Single Axis Controller + Driver	1	ea	\$199.98	\$199.98	
RMS Technologies	N/A	R356 Controller, Single Axis Controller + Driver	1	ea	\$249.00	\$249.00	*
Lin Engineering	N/A	R356 Controller, Single Axis Controller + Driver	1	ea	\$249.00	\$249.00	
Lin Engineering	PW-100-24	PW-100 Series Power Supply	1	ea	\$99.84	\$99.84	
Lin Engineering	083-00036	Designer's Kit w/ USB485 for SP 23C	1	ea	\$99.00	\$99.00	
Radio Shack	22-508	13.8 VCD 15-Amp Power Supply	1	ea	\$84.99	\$84.99	*
US Digital	CA-LC5-SH-NC-6	Shielded cable, 5-pin locking, unterminated, 6 ft long	1	ea	\$13.88	\$13.88	
Measurement Computing	PCI-QUAD04	4 Channel quadrature encoder board	1	ea	\$399.00	\$399.00	
Measurement Computing	CIO-MINI37	4x4 Universal screw terminal	1	ea	\$69.00	\$69.00	
Measurement Computing	C37FFS-5	37-conductor shielded cable, female to female, 5 ft long	1	ea	\$35.00	\$35.00	
Barcode Giant	1550-201531	Unitech cable RS-232, DB-9	1	ea	\$25.80	\$25.80	
Futek	FSH00103	5 lb JR S-Beam Load Cell	1	ea	\$450.00	\$450.00	
Futek	SLT00002	Tension calibration for load cell	1	ea	\$0.00	\$0.00	
Futek	FSH02465	TEDS chip for load cell	1	ea	\$150.00	\$150.00	
Lion Precision	C23-C	Capacitance Probe, 250 micrometer range, 5 or 10 nm resolution	2	ea	\$675.00	\$1,350.00	
Lion Precision	CPL290-2-2	Two channel driver	1	ea	\$7,380.00	\$7,380.00	
Thor Labs	MS1	Micrometer stage	2	ea	\$172.40	\$344.80	
Thor Labs	MS102	Micrometer stage bracket	2	ea	\$29.60	\$59.20	
Thor Labs	MB1224	Aluminum bread board,	1	ea	\$282.30	\$282.30	

		12"x18"x1/2"					
Thor Labs	VB01	Vertical bracket for bread boards	2	ea	\$83.60	\$167.20	
Custom Fabricated		Grips	2	ea	\$65.00	\$130.00	
Custom Fabricated		Clamp plates	2	ea	\$40.00	\$80.00	
Henze Industries		Flexure	1	ea	\$650.00	\$650.00	^
Henze Industries		Flexure	1	ea	-\$650.00	-\$650.00	#
Arnold Tool & Die Co.		Motor mount	1	ea	\$200.00	\$200.00	^
Arnold Tool & Die Co.		Motor mount	1	ea	-\$200.00	-\$200.00	#
McMaster-Carr	97395A461	3/16" SS Dowel	1	ea	\$7.42	\$7.42	
McMaster-Carr	97395A451	1/8" SS Dowel	1	ea	\$7.18	\$7.18	
McMaster-Carr	2463K3	5mm Helical Shaft Coupling	1	ea	\$28.16	\$28.16	
McMaster-Carr	6391K443	5/16" ID, 1/2" OD Bronze Sleeve Bearing	3	ea	\$1.29	\$3.87	
McMaster-Carr	6391K178	3/8" ID, 1/2" OD Bronze Sleeve Bearing	2	ea	\$0.97	\$1.94	
McMaster-Carr	93600A150	14mm SS Dowel	1	ea	\$5.46	\$5.46	
McMaster-Carr	98381A525	3/16" Dowel	1	ea	\$9.26	\$9.26	
McMaster-Carr	91829A523	4-40 x 1/8" Shoulder Screw	3	ea	\$1.80	\$5.40	
McMaster-Carr	95412A409	4-40 threaded Stud	1	ea	\$4.06	\$4.06	
McMaster-Carr	8873K36	Copper wire, 0.005" diameter	1	ea	\$7.12	\$7.12	
Alro Metals Plus		1/2" Al plate	1	ea	\$30.15	\$30.15	
Alro Metals Plus		1/4" Al plate	1	ea	\$3.35	\$3.35	
Alro Metals Plus		1/4" sq Al, 0.014" wall	1	ea	\$18.56	\$18.56	
Alro Metals Plus		3" x 2.5" Al	1	ea	\$16.75	\$16.75	
Grainger	MCLX-5-5-A	Rigid clamp coupling, 5 mm bore	1	ea	\$26.20	\$26.20	
Stadium Hardware		bolts and 3/32" dowels	31	ea	--	\$5.11	
Stadium Hardware		electrical connectors	40	ea	\$ 0.25	\$10.00	
		tax			--	\$5.03	
		shipping			--	\$200.00	^
					Total	\$14,034.01	
					Total (**)	\$5,304.01	

^ estimate; * replacement; # donation; ** total not including the capacitance probes

APPENDIX H

Load Cell Calculations

Data Acquisition System:

24 bit resolution
±25 mV/V inputs

Load Cell:

5 lbf Capacity
±2 mV/V read out

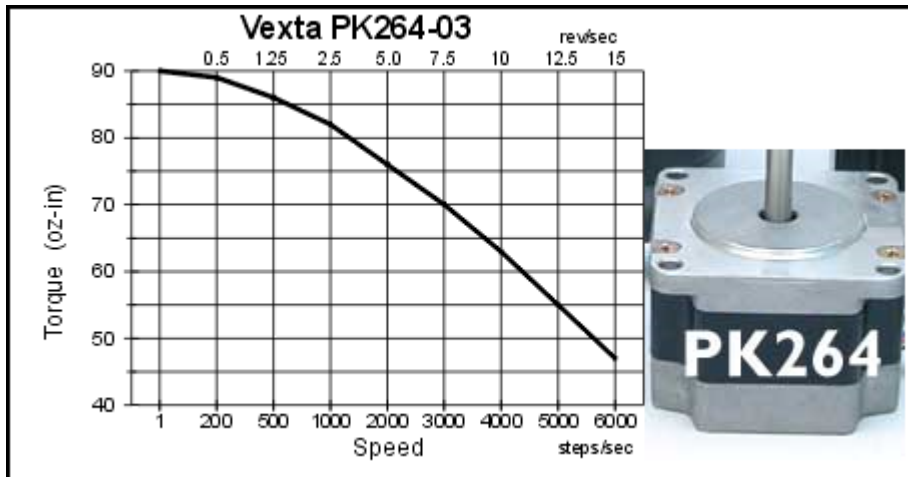
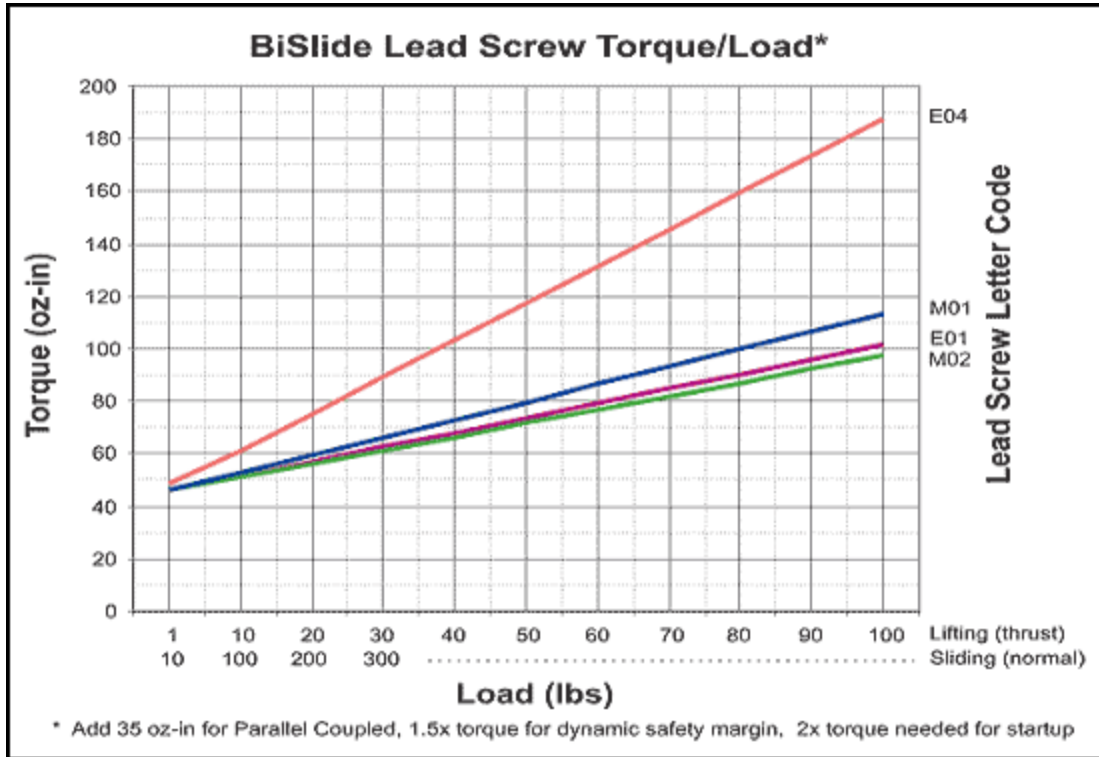
Resolution of DAQ: $2^{24} = 1.68(10^7)$ points

With the ±2 mV/V read out we are only using about 0.08 of our DAQ and therefore can achieve $1.34(10^6)$ data points with the load cell.

Using the 5 lbf load cell, this gives a resolution of $3.72(10^{-6})$ lbf ($1.65(10^{-5})$ N).

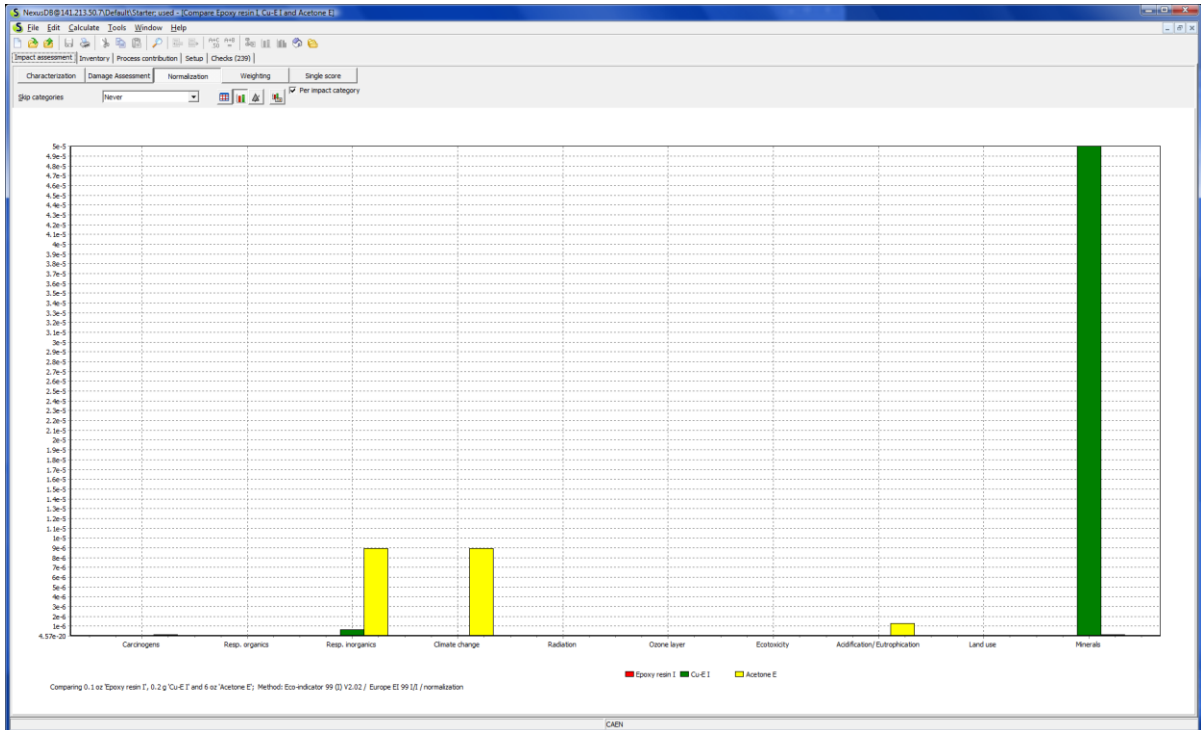
APPENDIX I

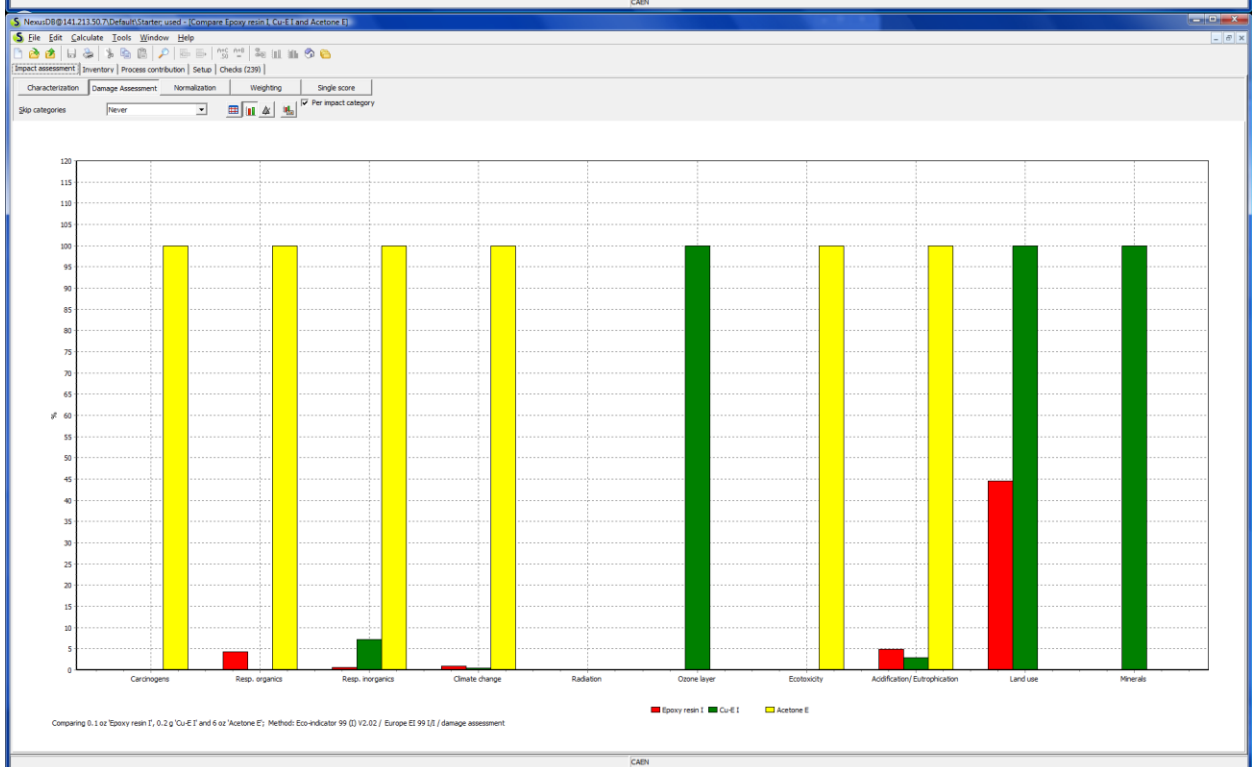
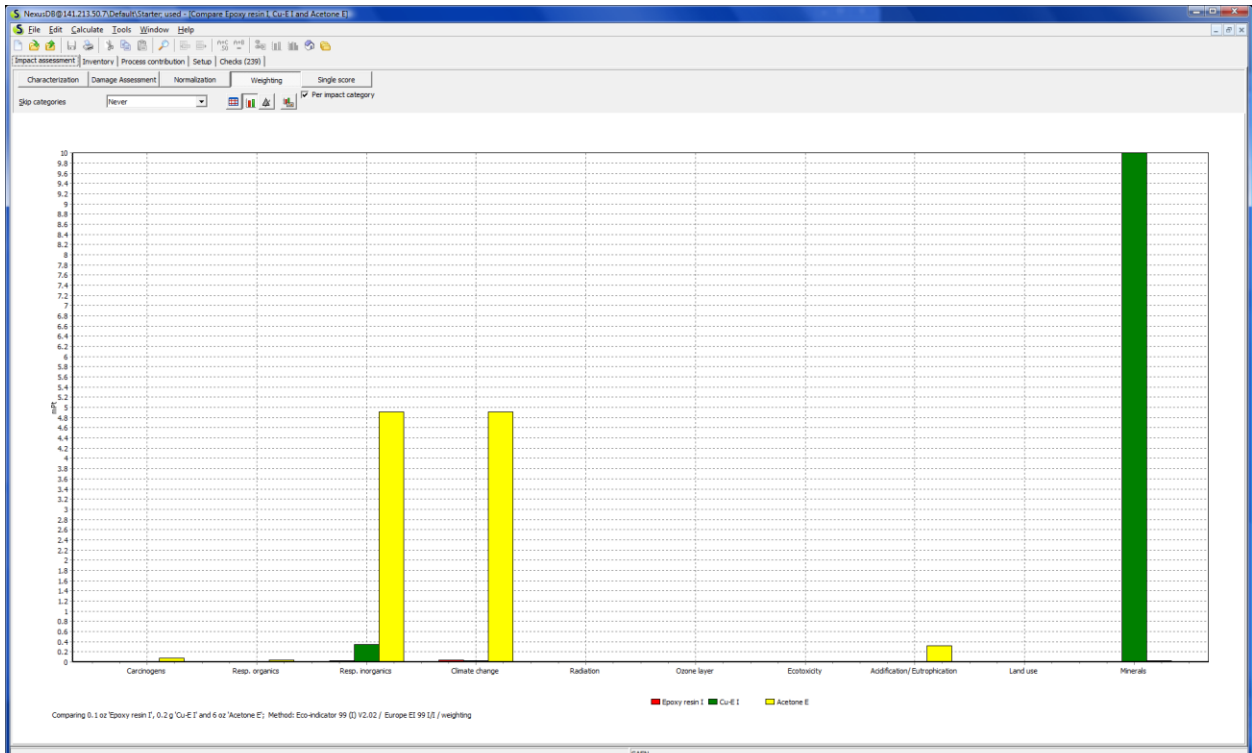
Tension Motor Graphs

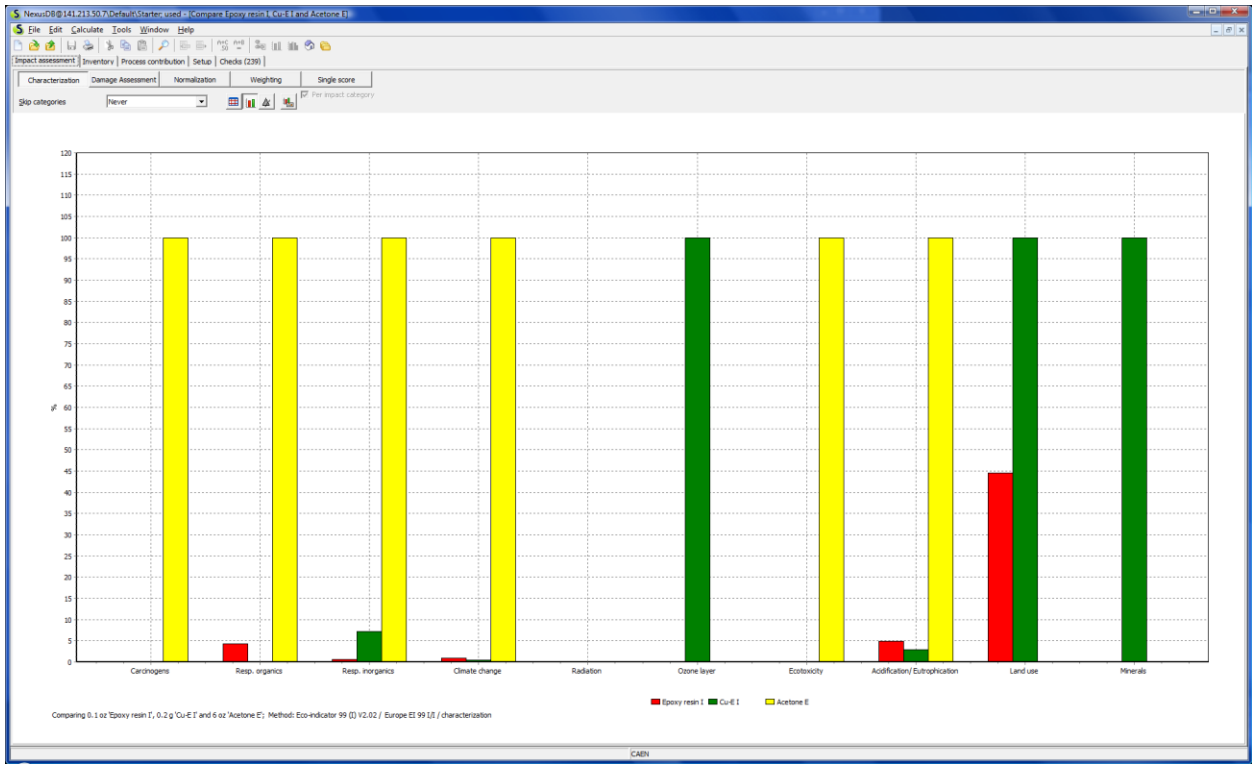


http://velmex.com/motor_torque.html

APPENDIX J

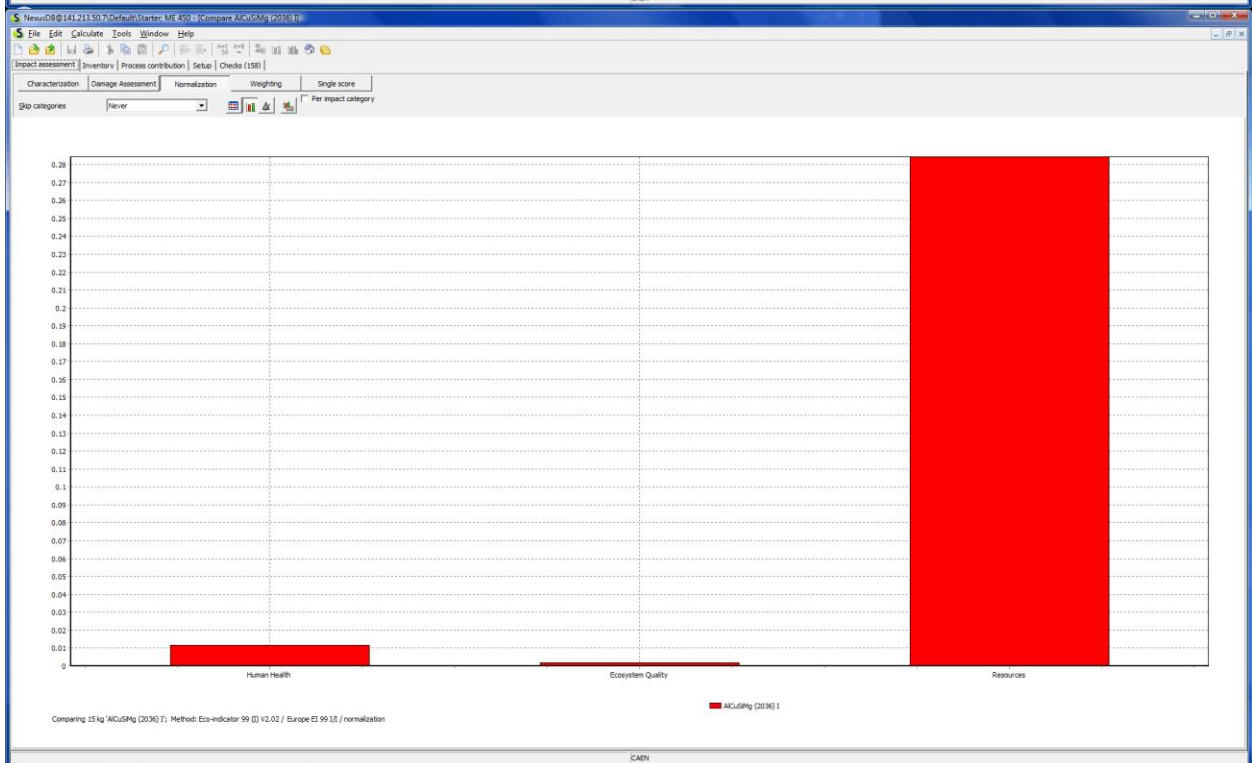
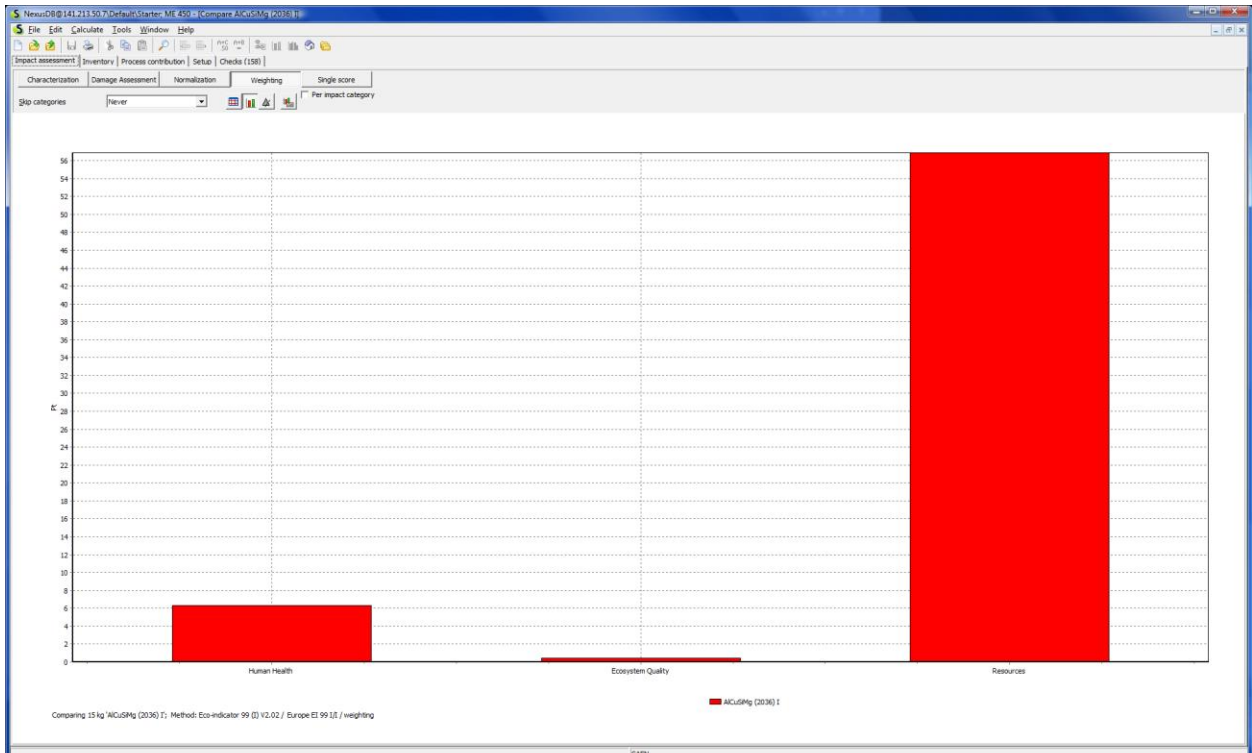


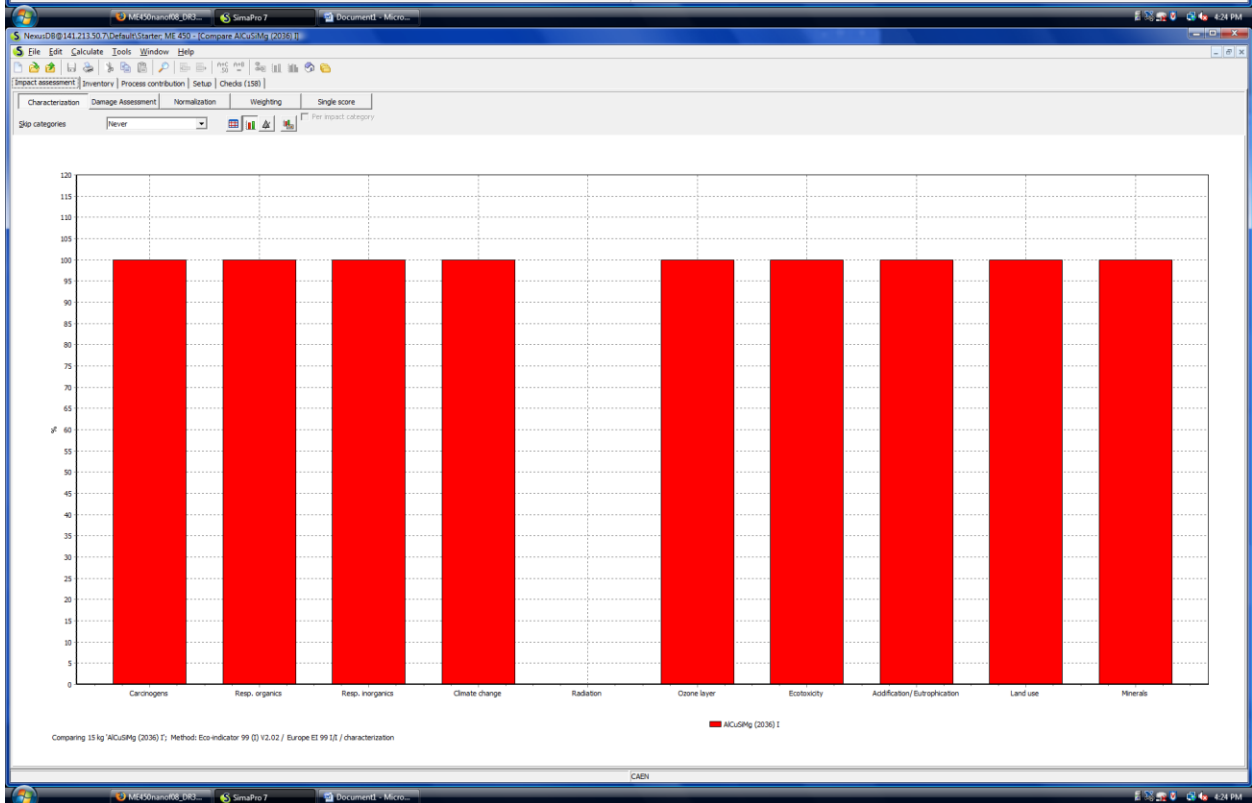
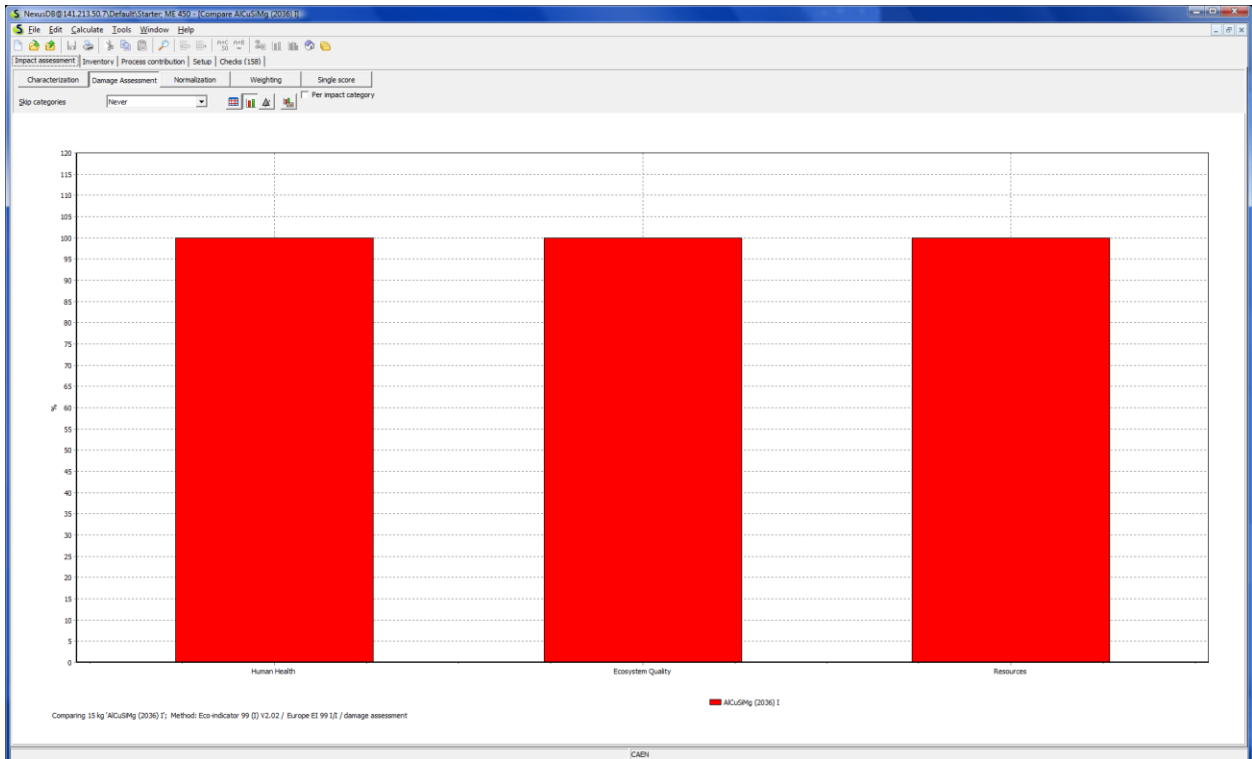




Aluminum

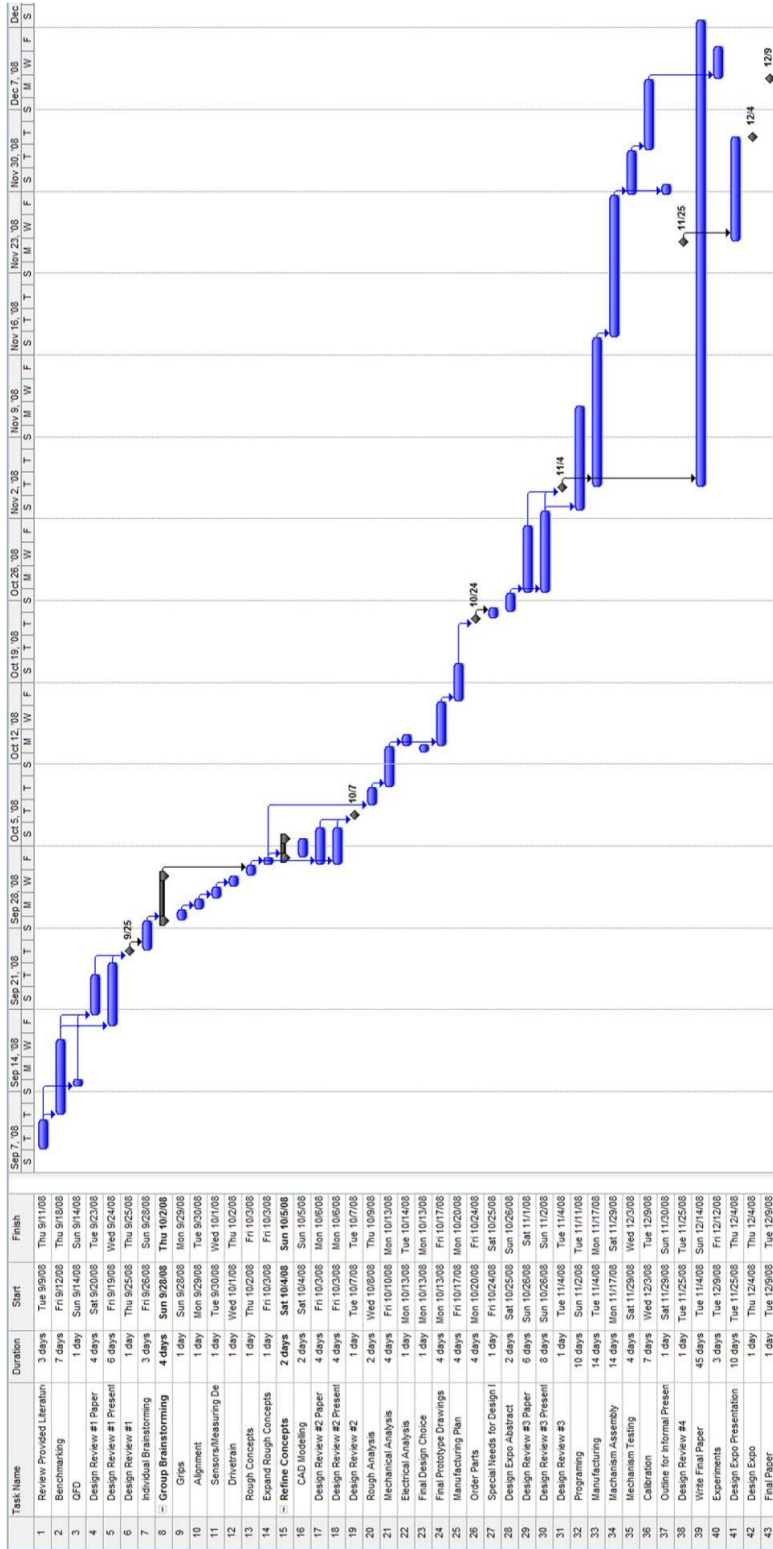






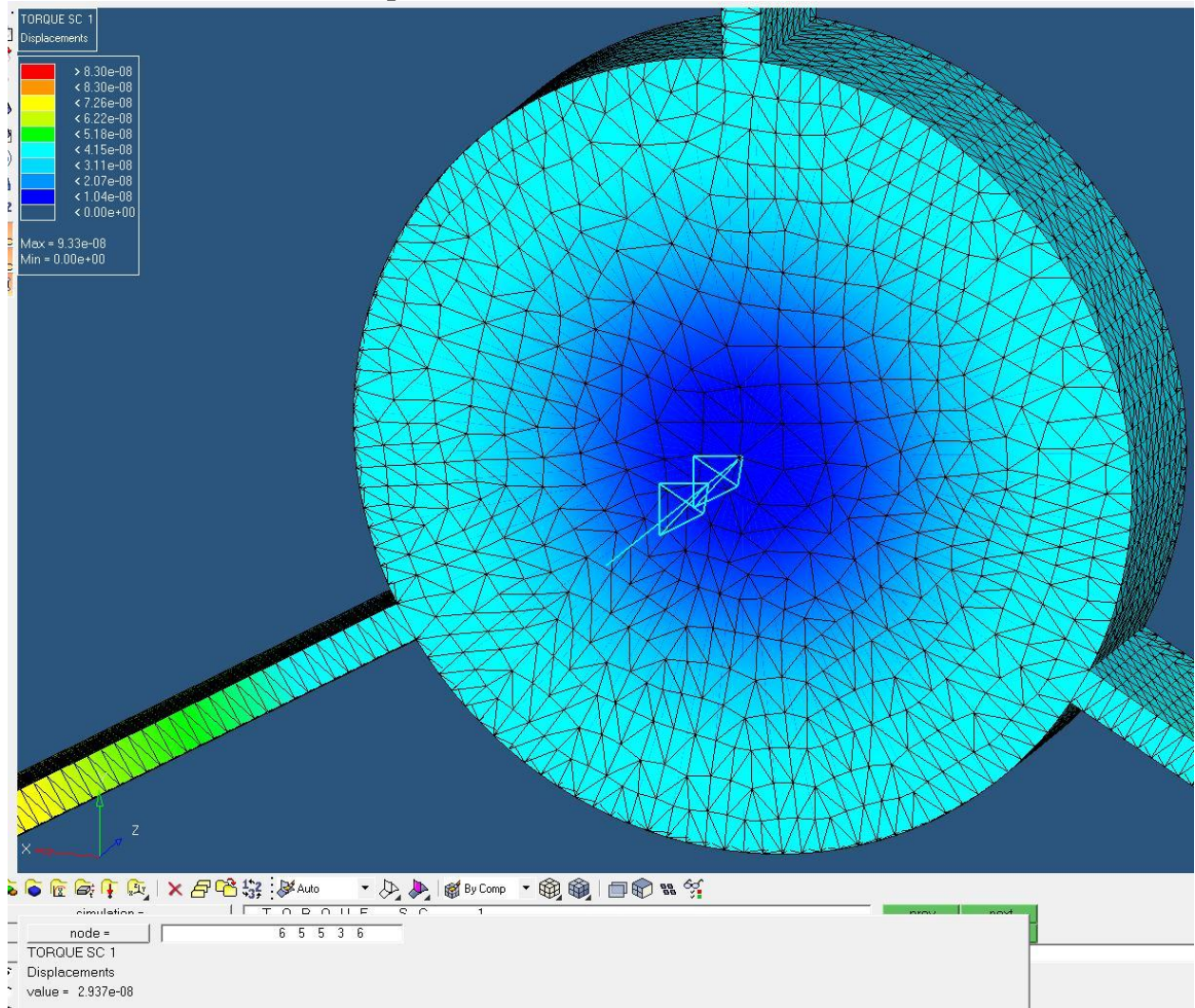
APPENDIX K

Gantt Chart



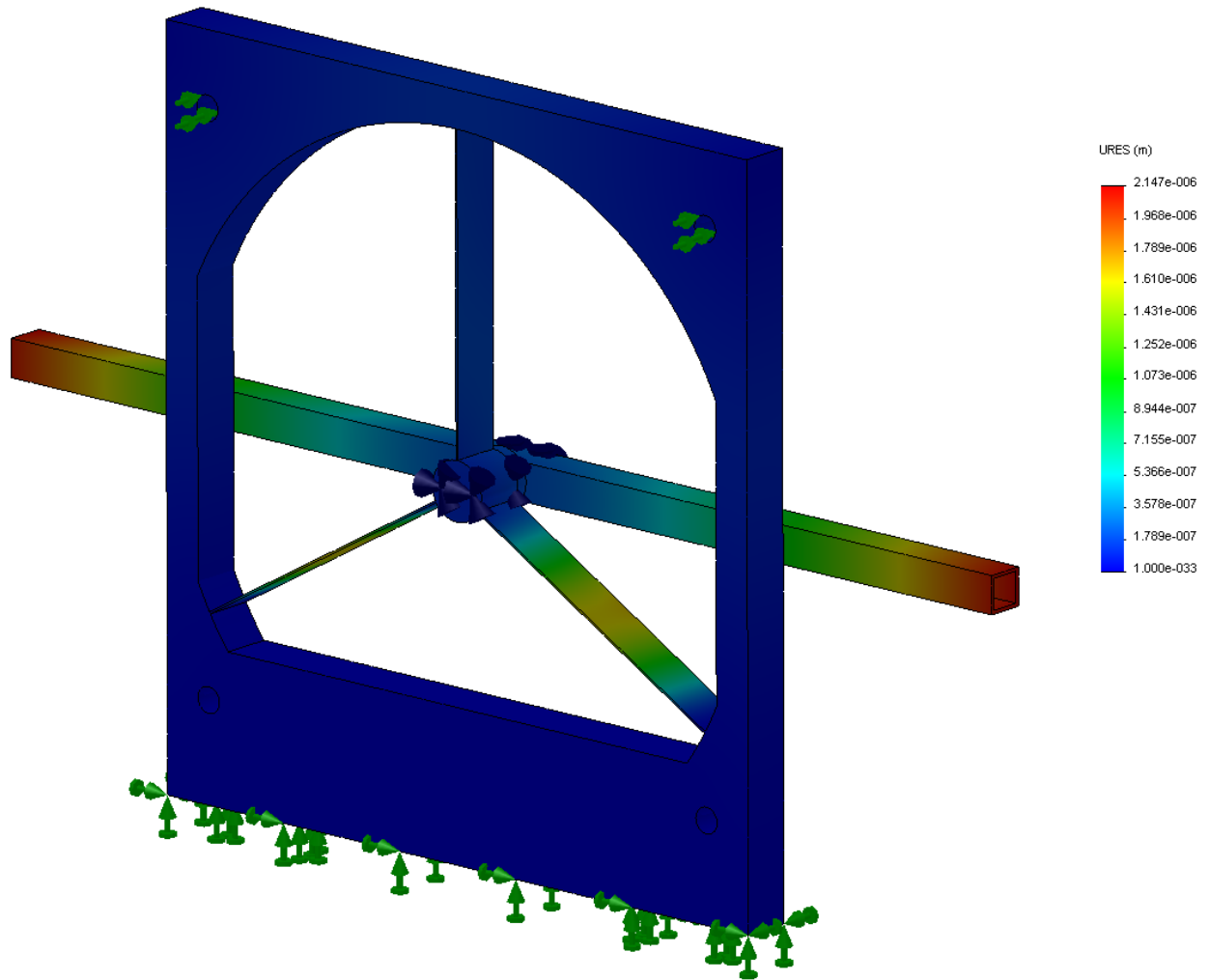
Hypermesh

Pure 2.49E-9 Nm Torsion Displacement in mm

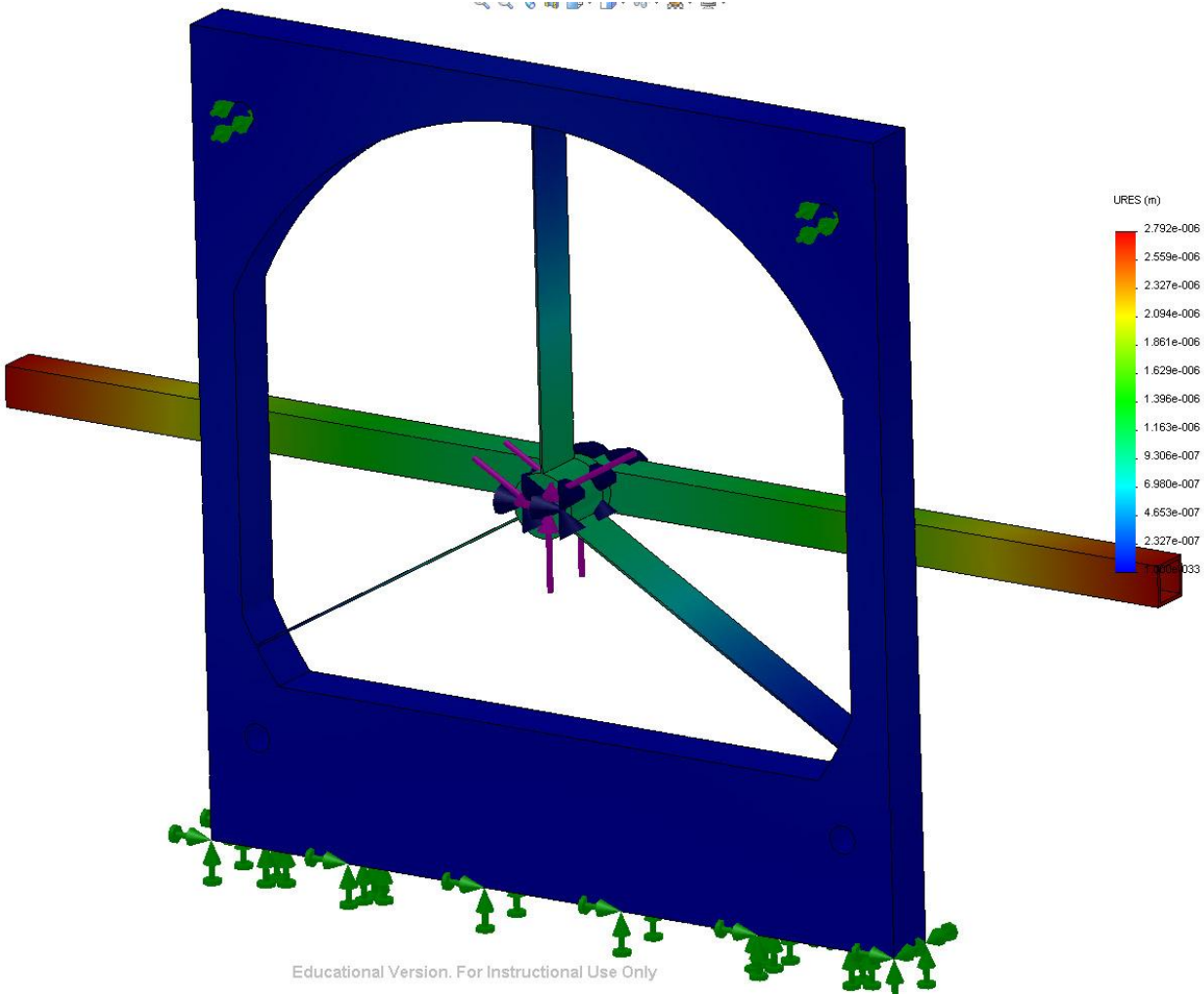


SolidWorks CosmosWorks

Displacement due to Weight

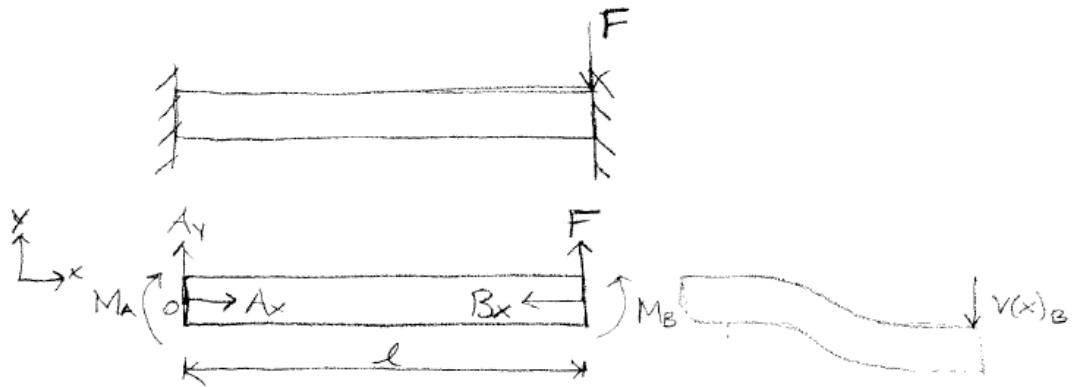


Displacement Due to Weight and 5E-9 Nm Torque



APPENDIX M

First Derivation of Flexure Math Model



$$\sum F_y: A_y + F = 0$$

$$\sum F_x: A_x - B_x = 0$$

$$\sum M_{z,pt.o}: -M_A + M_B + lF = 0$$

$$V_A = 0$$

$$\frac{dv}{dx} \Big|_B = 0$$

$$\frac{dv}{dx} \Big|_A = 0$$

$$\frac{\partial U}{\partial F} = V_B$$

$$= \int_0^l \frac{1}{EI} M(x) \frac{\partial M(x)}{\partial F} dx$$

$$\frac{\partial U}{\partial A_y} = 0$$

$$0 = \int_0^l \frac{1}{EI} (M_A + xA_y) x dx$$

$$0 = \int_0^l \frac{1}{EI} (M_A - xF) x dx = \frac{M_A}{EI} \int_0^l x dx - \frac{F}{EI} \int_0^l x^2 dx$$

$$0 = \frac{M_A}{EI} \frac{x^2}{2} \Big|_0^l - \frac{F}{EI} \frac{x^3}{3} \Big|_0^l$$

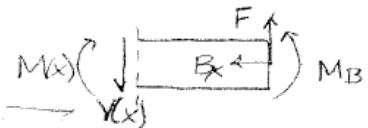


$$\sum F_y: -M_A + M(x) + xV(x) = 0$$

$$A_y + V(x) = 0$$

$$M(x) = M_A + xA_y$$

$$= M_A - xF$$



$$\sum F_y: -M(x) + M_B + (l-x)F = 0$$

$$F - V(x) = 0$$

$$M(x) = M_B + (l-x)F$$

$$= -\frac{1}{3}Fl + (l-x)F$$

$$0 = \frac{M_A}{EI} \frac{l^2}{2} - \frac{F}{EI} \frac{l^3}{3}$$

$$\frac{F}{EI} \frac{l^3}{3} \frac{(2EI)}{l^2} = M_A$$

$$M_A = \frac{2Fl}{3}$$

$$M_B = -lF + M_A = -lF + \frac{2Fl}{3}$$

$$M_B = -\frac{1}{3}Fl$$

$$V_B = \int_0^l \frac{1}{EI} \left(-\frac{1}{3}Fl + (l-x)F \right) \left(-\frac{1}{3}l + (l-x) \right) dx$$

$$= \int_0^l \frac{1}{EI} \left(-\frac{1}{3}Fl + lF - xF \right) \left(-\frac{1}{3}l + l - x \right) dx$$

$$= \int_0^l \frac{1}{EI} \left(\frac{1}{9}Fl^2 - \frac{1}{3}Fl^2 + \frac{1}{3}Flx - \frac{1}{3}l^2F + l^2F - lxF \right. \\ \left. + \frac{1}{3}Flx - lFx + x^2F \right) dx$$

$$= \int_0^l \frac{1}{EI} \left(\frac{4}{9}Fl^2 - \frac{4}{3}Flx + x^2F \right) dx$$

$$= \frac{1}{EI} \left(\frac{4}{9}Fl^2 \int_0^l dx - \frac{4}{3}Fl \int_0^l x dx + F \int_0^l x^2 dx \right)$$

$$= \frac{1}{EI} \left(\frac{4}{9}Fl^2 x \Big|_0^l - \frac{4}{3}Fl \frac{x^2}{2} \Big|_0^l + F \frac{x^3}{3} \Big|_0^l \right)$$

$$= \frac{1}{EI} \left(\frac{4}{9}Fl^3 - \frac{4}{3}Fl^3 + \frac{Fl^3}{3} \right)$$

$$V_B = \frac{1}{EI} \left(\frac{1}{9}Fl^3 \right)$$

Second Derivation of Flexure Math Model

$$EI \frac{d^2 v}{dx^2}(x) = M_B + (l-x)F$$

$$EI \frac{dv}{dx}(x) = M_B x + F l x - \frac{F x^2}{2} + C_1$$

$$EI v(x) = \frac{M_B x^2}{2} + \frac{F l x^2}{2} - \frac{F x^3}{6} + C_1 x + C_2$$

$$\frac{dv}{dx}(l) = 0$$

$$\frac{dv}{dx}(0) = 0$$

$$v(0) = 0$$

$$0 = C_2$$

$$0 = C_1$$

$$0 = M_B l + \frac{F l^2}{2} - \frac{F l^2}{6}$$

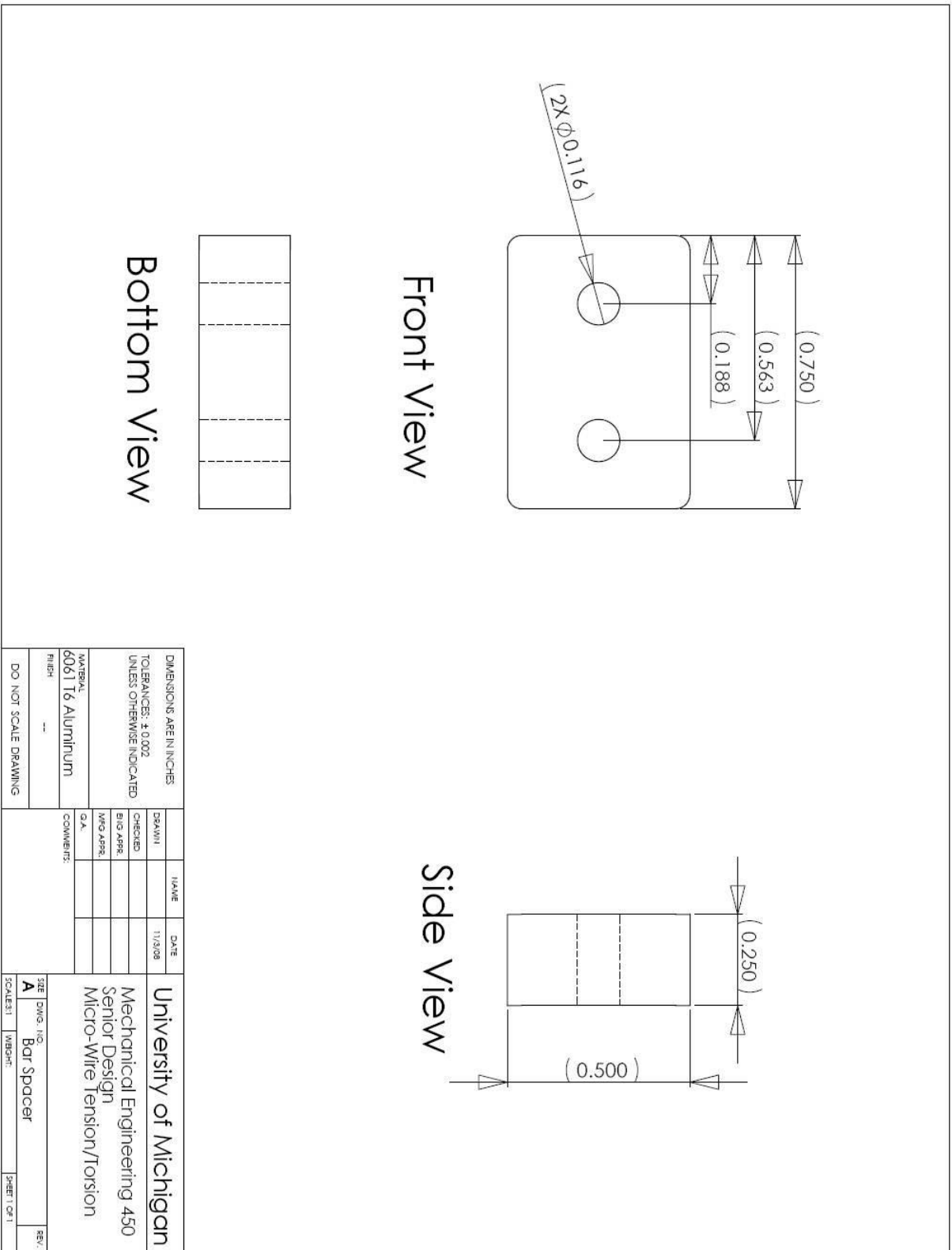
$$M_B = \frac{\frac{F l^2}{2} - \frac{F l^2}{6}}{l} = -\frac{1}{3} F l$$

$$\begin{aligned} v(x) &= \frac{1}{EI} \left(-\frac{1}{3} F l \frac{x^2}{2} + \frac{F l x^2}{2} - \frac{F x^3}{6} \right) \\ &= \frac{1}{EI} \left(-\frac{1}{6} F l^3 + \frac{F l^3}{2} - \frac{F l^3}{6} \right) \\ &= \frac{1}{EI} \left(\frac{1}{3} F l^3 \right) \end{aligned}$$

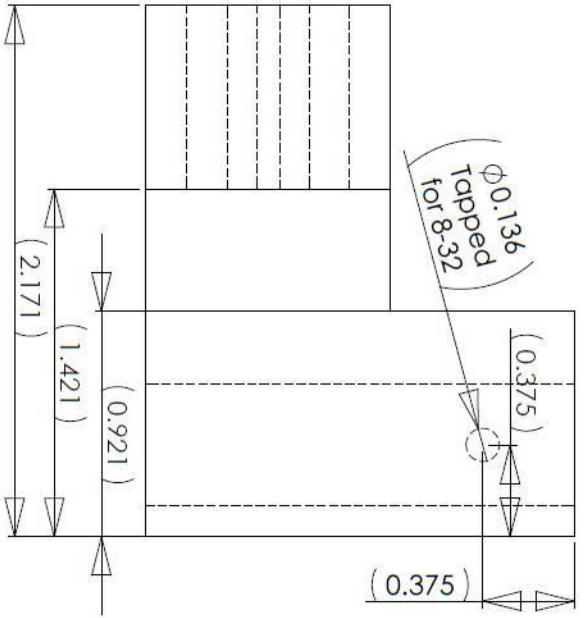
$$\begin{aligned} v(x) &= \frac{1}{EI} \left(\frac{1}{12} \frac{I}{3r} l^3 \right) \\ &= \frac{1}{E b h^3} \frac{I}{3r} l^3 \end{aligned}$$

APPENDIX N

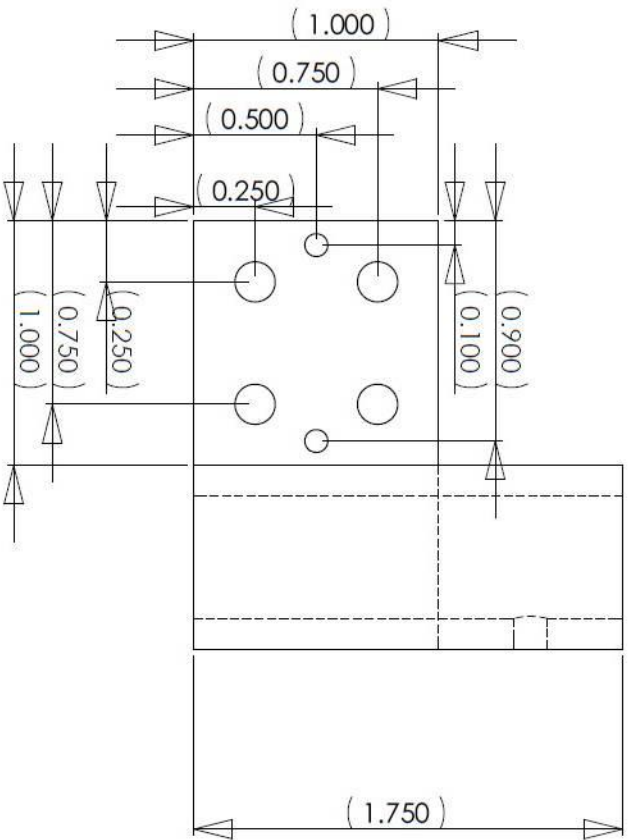
Engineering Drawings



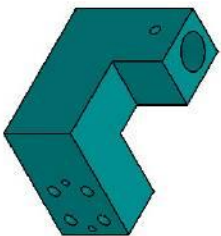
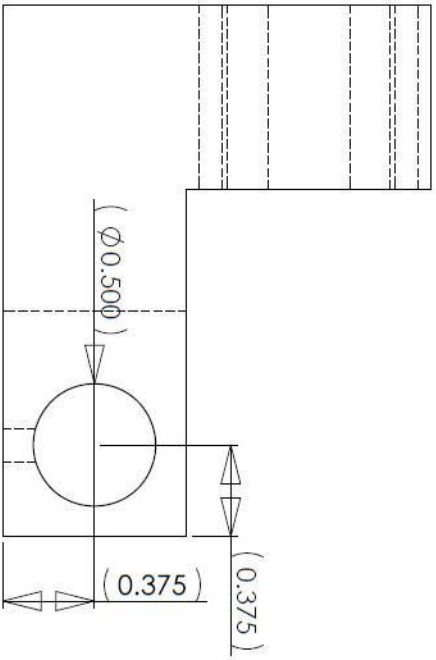
Front View



Side View



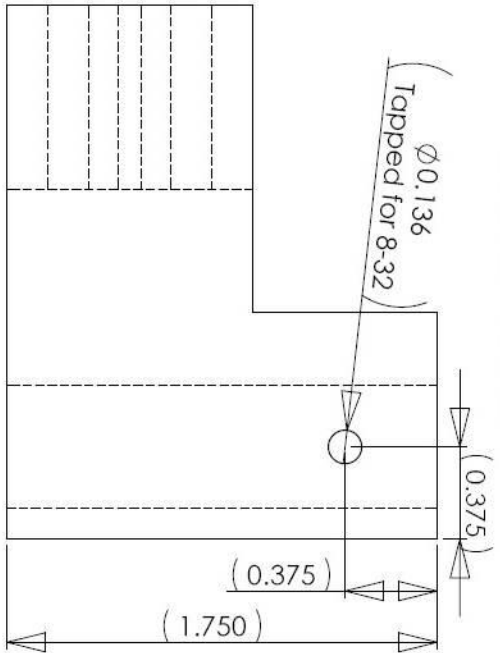
Bottom View



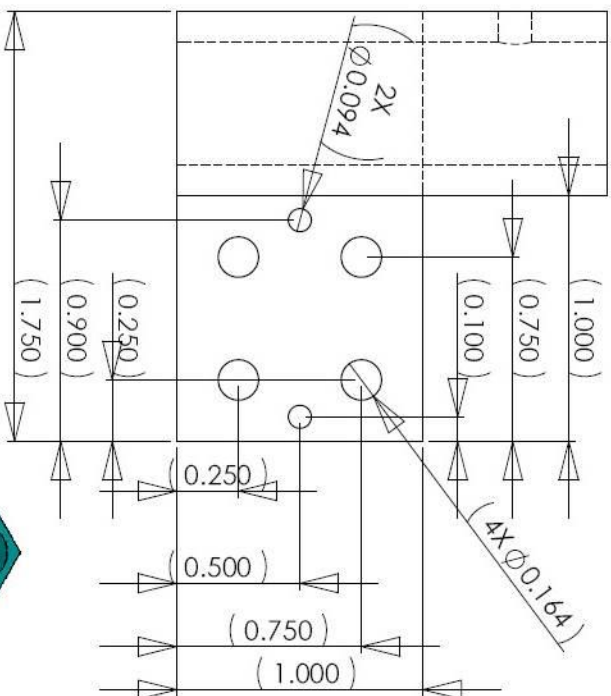
DIMENSIONS ARE IN INCHES		DATE	11/2008
TOLERANCES: ± 0.002		DRAWN	
UNLESS OTHERWISE INDICATED		CHECKED	
MATERIAL		ENG APPR	
6061 T6 Aluminum		MFG APPR	
FINISH		G.A.	
--		COMMENTS	
DO NOT SCALE DRAWING		SIZE	DWG. INC.
		SCALE	A
		WEIGHT	Capacitance Probe Mount 1
		SHEET	1 OF 1
		REV.	

University of Michigan
 Mechanical Engineering 450
 Senior Design
 Micro-Wire Tension/Torsion

Front View

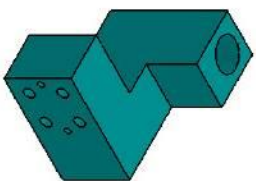
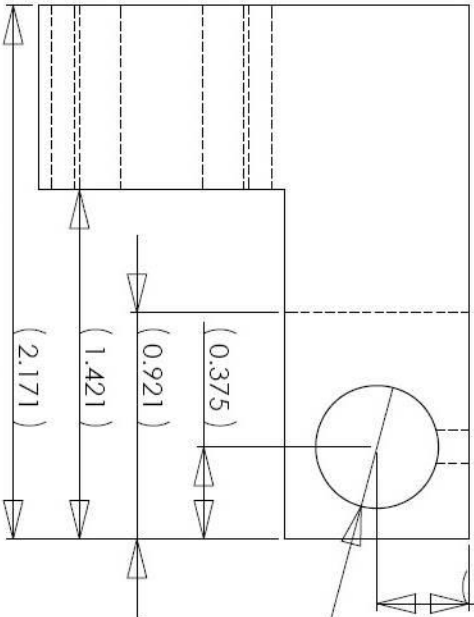


Side View

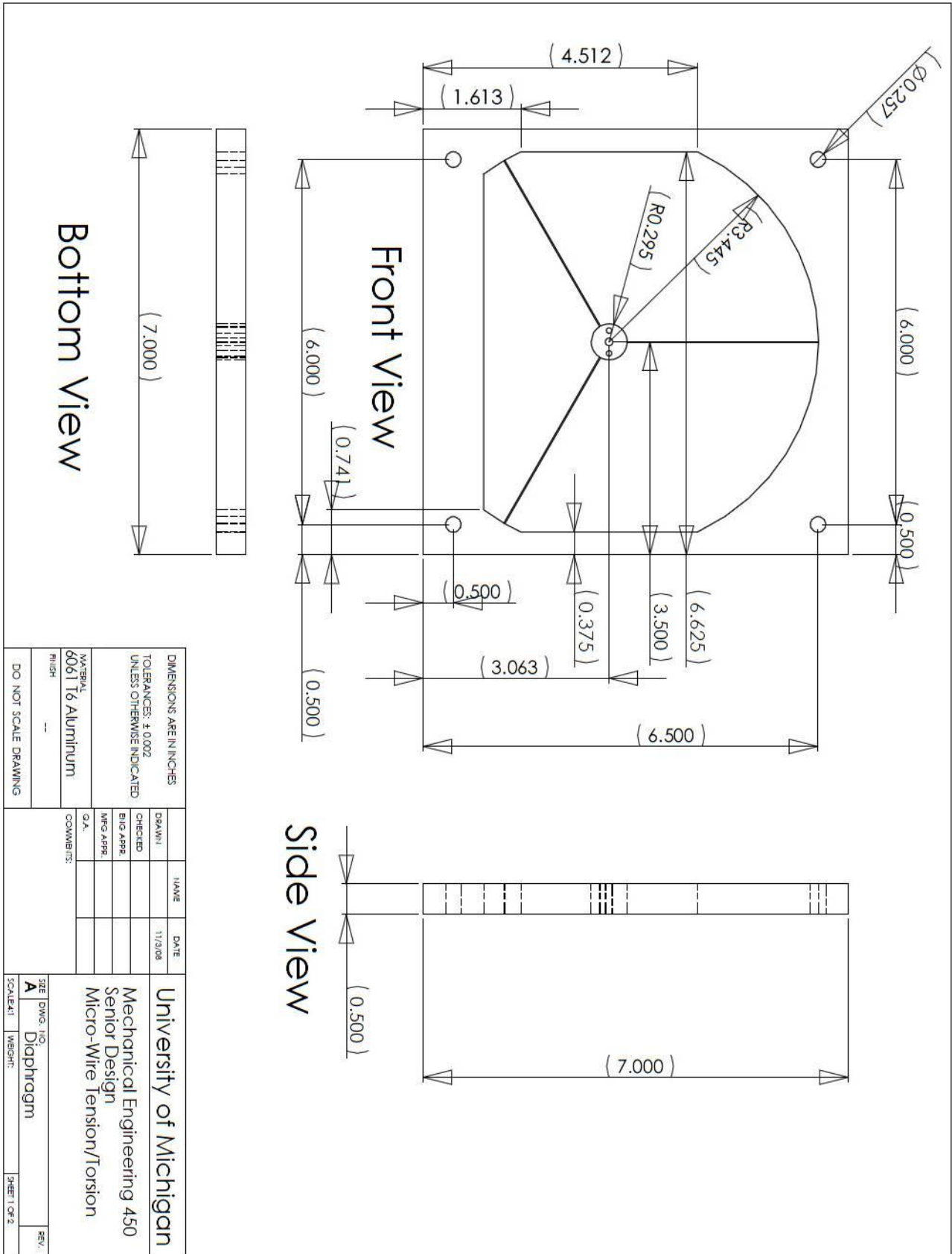


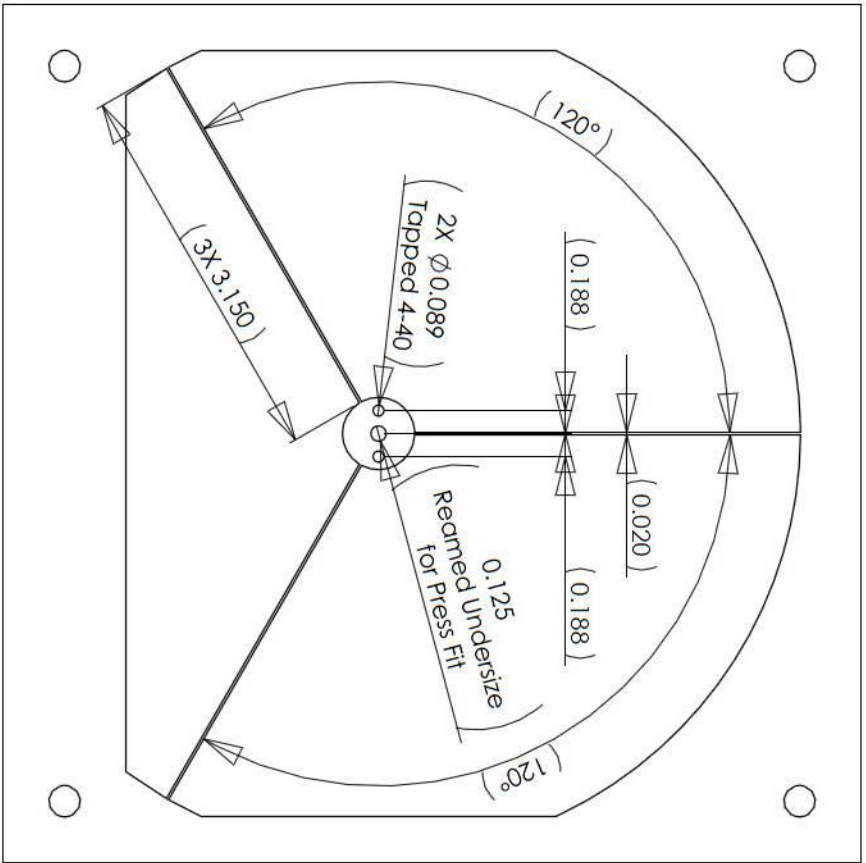
$\phi 0.500$
 Reamed
 Oversize

Bottom View

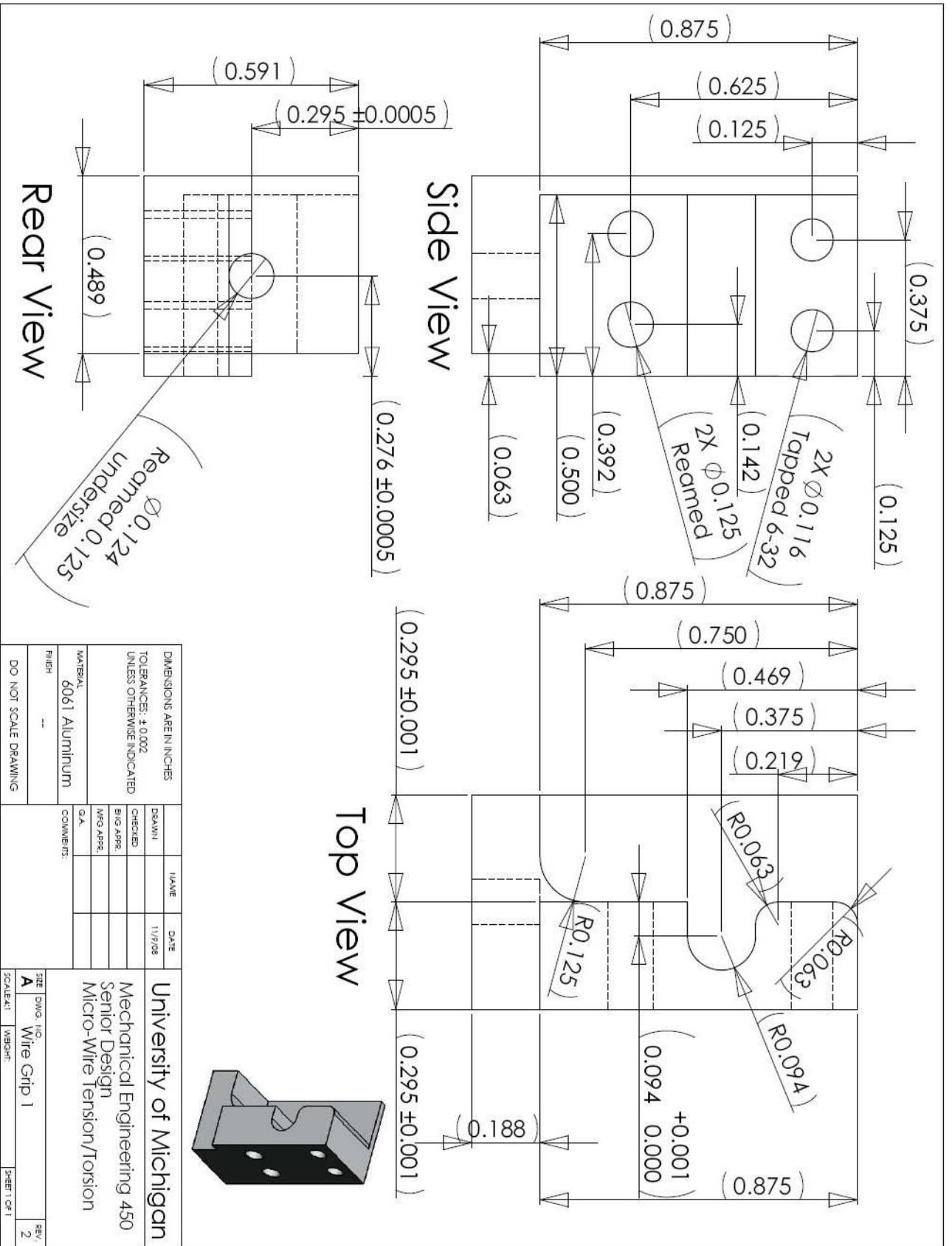


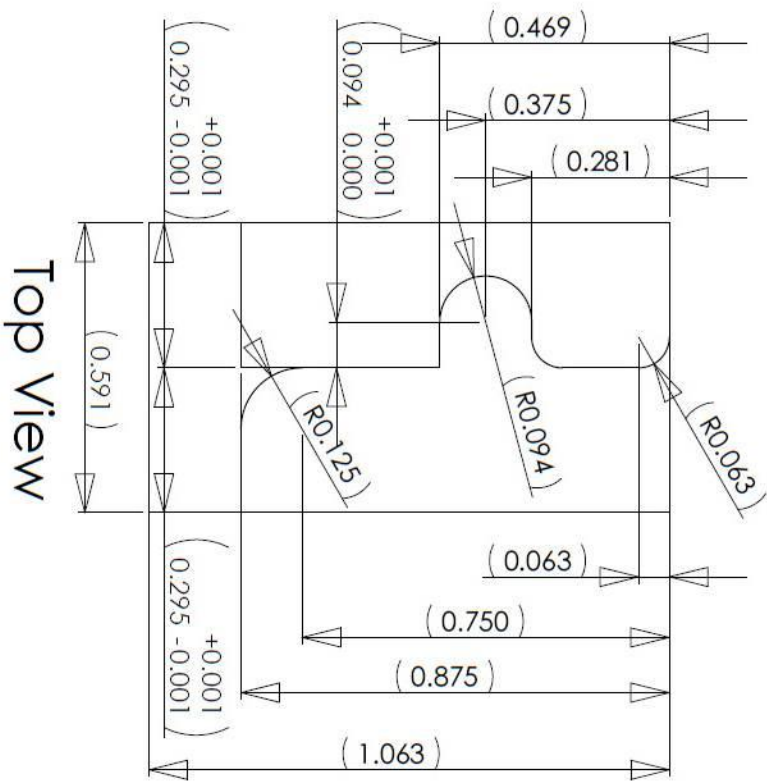
DIMENSIONS ARE IN INCHES		DATE	11/9/08
TOLERANCES: ± 0.002		DRAWN	
UNLESS OTHERWISE INDICATED		CHECKED	
MATERIAL: 6061 T6 Aluminum		ENG APPR.	
FINISH: --		MFG APPR.	
DO NOT SCALE DRAWING		Q.A.	
COMMENTS:		UNIVERSITY OF MICHIGAN	
MECHANICAL ENGINEERING 450		SENIOR DESIGN	
MICRO-WIRE TENSION/TORSION			
SIZE	DWG. NO.	SHEET	REV.
A	Capacitance Probe Mount 2	2	
SCALE:	1:1	SHEET	1 OF 1



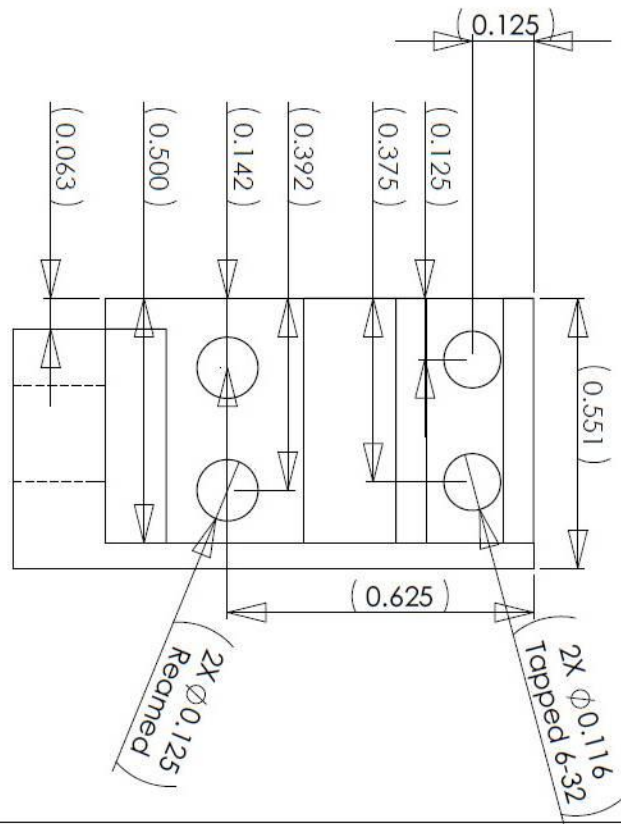


DIMENSIONS ARE IN INCHES		DRAWN	NAME	DATE
TOLERANCES: ± 0.002		CHECKED		11/29/08
UNLESS OTHERWISE INDICATED		ENG. APPR.		
		MFG. APPR.		
		Q.A.		
MATERIAL: 6061 T6 Aluminum		COMMENTS:		
FINISH: —				
DO NOT SCALE DRAWING				
SIZE A	DWG. NO. Dichprogm	University of Michigan		REV.
SCALE: 1:1	WEIGHT:	Mechanical Engineering 450		
		Senior Design		
		Micro-Wire Tension/Torsion		
		SHEET 2 OF 2		

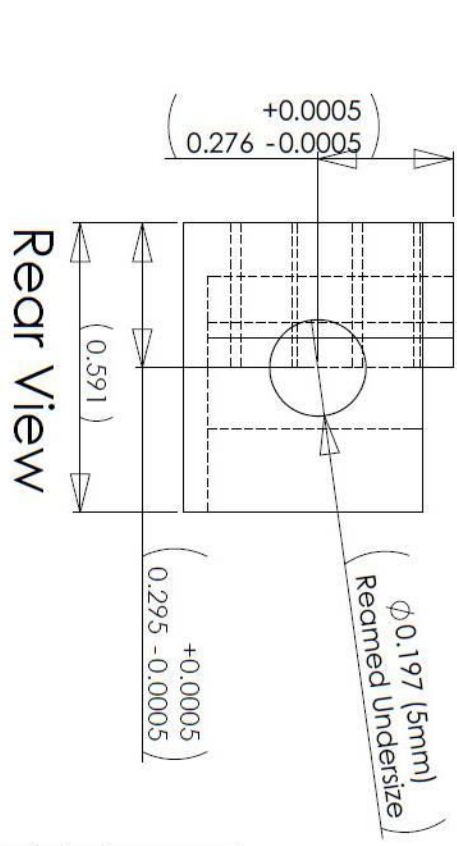




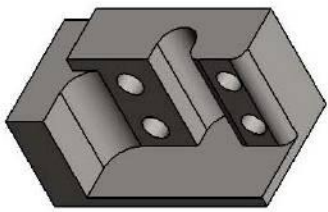
Top View



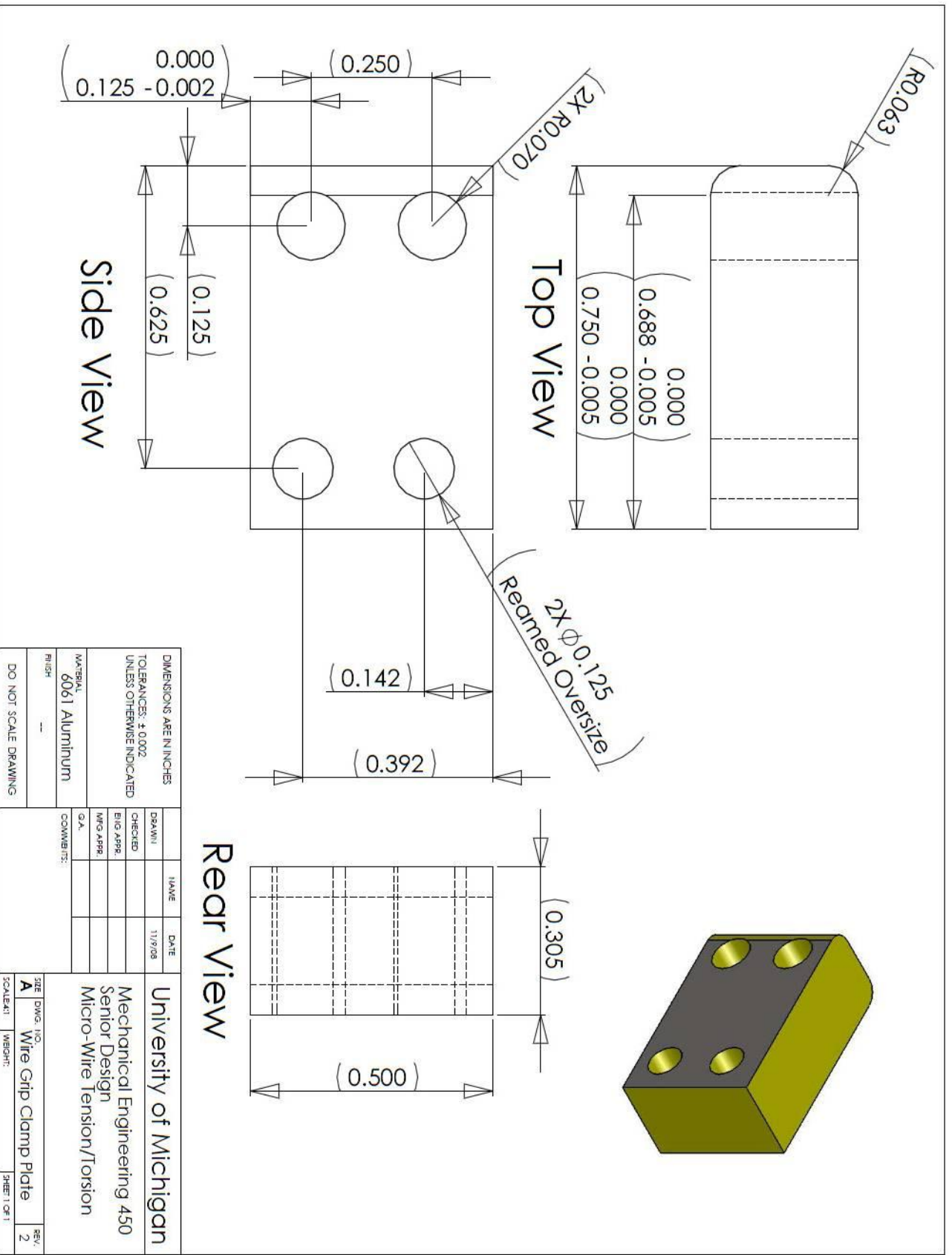
Side View



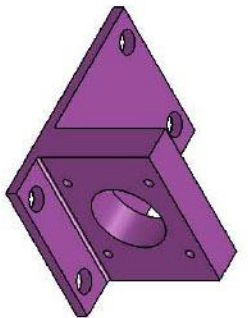
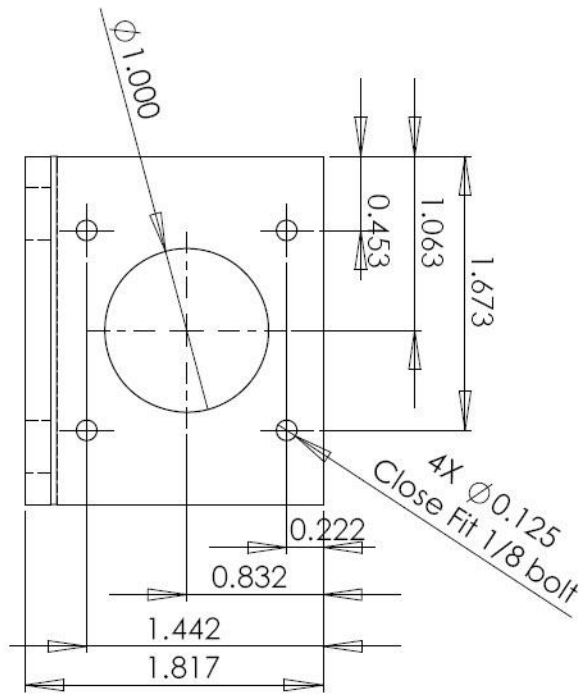
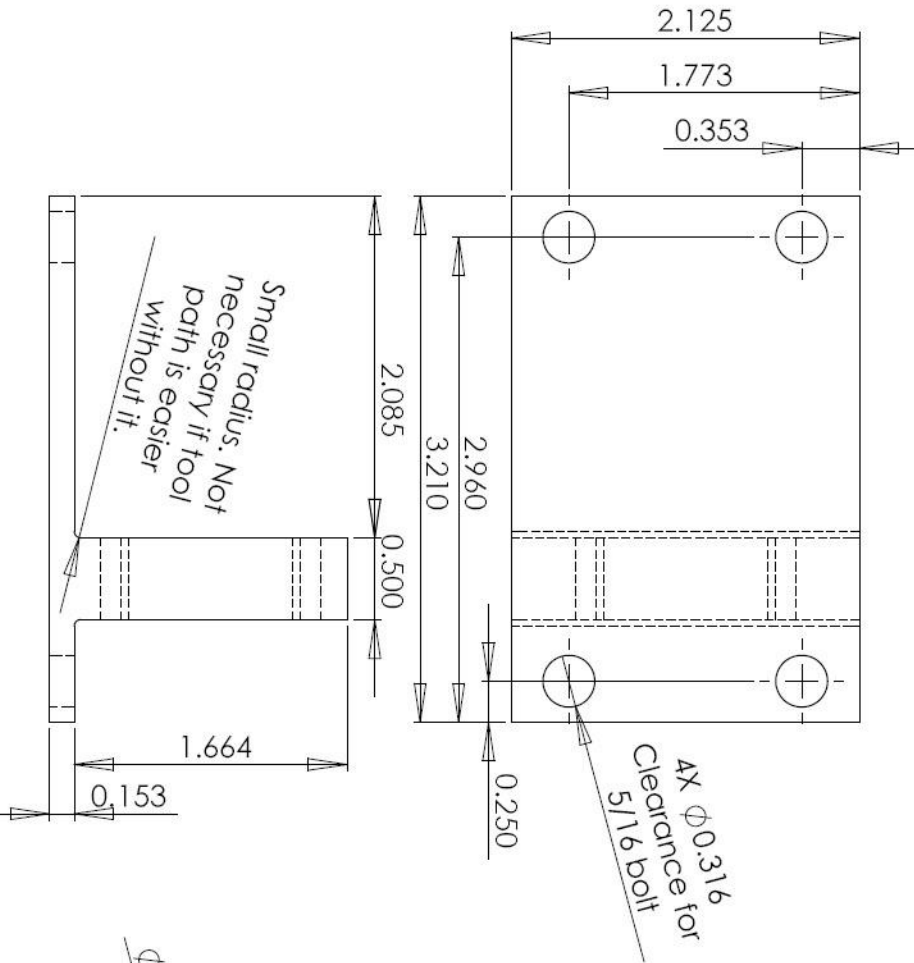
Rear View



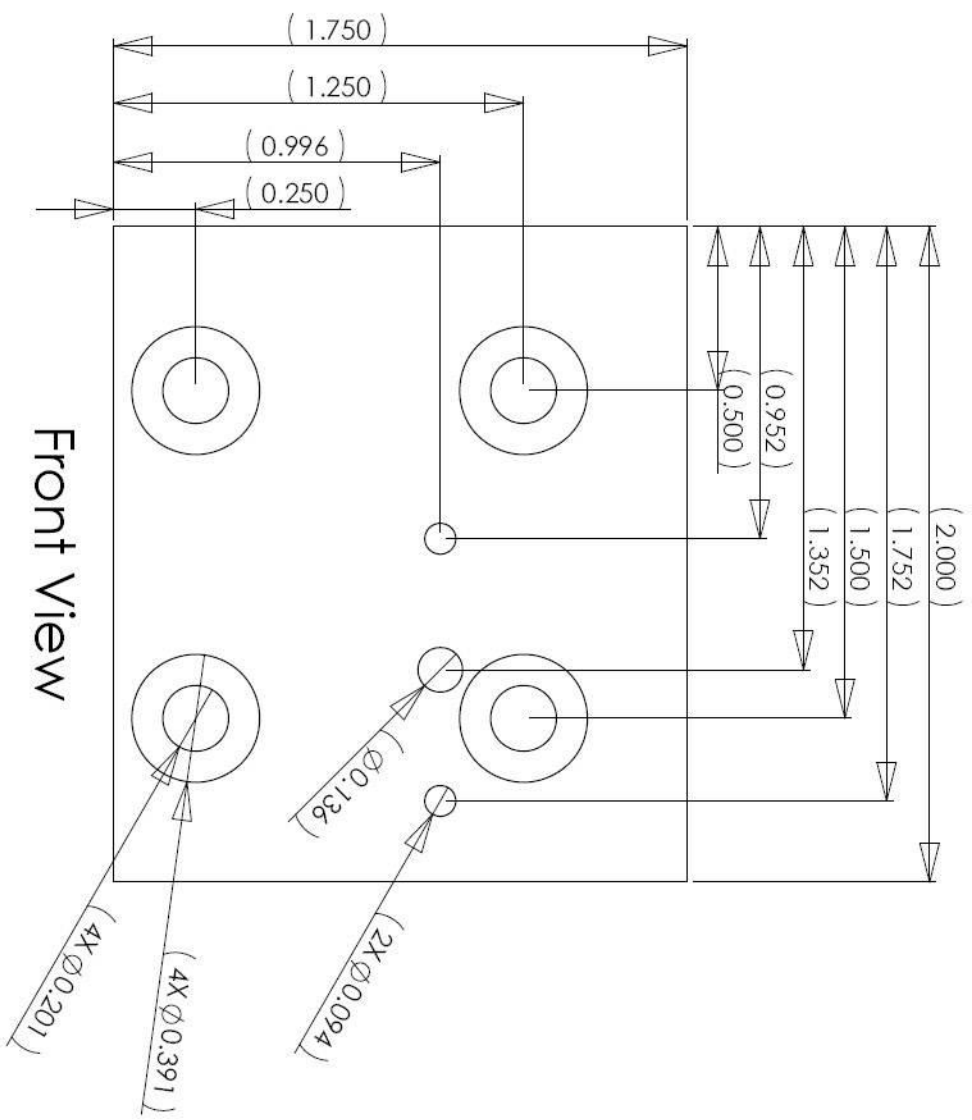
DIMENSIONS ARE IN INCHES		NAME	DATE
TOLERANCES: ± 0.002			11/9/08
UNLESS OTHERWISE INDICATED		CHECKED	
MATERIAL		ENG APPR	
6061 Aluminum		MFG APPR	
FINISH		G.A.	
DO NOT SCALE DRAWING		COMMENTS	
UNIVERSITY OF MICHIGAN		MECHANICAL ENGINEERING 450	
		SENIOR DESIGN	
		MICRO-WIRE TENSION/TORSION	
SIZE	DWG. NO.	SCALE	REV.
A	Wire Grip 2		2
SHEET 1	OF 1		



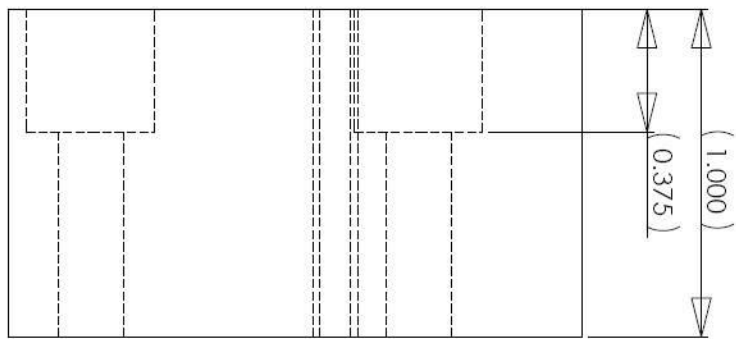
DIMENSIONS ARE IN INCHES		DATE	11/9/08
TOLERANCES: ± 0.002		DRAWN	
UNLESS OTHERWISE INDICATED		CHECKED	
MATERIAL: 6061 Aluminum		ENG APPR	
FINISH: --		MFG APPR	
DO NOT SCALE DRAWING		Q.A.	
COMMENTS:			
UNIVERSITY OF MICHIGAN		SIZE	DWG. NO.
MECHANICAL ENGINEERING 450		A	Wire Grip Clamp Plate
SENIOR DESIGN		SCALE	1/8" = 1"
MICRO-WIRE TENSION/TORSION		WEIGHT	
		SHEET	1 OF 1
		REV.	2



UNLESS OTHERWISE SPECIFIED:		NAME	DATE
DIMENSIONS ARE IN INCHES			11/17/08
TOLERANCES: ±0.002 general ±0.001 hole locations		CHECKED	
INTERPRET GEOMETRIC TOLERANCING PER:		ENG APPR.	
MATERIAL:		MFG APPR.	
FINISH		O.A.	
DO NOT SCALE DRAWING		COMMENTS:	
DWG. NO.		TITLE:	
Torsion Motor Mount		1	
SCALE: 1:1	WEIGHT:	SHEET 1 OF 1	
REV		1	

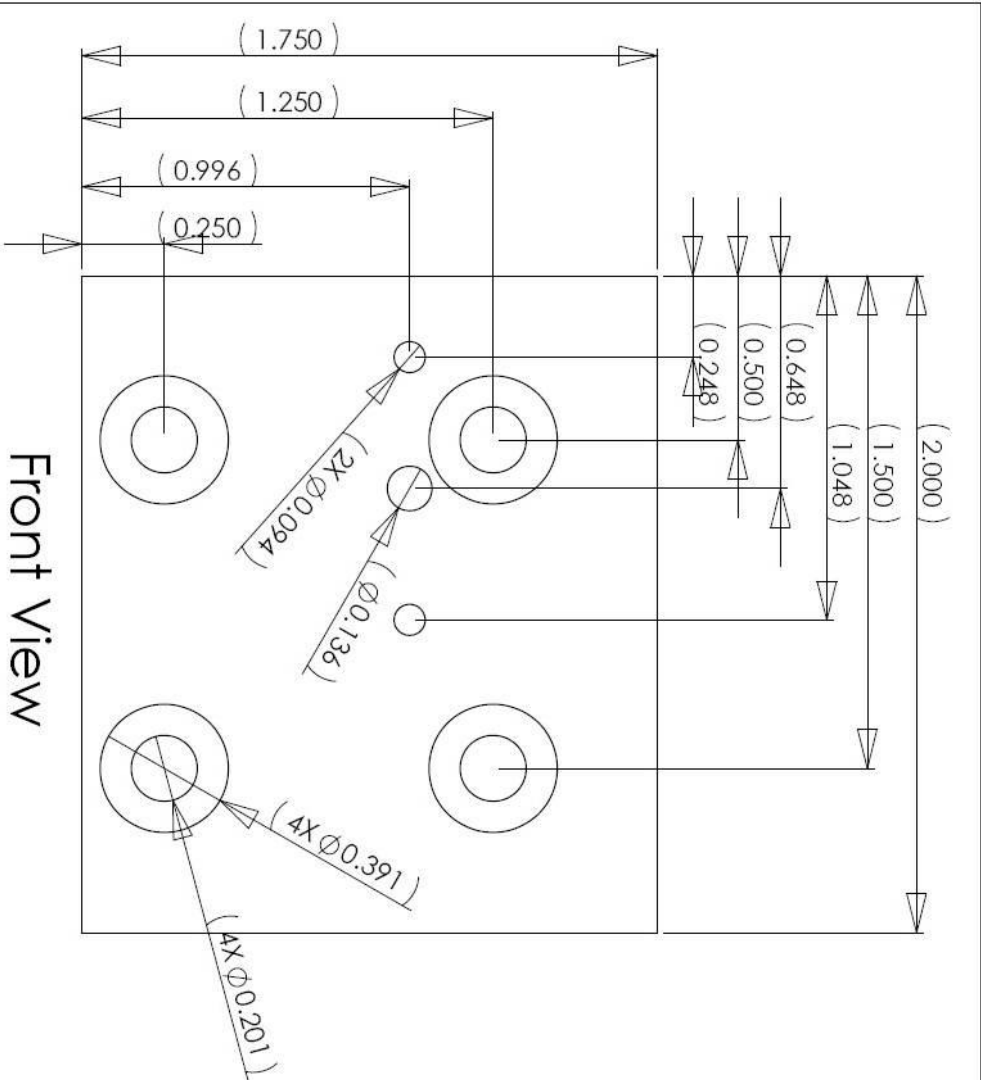


Front View

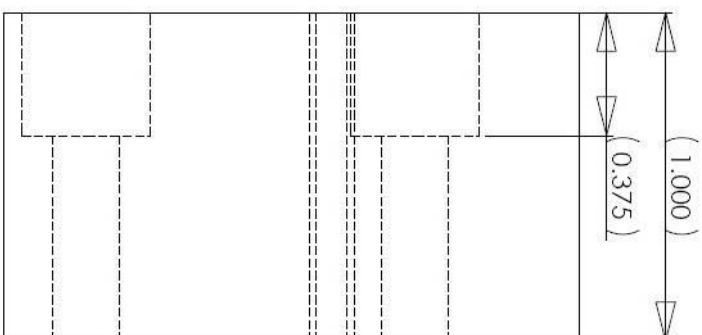


Side View

DIMENSIONS ARE IN INCHES		DRAWN	NAME	DATE
TOLERANCES: ± 0.002		CHECKED		11/9/08
UNLESS OTHERWISE INDICATED		ENG APPR.		
		MFG APPR.		
		Q.A.		
COMMENTS:				
MATERIAL: 6061 T6 Aluminum				
FINISH: ---				
DO NOT SCALE DRAWING				
UNIVERSITY OF MICHIGAN	MECHANICAL ENGINEERING 450			
	SENIOR DESIGN			
	MICRO-WIRE TENSION/TORSION			
SIZE: A	DWG. NO.: Stage Mount Block 1	SCALE: 1:1	SHEET: 1 OF 1	REV.:

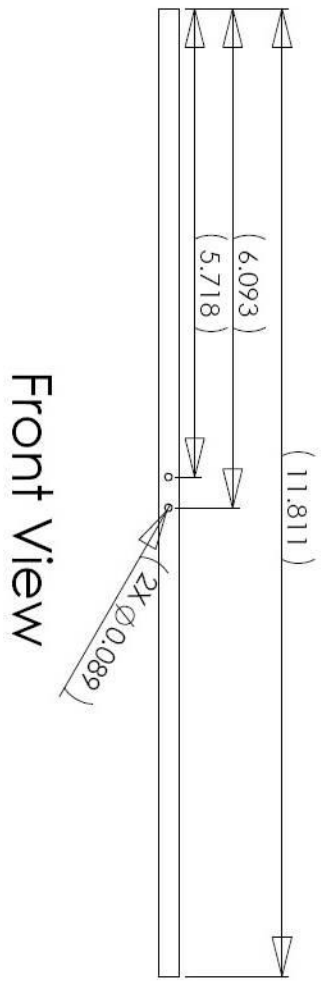


Front View

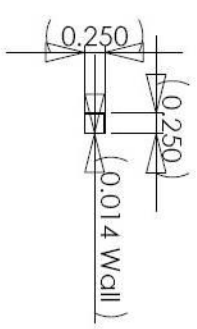


Side View

DIMENSIONS ARE IN INCHES TOLERANCES: ±0.002 UNLESS OTHERWISE INDICATED		DRAWN	NAME	DATE
		CHECKED		11/13/08
		ENG APPR.		
		MFG APPR.		
		QA		
COMMENTS:				
MATERIAL 6061 T6 Aluminum				
FINISH --				
DO NOT SCALE DRAWING				
UNIVERSITY OF MICHIGAN				
MECHANICAL ENGINEERING 450				
SENIOR DESIGN				
MICRO-WIRE TENSION/TORSION				
SIZE	DWG. NO.			REV.
A	Stage Mount Block 2			
SCALE: 2:1	WEIGHT:			SHEET 1 OF 1



Front View



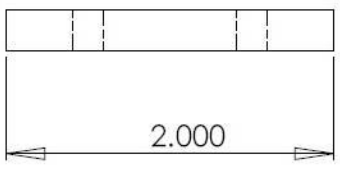
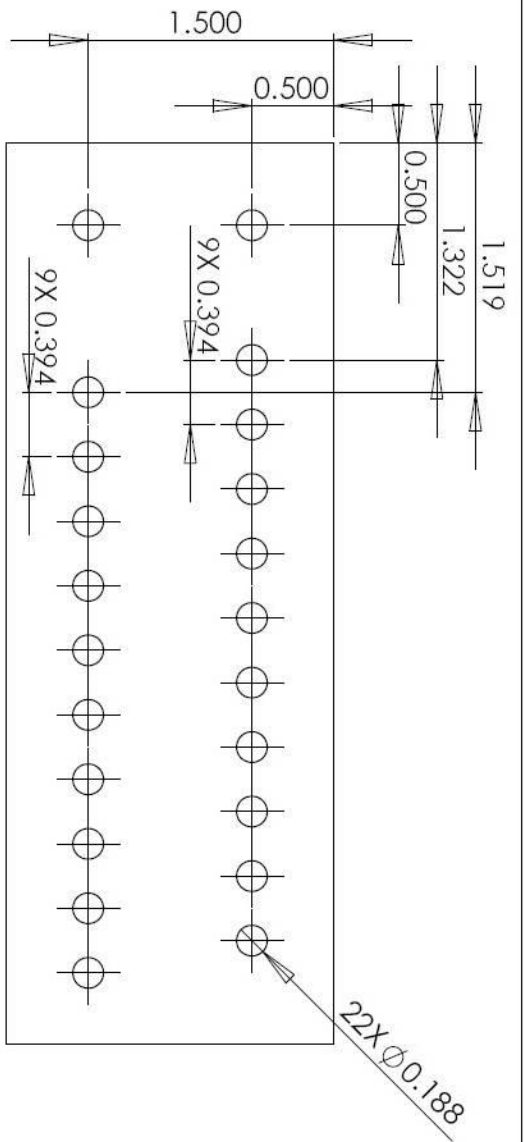
Side View



Bottom View

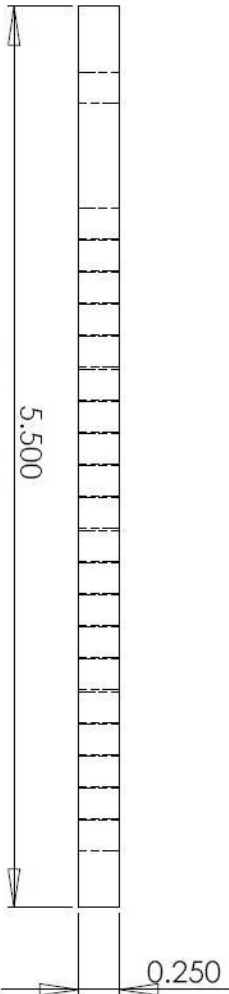


DIMENSIONS ARE IN INCHES		DRAWN	NAME	DATE
TOLERANCES: ±0.002		CHECKED		11/19/08
UNLESS OTHERWISE INDICATED		ENG APPR		
		MFG APPR		
		Q.A.		
MATERIAL:		COMMENTS:		
6061 T6 Aluminum				
FINISH:				
DO NOT SCALE DRAWING				
UNIVERSITY OF MICHIGAN		MECHANICAL ENGINEERING 450		
SENIOR DESIGN		MICRO-WIRE TENSION/TORSION		
SIZE	DWG. NO.	SHEET 1 OF 1		REV.
A	Amplification Bar			
SCALE: 1:2	WEIGHT:			

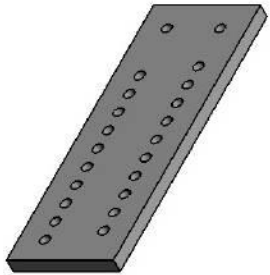


Top View

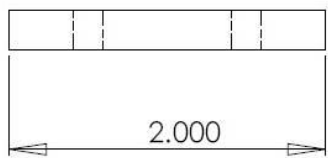
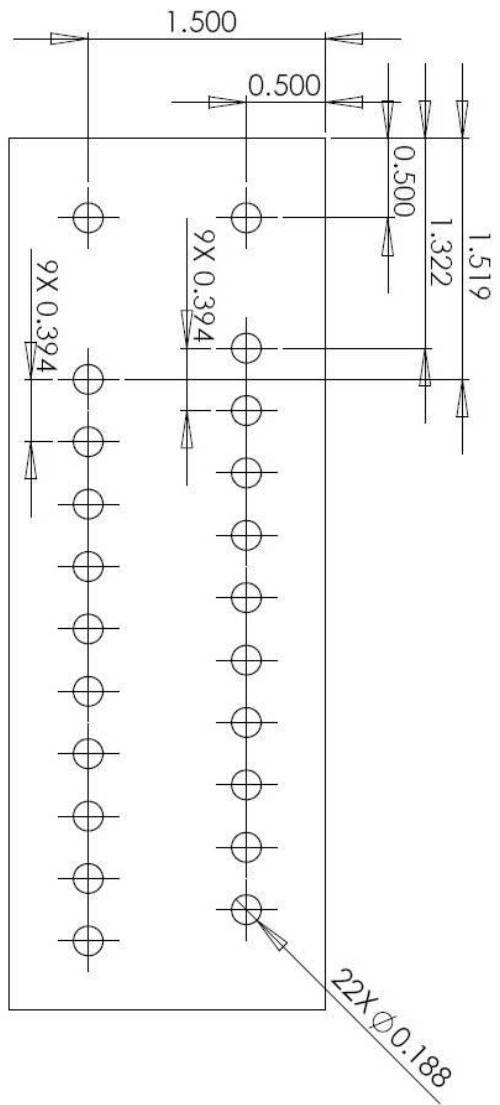
Rear View



Side View

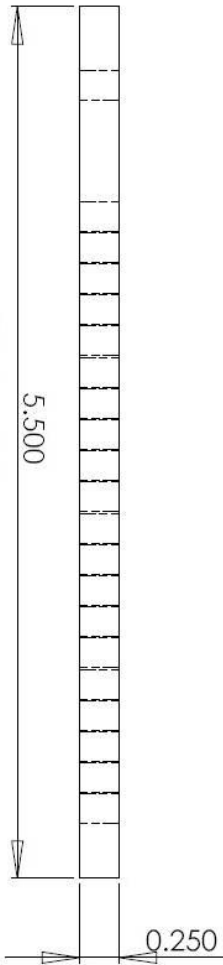


UNLESS OTHERWISE SPECIFIED:		DRAWN	NAME	DATE	TITLE:	
DIMENSIONS ARE IN INCHES		CHECKED		11/17/08		
TOLERANCES: ±0.002 general		ENG APPR.				
±0.001 hole locations		MFG APPR.				
		Q.A.				
INTERPRET GEOMETRIC TOLERANCING PER:		COMMENTS:			DWG. NO. Wire Set-Up Tray	
MATERIAL						
FINISH						
DO NOT SCALE DRAWING		SCALE: 1:1			WEIGHT:	SHEET 1 OF 1
		REV			1	

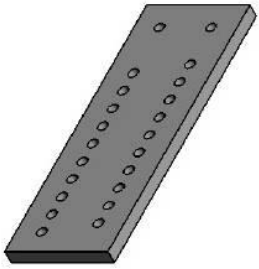


Top View

Rear View



Side View



UNLESS OTHERWISE SPECIFIED:		DRAWN	NAME	DATE
DIMENSIONS ARE IN INCHES		CHECKED		11/17/08
TOLERANCES: ±0.002 general		ENG APPR.		
±0.001 hole locations		MFG APPR.		
INTERPRET GEOMETRIC TOLERANCING PER:		O.A.		
MATERIAL		COMMENTS:		
FINISH				
DO NOT SCALE DRAWING				
DWG. NO.		TITLE:		REV
Wire Set-Up Tray				1
SCALE: 1:1	WEIGHT:	SHEET 1 OF 1		

APPENDIX O

Table O1: Summary of Performance

Parameter	Part	Value	Target	Design Change Needed
Linear Travel	Linear Encoder	1 μm	4 μm	No
Twist Angle	Rotary Encoder/Motor Position	0.056°	.096°	No
Tension Load	Load Cell	1.65E-5 N	5.00E-04	No
Torsion Load	Flexure/Capacitance Probes	~7E-8 Nm	2.49E-9 N*m	Yes
Alignment	Grips	Part Flaw	0.5°	No
Travel	Bi-Slide	127 mm	125 mm	No
Max Load	Load Cell/Torsion Motor	22.3 N	33 N	No
Grip Force Grip Friction	Grips	Successful Wire Test	43.75 N	No
Gauge Length	Grips/Bi-Slide	5-100 mm	1-75 mm	No